EFFECTIVE FIELD THEORIES FOR VECTOR PARTICLES AND CONSTRAINT ANALYSIS

ANDREAS NEISER

Diplomarbeit

Institut für Kernphysik

JOHANNES GUTENBERG UNIVERSITÄT MAINZ

September 2011

Andreas Neiser:
Effective Field Theories for Vector Particles and Constraint Analysis,
Diplomarbeit

ERSTGUTACHTER:
Prof. Dr. Stefan Scherer

ZWEITGUTACHTER:
Prof. Dr. Martin Reuter

CONTENTS

LIST OF FIGURES

LIST OF TABLES

Part I

INTRODUCTION AND THEORETICAL FOUNDATIONS

The main motivation for working in chiral dynamics is that it is fun…

— Heinrich Leutwyler [1]

1 MOTIVATION AND OVERVIEW

The strong interaction is one of the four fundamental forces in physics known today, besides gravitation, the weak interaction, and electromagnetism. It was firstly postulated as a short-ranged counterforce to explain the stability of nuclei as bound states of neutrons and protons since the latter are subject to electromagnetic repulsion due to their positive charge. Later, it was discovered in scattering experiments that nucleons are not fundamental particles but consist of point-like quarks and gluons [2, 3, 4]. In fact, quarks had already been discussed as hypothetical particles to explain the observed particle spectrum prior to their experimental discovery [5, 6]. Besides the leptons and the gauge bosons of electroweak theory, quarks and gluons are constituents of the Standard Model of particle physics and are therein described by an SU(3) gauge theory called quantum chromodynamics (QCD) [7, 8, 9]. It bears its name from the analogy to quantum electrodynamics (QED) that quarks interact with each other through gluons representing the gauge bosons. In contrast to QED, quarks carry three different color charges and the eight gluons themselves are color-charged. Due to the latter, three- and four-vertex gluon self-interactions arise.

QCD exhibits two intriguing features. So far, no free isolated quarks have been observed experimentally, although they are the constituents of matter. Only color-neutral bound states of quarks, so-called hadrons, seem to appear in nature. It is still an open question of high interest how to derive this phenomenon known as color confinement from QCD [10]. The second remarkable phenomenon, called asymptotic freedom, might be related to confinement [7, 10, 11]. It states that the running coupling constant g of QCD decreases for increasing energies. This implies that a perturbative treatment as an expansion in g is feasible and successfully describes experiments for energies higher than $\Lambda \approx 1\,\mathrm{GeV}$. On the other hand, the coupling g diverges for lower energies, which corresponds roughly speaking to larger distances, and thus could explain confinement.

Hence, in the low-energy regime, a perturbative treatment is meaningless and an analytical solution of QCD is yet unknown. Therefore, one could resort to a numerical approach called Lattice QCD, which is cur-

rently limited by available computing power. Another option—pursued in this work—is an effective field theory (EFT) where the degrees of freedom are not gluons and quarks anymore but pions, kaons, vector mesons and baryons, i.e. the low-energy degrees of freedom of the strong interaction. This approximation to the fundamental theory can be formulated as a quantum field theory, if Lorentz invariance and the cluster-decomposition principle hold. The cluster-decomposition principle states that sufficiently separated experiments do not influence each other [12]. Furthermore, the most general Lagrangian is only required to be consistent with the assumed symmetries of the underlying theory [13]. In general, this implies that the corresponding Lagrangian contains an infinite number of interaction terms, each accompanied by an unknown low-energy constant (LEC). Note that if one had solved the fundamental theory, one could calculate these LECs in principle. However, in order to give the effective theory predictive power, two concepts are necessary. First, the results of an EFT are obtained as a perturbative series in q/Λ up to a certain order, where q denotes a small quantity such as the pion mass or momentum. This renders the EFT only applicable for energies sufficiently below the intrinsic scale Λ, otherwise the series would not make any sense. Second, only terms in the Lagrangian which contribute in this finite series of small quantities are taken into account. Thus, one is left with a finite number of unknown LECs, which can be determined by comparison with experimental data if the fundamental theory is unknown. Since the LECs are independent of the particular physical process from which they have been determined, one can describe several physical processes with the same set of LECs, at least up to a certain accuracy.

In the case of chiral perturbation theory (ChPT), which is an effective field theory for Goldstone bosons only,[1] these concepts work reasonably well [14]. There exists a correspondence between the number of loops of a Feynman diagram and its lowest possible chiral order. In this sense, one can systematically neglect contributions of higher order. This so-called power counting scheme was firstly developed by Weinberg [15] and has been successfully used for various calculations. Though, there are two subtleties concerning this concept. First, due to the arbitrary negative mass dimension of the LECs, an EFT is not renormalizable

1 In this work, the term ChPT is distinguished from the term chiral effective field theory. The latter includes heavy degrees of freedom such as vector mesons. Moreover, the term Goldstone bosons is used for pions and additional kaons if the flavor symmetry is irrelevant in the particular context.

in the traditional sense, i.e. divergences stemming from loop integrals cannot be absorbed in a finite number of coupling constants. Nevertheless, this problem is simply overcome by requiring renormalizability for an EFT in a modern sense, i.e. appearing divergences are absorbed only up to the finite order of the calculation [12]. Second, the question arises whether the series in the small quantities converges. Naïvely, one would expect a correction factor of q/Λ for the next order not taken into account. In ChPT, where the order of q is given by the pion mass and $\Lambda \approx 1\,\text{GeV}$, this rough estimate of about 20 % seems accurate.[2]

The inclusion of heavy degrees of freedom such as nucleons and vector mesons is obviously desirable, since it extends the applicability of an EFT in two ways. Not only the energy regime is increased but also a wider range of hadronic processes can be described. On the other hand, it introduces several novel problems, which have been firstly encountered in the case of nucleons [16]. In the chiral limit, in which the masses of the light quarks and thus the masses of the Goldstone bosons vanish, the nucleon mass stays finite. Thereby, one introduces an intrinsic large scale in the theory, which is the main reason that a simple power counting as in ChPT fails. It follows that diagrams containing heavy degrees of freedom contribute to a lower chiral order than a naïvely adapted power counting would imply. Nevertheless, one can recover power counting by the price of a more complicated renormalization scheme. Basically, the parameters of a Lagrangian are redefined by finite quantities in order to absorb the power-counting-violating terms of the diagrams. Several manifestly Lorentz-invariant renormalization schemes have been developed to cover this issue. In this work, the commonly used infrared regularization [17] in its reformulated version of [18] is employed. Moreover, if heavy degrees of freedom are included, the convergence of the expansion in small quantities is worse in comparison to ChPT, even after renormalization. For example, some quantities in the nucleon sector receive large higher-order corrections, which renders the validity of the series expansion questionable.

This thesis deals with describing strongly interacting spin-one particles, so-called vector mesons, in the low-energy regime up to 1 GeV. They were postulated in the late 1950's in order to explain the charge distribution of protons and neutrons [24] and were discovered as resonances in various scattering experiments from 1961 to 1963 [25]. In this work, mainly the lightest vector mesons are considered: the three

2 Note that in ChPT the series is given in powers of $(q/\Lambda)^2$.

Name	I	Y	J^{PG}	Reference
$\rho(770)$	1	0	1^{-+}	[19]
$\omega(780)$	0	0	1^{--}	[20]
$\phi(1020)$	0	0	1^{--}	[21, 22]
$K^*(890)$	1/2	±1	1^-	[23]

Table 1.1: Firstly discovered vector mesons (mass in MeV) with their isospin I, hypercharge Y, and Poincaré transformation properties J^{PG} including G-parity if applicable.

isovectorial mesons ρ^+, ρ^0, ρ^- and the isoscalar meson ω, see table 1.1. Since the neutral ρ^0 has the same properties as the photon except for its mass, the inclusion of vector mesons typically improves the calculation of electromagnetic form factors [26, 27]. In particular, their q^2 dependence is better described since the quantity q^2 is a measure for the mass of the virtual photon. This is reflected in the vector meson dominance model, where the interaction of the photon with a hadron is mostly determined by the direct photon-rho coupling [25].

In comparison to nucleons, the inclusion of vector mesons as heavy degrees of freedom is further complicated by their decay to pions. This leads to diagrams which exhibit a power-counting-violating imaginary part, which must be compensated by imaginary counter-terms. Furthermore, unstable particles could be implemented in a quantum field theory with a complex mass [28]. Calculations using such a complex mass renormalization scheme have been performed, e.g. for the mass of the rho meson [29]. It leads to the question whether the unitarity of the S-matrix is violated or not by this renormalization scheme order by order. Additionally, the construction of Lorentz-invariant scalars for vector meson fields usually introduces more degrees of freedom than physically meaningful. Hence, constraints are necessary to reduce the number of degrees of freedom to the physical number. However, these constraints must be conserved in time, which represents a self-consistency condition. This reasoning implies additional relations among the introduced LECs in general, e.g. the well-known KSRF relation can be derived with the help of such a constraint analysis [30].

This work is organized as follows. In chapter 2, the basic concepts of QCD with an emphasis on symmetries are presented in order to motivate the construction of ChPT. Furthermore, ChPT is extended to

include vector mesons, which is then denoted as a chiral effective field theory. In chapter 3, some aspects of power counting and reformulated infrared regularization are briefly highlighted. Finally, the methods of a constraint analysis on a classical level are described in chapter 4, complemented by considering the free antisymmetric tensor model as an example. In the second part, an already existing self-consistency calculation of a general EFT for vector particles is extended to the SU(3) sector in chapter 5, which is the only part of this work dealing with flavor SU(3). Next, the quantization of an effective field theory is investigated for three massive vector particles using the antisymmetric tensor field formalism including a constraint analysis in chapter 6. Finally, the magnetic moment of the rho meson is calculated using a chiral effective field theory incorporating pions, rho- and omega-mesons in chapter 7. The findings are summarized and conclusions are drawn in chapter 8.

2

QCD AND CHIRAL EFFECTIVE FIELD THEORY

In this chapter, the well-established quantum field theory describing the strong interaction, quantum chromodynamics (QCD), is presented. In the so-called chiral limit, it reveals symmetries which motivate an effective field theory, chiral perturbation theory (ChPT). It can be extended to a chiral effective field theory, which includes heavy degrees of freedom, such as vector mesons. This introduction is loosely based on [31, 32, 33].

2.1 QUANTUM CHROMODYNAMICS

As already mentioned, the strong interaction can be described by an SU(3) gauge theory called quantum chromodynamics (QCD). The full QCD Lagrangian is given by [34, 35]

$$\mathcal{L}_{\text{QCD}} = \sum_{f=1}^{6} \bar{q}_f (i\gamma^\mu D_\mu - m_f) q_f - \frac{1}{2} \operatorname{Tr}\left(\mathcal{G}_{\mu\nu}\mathcal{G}^{\mu\nu}\right), \tag{2.1}$$

where

$$q_f = \begin{pmatrix} q_{f,1} \\ q_{f,2} \\ q_{f,3} \end{pmatrix} \tag{2.2}$$

is the Dirac spinor quark field written down as a color triplet for each of the six quark flavors f, usually denoted up (u), down (d), strange (s), charm (c), bottom (b) and top (t). In addition, the quantity[1]

$$\mathcal{A}_\mu \equiv \mathcal{A}_\mu^a \frac{\lambda^a}{2} \tag{2.3}$$

represents the eight gluon gauge fields and its field strength tensor is given by

$$\mathcal{G}_{\mu\nu} \equiv \mathcal{G}_{\mu\nu}^a \frac{\lambda^a}{2} = \left(\partial^\mu \mathcal{A}_\nu^a - \partial_\nu \mathcal{A}_\mu^a - g f^{abc} \mathcal{A}_\mu^b \mathcal{A}_\nu^c\right) \frac{\lambda^a}{2}. \tag{2.4}$$

1 See section A.1 on page 95 for the notation used.

Flavor	Charge	Mass
up	2/3	(1.7–3.3) MeV
down	–1/3	(4.1–5.8) MeV
strange	–1/3	(101 ± 29) MeV
charm	2/3	(1.27 ± 0.09) GeV
bottom	–1/3	(4.19 ± 0.18) GeV
top	2/3	(172.0 ± 1.3) GeV

Table 2.1: Quark masses and their charge in units of e for each flavor. The masses are heavily model dependent due to the experimental fact that quarks cannot be observed as free particles but only by indirect measurements of color singlet states. Values are taken from [36].

Finally, one finds

$$D_\mu q_f \equiv (\partial_\mu + ig\mathcal{A}_\mu) q_f \tag{2.5}$$

as the covariant derivative, which transforms as the object it acts on by definition. Note that the coupling constant g is independent of the quark flavor.

As indicated earlier, the Lagrangian is constructed such that it is invariant under a *local* SU(3) gauge transformation of the quark fields in color space, i.e.

$$q_f(x) \to q'_f(x) = \exp\Big(-i\theta^a(x)\frac{\lambda^a}{2}\Big) q_f(x) \equiv U(x) q_f(x) \tag{2.6a}$$

$$\text{and} \quad \mathcal{L}_{\text{QCD}} \to \mathcal{L}'_{\text{QCD}} = \mathcal{L}_{\text{QCD}} \,. \tag{2.6b}$$

This implies the transformation of the gauge fields to read

$$\mathcal{A}_\mu \to \mathcal{A}'_\mu = U\mathcal{A}_\mu U^\dagger + \frac{i}{g}\partial_\mu U U^\dagger \tag{2.7}$$

and it renders both parts of the Lagrangian in equation (2.1) independently invariant. Note that in contrast to quantum electrodynamics, the Lagrangian contains three-vertex and four-vertex interactions between the gluon fields. This key feature of quantum chromodynamics stems from the fact that the underlying gauge group SU(3) is non-abelian.

There exists an accidental global symmetry due to the numerical values of the so-called current quark masses, see table 2.1. One can divide the six quark flavors into the „light" quarks up, down, strange, and into the „heavy" quarks charm, bottom, and top. The splitting scale of about 1 GeV is justified by the mass of the lightest[2] strongly interacting particles, i.e. the rho meson with a mass of 770 MeV, and by the scale of spontaneous symmetry breaking $4\pi F \approx 1170\,\mathrm{MeV}$. This leads to a Lagrangian approximately describing low-energy processes of the strong interaction

$$\mathcal{L}^0_{\mathrm{QCD}} = \sum_{f=u,d,s} \bar{q}_f i\gamma^\mu D_\mu q_f - \frac{1}{2}\,\mathrm{Tr}\big(\mathcal{G}_{\mu\nu}\mathcal{G}^{\mu\nu}\big)\,, \tag{2.8}$$

where the light quark masses are set to zero and the heavy quarks are omitted in comparison to equation (2.1). This approximation is called chiral limit. By introducing the projection operators,

$$P_{\mathrm{R}} = \frac{1}{2}(1+\gamma_5) \quad \text{and} \quad P_{\mathrm{L}} = \frac{1}{2}(1-\gamma_5)\,, \tag{2.9}$$

which project the quark fields q_f onto their right-handed $q_f^{\mathrm{R}} = P_{\mathrm{R}} q_f$ and left-handed $q_f^{\mathrm{L}} = P_{\mathrm{L}} q_f$ components, respectively, the Lagrangian can be rewritten as

$$\mathcal{L}^0_{\mathrm{QCD}} = \sum_{f=u,d,s} \Big(\bar{q}_f^{\mathrm{R}} i\gamma^\mu D_\mu q_f^{\mathrm{R}} + \bar{q}_f^{\mathrm{L}} i\gamma^\mu D_\mu q_f^{\mathrm{L}}\Big) - \frac{1}{2}\,\mathrm{Tr}\big(\mathcal{G}_{\mu\nu}\mathcal{G}^{\mu\nu}\big)\,. \tag{2.10}$$

Since the covariant derivative D_μ is flavor independent, it follows that $\mathcal{L}^0_{\mathrm{QCD}}$ is invariant under a transformation associated with a $\mathrm{U}(3)_{\mathrm{R}} \times \mathrm{U}(3)_{\mathrm{L}}$ symmetry group in flavor space, which is isomorphic to the symmetry group $\mathrm{SU}(3)_{\mathrm{R}} \times \mathrm{SU}(3)_{\mathrm{L}} \times \mathrm{U}(1)_{\mathrm{V}} \times \mathrm{U}(1)_{\mathrm{A}}$. Here and henceforth, the basis[3] V = R + L and A = R − L with well-defined parity +1 and −1, respectively, is used. Naïvely, one would expect $2 \times 8 + 2 = 18$ conserved currents according to Noether's theorem [37]. However, an anomaly in QCD due to quantum corrections breaks the conservation of the singlet axial-vector current associated with $\mathrm{U}(1)_{\mathrm{A}}$ [38, 39, 40], so that QCD in the chiral limit possesses the symmetry group

$$\mathrm{SU}(3)_{\mathrm{R}} \times \mathrm{SU}(3)_{\mathrm{L}} \times \mathrm{U}(1)_{\mathrm{V}}\,, \tag{2.11}$$

2 The pseudoscalar pions and kaons are regarded as pseudo-Goldstone bosons and are therefore treated specially, see section 2.2.

3 Note that this notation is rather symbolic, in some cases a prefactor 1/2 or $1/\sqrt{2}$ is inserted by convention.

where the subgroup $G = \mathrm{SU}(3)_\mathrm{R} \times \mathrm{SU}(3)_\mathrm{L}$ is often referred to as the chiral group. The conservation of the singlet vector current associated with $\mathrm{U}(1)_\mathrm{V}$ corresponds to the conservation of baryon number B observed in experiments. Therefore, one divides hadrons into mesons with $B = 0$ and baryons with $B = 1$.

2.2 CHIRAL EFFECTIVE FIELD THEORY

In the scope of this thesis, it is sufficient to restrict the following considerations to the case of a global $G = \mathrm{SU}(2)_\mathrm{R} \times \mathrm{SU}(2)_\mathrm{L}$ symmetry, i.e. only the up and down quarks are regarded as light, which is a far better approximation than including the strange quark.

Spontaneous Symmetry Breaking

According to the approximate symmetry of QCD in equation (2.11), one would expect that observed particle states in a certain mass region can be arranged approximately in irreducible multiplets of SU(2) with positive *and* negative parity. However, one finds at the lowest mass scale multiplets with positive parity only, e.g. the baryon doublet, and rather light pseudoscalar pions. This leads to the conclusion that the chiral group $G = \mathrm{SU}(2)_\mathrm{R} \times \mathrm{SU}(2)_\mathrm{L}$ with $n_G = 6$ generators is spontaneously broken to the subgroup $H = \mathrm{SU}(2)_\mathrm{V}$ with $n_H = 3$ generators. Spontaneous symmetry breaking means that, although the Hamiltonian is invariant under G, its physically realized ground state is only invariant under a subgroup H of G. In this case, Goldstone's theorem [41, 42] requires the appearance of $n_G - n_H = 3$ massless and spinless particles. These particles are identified with the pions, whose finite mass is attributed to the explicit breaking of chiral symmetry due to the finite masses of the light quarks. Note that the symmetry of the system is determined by the ground state and not by the Hamiltonian, owing to Coleman's theorem [43].

Ward Identities and Local Chiral Invariance

Vacuum expectation values of time-ordered products of operators, so-called Green's functions, are connected to the physical scattering amplitudes according to the Lehmann-Symanzik-Zimmermann (LSZ) formalism [44, 45]. Thereby, they represent the crucial link between theory and

experimental data in a quantum field theory. The aforementioned global chiral symmetry leads to relations among different Green's functions if promoted to a local one. This was firstly discovered in QED with respect to a U(1) symmetry and these relations are thus denoted shortly as Ward identities [46, 47, 48]. Note that chiral Ward identities are still useful in a modified form if the underlying chiral symmetry is explicitly broken, i.e. in the physical case of non-vanishing quark masses [49].

Green's functions can be obtained elegantly by functional derivatives with respect to external fields in the path integral formalism. To that end, the SU(2)-adapted Lagrangian in equation (2.10) is extended by such external fields, which couple to the vector-, axial-vector-, scalar- and pseudoscalar quark currents as follows:

$$\mathcal{L} = \mathcal{L}^0_{\mathrm{QCD}} + \mathcal{L}_{\mathrm{ext}} = \mathcal{L}^0_{\mathrm{QCD}} + \bar{q}\gamma_\mu\Big(v^\mu + \frac{1}{3}v^\mu_{(\mathrm{s})} + \gamma_5 a^\mu\Big)q - \bar{q}\Big(s - i\gamma_5 p\Big)q\,. \quad (2.12)$$

The color-neutral external fields acting in flavor space are defined with the help of the Pauli matrices[4] as

$$\begin{aligned} v^\mu &= \sum_{i=1}^{3}\frac{\tau_i}{2}v^\mu_i\,, \quad v^\mu_{(\mathrm{s})} = \tau_0 v^\mu_0\,, \quad a^\mu = \sum_{i=1}^{3}\frac{\tau_i}{2}a^\mu_i\,, \\ s &= \sum_{i=0}^{3}\tau_i s_i\,, \qquad\qquad p = \sum_{i=0}^{3}\tau_i p_i\,. \end{aligned} \quad (2.13)$$

Note that the vector current possesses an isovectorial and isoscalar part.[5] The original QCD Lagrangian with finite quark masses can be obtained by setting $s = \mathrm{diag}(m_u, m_d)$ and $v = a = p = 0$. Finally, the generating functional Z is given by

$$\exp\big(iZ[v,a,s,p]\big) = \big\langle 0\big|T\exp\big[i\int d^4x\mathcal{L}_{\mathrm{ext}}(x)\big]\big|0\big\rangle_{(\text{chiral limit})}\,. \quad (2.14)$$

This functional represents the crucial link between QCD in the low-energy limit and effective field theories for the strong interaction.

4 The definition is given in equation (A.5) on page 95.

5 The isoscalar vector current plays an important role in the SU(2) sector and is hence included explicitly. The isoscalar axial-vector current has an anomaly and is hence omitted [14, 50].

Furthermore, the Lagrangian $\mathcal{L}$ in equation (2.12) is invariant under a *local* chiral transformation if the external currents behave as

$$\begin{aligned}
\big(v^\mu + a^\mu\big) &\to V_\mathrm{R}\big(v^\mu + a^\mu\big)V_\mathrm{R}^\dagger + iV_\mathrm{R}\partial^\mu V_\mathrm{R}^\dagger\,,\\
\big(v^\mu - a^\mu\big) &\to V_\mathrm{L}\big(v^\mu - a^\mu\big)V_\mathrm{L}^\dagger + iV_\mathrm{L}\partial^\mu V_\mathrm{L}^\dagger\,,\\
\big(s + ip\big) &\to V_\mathrm{R}\big(s + ip\big)V_\mathrm{L}^\dagger\,,\\
\big(s - ip\big) &\to V_\mathrm{L}\big(s - ip\big)V_\mathrm{R}^\dagger\,,
\end{aligned} \tag{2.15}$$

where $\big(V_\mathrm{R}(x), V_\mathrm{L}(x)\big) \in G = \mathrm{SU}(2)_\mathrm{R} \times \mathrm{SU}(2)_\mathrm{L}$. Promoting the global chiral symmetry to a local one serves two purposes. First, in absence of anomalies, the chiral Ward identities are equivalent to the invariance of the generating functional under a *local* chiral transformation, i.e. the effective Lagrangian reproducing the Green's functions resulting from equation (2.14) is invariant under a local chiral transformation. This imposes strong constraints on the construction of an effective field theory [51]. Second, local invariance allows for a coupling of the effective degrees of freedom to external gauge fields. For example, the electromagnetic four-vector potential A^μ is implemented as

$$v^\mu_{(\mathrm{s})} = -\frac{e}{2}A^\mu\,, \quad v^\mu = -\frac{e}{2}\tau_3 A^\mu\,. \tag{2.16}$$

Weinberg's Power Counting

As already indicated, an effective Lagrangian contains an infinite number of interaction terms and, hence, an infinite number of Feynman diagrams contribute to a physical process even up to one-loop level. Therefore, a power counting scheme, which assigns to each diagram a so-called chiral order D, is necessary. In the case of pions, this scheme is called Weinberg's power counting [15] and allows for neglecting higher-order contributions in a systematic way. Consequently, the interaction terms of a Lagrangian are ordered by the number of derivatives[6] and powers of pion masses,

$$\mathcal{L} = \mathcal{L}_2 + \mathcal{L}_4 + \mathcal{L}_6 + \ldots\,. \tag{2.17}$$

As explained later, only even orders $\mathcal{L}_{2n}$ occur. In particular, the chiral order D is defined by the behavior of the invariant amplitude $\mathcal{M}(p, m_q)$

6 The derivatives can act on pion fields as well as on external ones. Of course, the latter are also assigned a chiral order which needs to be considered.

corresponding to some diagram under a linear rescaling of the external pion momenta, $p_i \to t p_i$, and a quadratic rescaling[7] of the quark masses, $m_q \to t^2 m_q$, as

$$\mathcal{M}(p, m_q) \to \mathcal{M}(tp, t^2 m_q) = t^D \mathcal{M}(p, m_q)\,. \tag{2.18}$$

The chiral order is then given by

$$\begin{aligned} D &= 2 + \sum_{n=0}^{\infty} 2(n-1) N_{2n} + 2N_{\mathrm{L}} \\ &= 4N_{\mathrm{L}} - 2N_{\mathrm{I}} + \sum_{n=0}^{\infty} 2n N_{2n}\,, \end{aligned} \tag{2.19}$$

where N_{2n} is the number of vertices from $\mathcal{L}_{2n}$, N_{L} the number of loop integrations and N_{I} the number of internal pion lines. Referring to equation (2.19), a loop integration counts as $D = 4$, an internal pion propagator as $D = -2$ and a vertex from $\mathcal{L}_{2n}$ as $D = 2n$. In conclusion, the importance of diagrams decreases with increasing chiral order D, which is directly proportional to the number of loops. Thus, by taking only diagrams into account up to a certain maximum chiral order, one approximates the invariant amplitude in a consistent way.

If vector mesons as heavy degrees of freedom are included and appear as external particles, the power counting scheme is necessarily extended and needs to be accompanied with a suitable renormalization scheme. This complicates matters significantly, as detailed in chapter 3.

Chiral Perturbation Theory

The next step is to construct an effective Lagrangian following [53, 54]. The pion fields π^+, π^0, π^- are represented by an unimodular unitary 2×2 matrix,

$$U(x) = \exp\Big(\frac{i}{F} \sum_{a=1}^{3} \tau_a \pi_a(x)\Big), \quad \text{with} \quad \sum_{a=1}^{3} \tau_a \pi_a = \begin{pmatrix} \pi^0 & \sqrt{2}\pi^+ \\ \sqrt{2}\pi^- & -\pi^0 \end{pmatrix}, \tag{2.20}$$

where F is associated with the pion decay constant in the chiral limit. The local chiral transformation of U is implemented as a non-linear realization,

$$U(x) \to V_{\mathrm{R}} U(x) V_{\mathrm{L}}^{\dagger}\,, \tag{2.21}$$

7 This rescaling can be motivated by the Gell-Mann, Oakes, and Renner relations [52].

where $\big(V_R(x), V_L(x)\big) \in G = \mathrm{SU}(2)_R \times \mathrm{SU}(2)_L$. Note that the ground state, represented by $U = \mathbb{1}$, is only invariant if $V_R = V_L$, which corresponds to the subgroup $H \cong \mathrm{SU}(2)_V$ as desired. The covariant derivative, which transforms as U itself, is defined as

$$D_\mu U = \partial_\mu U - i r_\mu U + i U l_\mu \,, \tag{2.22}$$

where the external currents $r_\mu = v_\mu + a_\mu$ and $l_\mu = v_\mu - a_\mu$ transform consistently according to equation (2.15). Eventually, the quantity

$$\chi = 2B(s + ip) \tag{2.23}$$

represents the scalar and pseudoscalar sources transforming as U. The constant B is related to the quark condensate $\langle \bar{q}q \rangle_0 = -2F^2B$ in the chiral limit. The chiral order of the building blocks in equations (2.21) to (2.23) is given by

$$U \sim \mathcal{O}(q^0)\,, \quad D_\mu U \sim \mathcal{O}(q^1)\,, \quad \chi \sim \mathcal{O}(q^2)\,. \tag{2.24}$$

Finally, the effective Lagrangian implementing local chiral invariance, spontaneous symmetry breaking and explicit breaking by the non-vanishing quark masses up to order two reads [14]

$$\mathcal{L}_2 = \frac{F^2}{4} \mathrm{Tr}\Big[D_\mu U \big(D^\mu U\big)^\dagger \Big] + \frac{F^2}{4} \mathrm{Tr}\Big(\chi U^\dagger + U \chi^\dagger \Big)\,. \tag{2.25}$$

Other possible terms are excluded due to Hermiticity as well as parity and charge conjugation invariance. Note that the pion mass at leading order is given by $M^2 = 2B\hat{m}$, where $\hat{m} = (m_u + m_d)/2$ is the average of the current quark masses [14]. By example of equation (2.25), only even chiral orders can appear in ChPT due to Lorentz invariance, since all Lorentz indices need to be fully contracted. Furthermore, F and B are the only LECs up to order two.

2.3 INCLUSION OF VECTOR MESONS

In this section, the mere construction of a leading-order effective Lagrangian describing spin-one particles is presented, whereas the difficulties concerning power counting are addressed in chapter 3.

Heavy degrees of freedom, such as vector mesons, are also termed resonances reminding of their short lifetime. In principle, such resonances are already implicitly included in chiral perturbation theory by the numerical values of the LECs. This can be illustrated by expanding the propagator of the resonance with heavy mass M_R as

$$\frac{1}{q^2 - M_R^2} = -\frac{1}{M_R^2}\left[1 + \left(\frac{q^2}{M_R^2}\right) + \left(\frac{q^2}{M_R^2}\right)^2 + \dots\right], \tag{2.26}$$

where the Lorentz structure is omitted for simplicity. Consequently, the contributions are absorbed order by order in the corresponding LECs. In contrast, the explicit inclusion of resonances replaces the finite expansion in equation (2.26) by its exact expression, which can be advantageous. This is denoted as resummation of higher-order terms and an example concerning nucleon form factors is given in [26].

Phenomenological Lagrangians including the interaction of vector mesons have already been discussed in the late 1960's [55, 56, 57]. Furthermore, it has been known for a long time that vector mesons play an important role in low-energy hadron physics, e.g. in the successful description of the pion form factor in terms of the vector meson dominance model, see [58, 59] for a review. Their experimental properties are given in table 1.1 on page 6. Thus, the approximation that both resonances included here possess the same mass, $M_R = M_\rho \approx M_\omega$, is valid within the accuracy of this work. In the framework of a chiral effective theory, several ways of implementing vector mesons exist [60]. Here, the Lorentz vector field representation is chosen for the description of rho and omega mesons. Additionally, only external vector currents are taken into account, i.e. $a^\mu = 0$ and $r^\mu = l^\mu = v^\mu$. In this case, it is convenient to introduce the following additional building blocks:

$$\begin{aligned}
\chi_+ &= u^\dagger \chi u^\dagger + u \chi^\dagger u\,, & \Gamma_\mu &= \frac{1}{2}\Big[u^\dagger \partial_\mu u + u \partial_\mu u^\dagger - i\big(u^\dagger v_\mu u + u v_\mu u^\dagger\big)\Big]\,,\\
u_\mu &= i u^\dagger (D_\mu U) u^\dagger\,, & \Gamma_{\mu\nu} &= \partial_\mu \Gamma_\nu - \partial_\nu \Gamma_\mu + \big[\Gamma_\mu, \Gamma_\nu\big]\,,\\
F^{\mu\nu} &= \partial^\mu v^\nu - \partial^\nu v^\mu\,, & f_+^{\mu\nu} &= u F^{\mu\nu} u^\dagger + u^\dagger F^{\mu\nu} u\,,
\end{aligned} \tag{2.27}$$

where u is defined as the square root of U, $u^2 = U$. Their chiral order is given as usual by

$$\begin{aligned} \chi_+ &\sim \mathcal{O}(q^2)\,, \quad \Gamma_\mu \sim \mathcal{O}(q^1)\,, \quad u_\mu \sim \mathcal{O}(q^1)\,, \\ \Gamma_{\mu\nu} &\sim \mathcal{O}(q^2)\,, \quad F^{\mu\nu} \sim \mathcal{O}(q^2)\,, \quad f_+^{\mu\nu} \sim \mathcal{O}(q^2)\,. \end{aligned} \tag{2.28}$$

The building blocks in equation (2.27) transform with the exception of Γ_μ homogeneously, e.g.

$$u_\mu \to K u_\mu K^\dagger\,, \tag{2.29}$$

with respect to the so-called compensator

$$K(V_\mathrm{R}, V_\mathrm{L}, U) = \left(\sqrt{V_\mathrm{R} U V_\mathrm{L}}\right)^{-1} V_\mathrm{R} \sqrt{U}\,, \tag{2.30}$$

which is unitary, $K^\dagger = K^{-1}$. Note that Γ_μ transforms inhomogeneously as

$$\Gamma_\mu \to K \Gamma_\mu K^\dagger - \partial_\mu K K^\dagger \tag{2.31}$$

and thus cannot be used separately in the construction of the Lagrangian. Next, the rho mesons—combined as an isotriplet—are represented by an SU(2)-valued Lorentz vector, which leads to the building blocks

$$\begin{aligned} V^\mu &= \sum_{a=1}^{3} \frac{\tau_a}{2} V_a^\mu\,, \\ V_{\mu\nu} &= \nabla_\mu V_\nu - \nabla_\nu V_\mu \quad \text{with} \quad \nabla_\mu V_\nu = \partial_\mu V_\nu + \big[\Gamma_\mu, V_\nu\big]\,. \end{aligned} \tag{2.32}$$

These transform homogeneously according to equation (2.29). At this point, the most general Lagrangian for rho mesons with mass M_ρ relevant to the magnetic moment can be written as

$$\begin{aligned} \mathcal{L} = &-\frac{1}{2}\,\mathrm{Tr}\Big(V_{\mu\nu} V^{\mu\nu}\Big) + \Big[M_\rho^2 + c_x\,\mathrm{Tr}(\chi_+)/4\Big]\,\mathrm{Tr}\Big(V_\mu V^\mu\Big) \\ &+ 4 i g_0\,\mathrm{Tr}\Big(V_\mu V_\nu \nabla^\mu V^\nu\Big) + 2 g_1\,\mathrm{Tr}\Big(V_\mu V_\nu\Big)\,\mathrm{Tr}\Big(V^\mu V^\nu\Big) \\ &+ 2 g_2\,\mathrm{Tr}\Big(V_\mu V^\mu\Big)\,\mathrm{Tr}\Big(V_\nu V^\nu\Big) + i d_x\,\mathrm{Tr}\Big(V_{\mu\nu}\Gamma^{\mu\nu}\Big) \\ &+ f_V\,\mathrm{Tr}\Big(V_{\mu\nu} f_+^{\mu\nu}\Big) + i g_{\rho\pi}\,\mathrm{Tr}\Big(V_\mu V_\nu f_+^{\mu\nu}\Big) + \dots\,, \end{aligned} \tag{2.33}$$

where $c_x, g_0, g_1, g_2, d_x, f_V, g_{\rho\pi}$ are unknown LECs. Here, the relevant linear terms in V_μ have been taken from [61]. Furthermore, terms with LECs having higher negative mass dimensions have been assumed to

be suppressed by the intrinsic scale Λ. Regarding interactions of vector fields only, the Lagrangian is equivalent to the hidden-gauge formalism [59]. However, it is still an open question how to construct a consistent Lagrangian with interactions among pions and more than one vector field. In this sense, the term proportional to $g_{\rho\pi}$ should be regarded as a first attempt to address this issue.

In [62], it was shown that starting from the most general Lagrangian for three massive vector particles one is led to a locally SU(2) invariant theory with an additional mass term by requiring global U(1) invariance, self-consistency, and renormalizability . This simplifies the Lagrangian in equation (2.33) with respect to the LECs g_0, g_1, g_2 and they can be re-expressed by a single LEC g. Additionally, employing a field redefinition

$$V_\mu = \rho_\mu - \frac{i}{g}\Gamma_\mu \tag{2.34}$$

and using the KSRF relation [63, 64]

$$M_\rho^2 = 2g^2F^2\,, \tag{2.35}$$

rho meson fields are transformed into the so-called Weinberg parametrization [57], which yields the Lagrangian in a form where renormalizability has been shown [30]. Note that the fields ρ^μ transform inhomogeneously with respect to the compensator. Eventually, taking the isosinglet omega meson ω_μ with mass M_ω into account,[8] the Lagrangian reads

$$\begin{aligned}\mathcal{L} = &-\frac{1}{2}\operatorname{Tr}\big(\rho_{\mu\nu}\rho^{\mu\nu}\big) + id_x\operatorname{Tr}\big(\rho_{\mu\nu}\Gamma^{\mu\nu}\big) + f_V\operatorname{Tr}\big(\rho_{\mu\nu}f_+^{\mu\nu}\big)\\ &+\frac{M_\rho^2 + c_x\operatorname{Tr}(\chi_+)/4}{g^2}\operatorname{Tr}\Big[\big(g\rho_\mu - i\Gamma_\mu\big)\big(g\rho^\mu - i\Gamma^\mu\big)\Big]\\ &+i\frac{g_{\rho\pi}}{g^2}\operatorname{Tr}\Big[\big(g\rho_\mu - i\Gamma_\mu\big)\big(g\rho_\nu - i\Gamma_\nu\big)f_+^{\mu\nu}\Big]\\ &-\frac{1}{4}\omega_{\mu\nu}\omega^{\mu\nu} + \frac{M_\omega^2}{2}\omega_\mu\omega^\mu + \frac{F}{2}g_{\omega\rho\pi}\epsilon_{\mu\nu\alpha\beta}\omega^\nu\operatorname{Tr}\big(\rho^{\alpha\beta}u^\mu\big)\,,\end{aligned} \tag{2.36}$$

where

$$\begin{aligned}\rho^\mu &= \sum_{a=1}^{3}\frac{\tau_a}{2}\rho_a^\mu\,,\\ \rho_{\mu\nu} &= \partial_\mu\rho_\nu - \partial_\nu\rho_\mu - ig\,[\rho_\mu,\rho_\nu]\,,\\ \omega_{\mu\nu} &= \partial_\mu\omega_\nu - \partial_\nu\omega_\mu\,.\end{aligned} \tag{2.37}$$

8 This interaction term can be found in [29]. However, there is a factor F missing in the Lagrangian $\mathcal{L}_{\omega\rho\pi}$ in order to define the LEC $g_{\omega\rho\pi}$ with mass unit eV^{-1}.

3 POWER COUNTING AND REGULARIZATION

3.1 POWER COUNTING WITH VECTOR MESONS

Implementing a consistent power counting scheme including the vector mesons as heavy degrees of freedom is a non-trivial task. They introduce a mass scale $M_\rho \approx M_\omega$, which is much larger than the pion mass M or typical energies of processes described by ChPT. Furthermore, the vector mesons as unstable particles should be implemented with a complex mass, i.e. $M_\rho^2 = (M_\chi - i\Gamma_\chi/2)^2$, where M_χ and Γ_χ denote the pole mass and width of the vector meson in the chiral limit, respectively. The implementation of unstable particles in a renormalizable quantum field theory was firstly discussed in [65]. There, it was shown that the S-matrix connecting stable particles only is unitary and causal. In perturbative calculations, one method of dealing with unstable particles is termed complex-mass renormalization scheme [66] and it has been applied in chiral effective field theories [29]. Recently, the perturbative unitarity of the S-matrix in the complex-mass scheme has been shown at the one-loop level [67].

Weinberg's power counting relies on the fact that only light degrees of freedom appear in loops and therefore the momentum integration undergoes a soft cut-off [15]. This assumption does not hold anymore if the theory contains vector mesons since then „hard" poles at large momenta contribute significantly. Hence, loop diagrams with a previously assigned order give contributions which have a lower order than expected. Fortunately, it turns out that these contributions are analytic in $M^2 = 2B\hat{m}$, i.e. in the quark mass expansion, as well as in the external momenta [68]. Therefore, the so-called power-counting-violating terms can be absorbed by the redefinition of the bare parameters of the Lagrangian, e.g.

$$g_0 = g_\mathrm{R} + \delta g = \underbrace{g_\mathrm{R} + \xi}_{=\tilde{g}_\mathrm{R}} + \underbrace{\delta g - \xi}_{=\delta\tilde{g}} \,. \tag{3.1}$$

Here, the bare g_0 stays real whereas the renormalized part g_R as well as the counter-term part δg can be complex. Furthermore, the splitting in equation (3.1) is not unique with respect to finite terms ξ as indicated

and thus the splitting *depends* on the used renormalization scheme. In conclusion, using an appropriate renormalization scheme enables us to restore a consistent power counting including heavy degrees of freedom.

The extended power counting rules, which allow for assigning a chiral order to each diagram, read as follows. First, the list of small quantities, collectively denoted as q, needs to be extended by the expression $K^2 - M_R^2 = \mathcal{O}(q^1)$ if K is a large momentum since the resonance is regarded as nearly on-shell, $K^2 \approx M_R^2$. Next, it is necessary to investigate every possible flux of the external momenta through each diagram. For each given flux the order of vertices and propagators are determined and summed up as detailed below. Finally, the lowest order resulting from the various flux assignments is defined to be the chiral order of the diagram. The order of the vertices can be read off the corresponding Feynman rules taking into account the previously assigned flux of large external momentum. Additionally, one considers that the pion mass counts as $\mathcal{O}(q^1)$, that the vector meson masses count as $\mathcal{O}(q^0)$, and that each loop integration counts as $\mathcal{O}(q^4)$, as usual. The order of the propagators for small and large momenta can be read off the following table:

Momentum	π	ρ or ω
Small	$\mathcal{O}(q^{-2})$	$\mathcal{O}(q^0)$
Large	$\mathcal{O}(q^0)$	$\mathcal{O}(q^{-1})$

Table 3.1

This can be motivated by the following approximative considerations of the typical pole structure of a propagator:

$$\begin{aligned}
&\frac{1}{k^2 - M^2} \approx \frac{1}{M^2} = \mathcal{O}(q^{-2})\,, \\
&\frac{1}{K^2 - M^2} \approx \frac{1}{K^2} = \mathcal{O}(q^0)\,, \\
&\frac{1}{k^2 - M_\rho^2} \approx \frac{1}{M_\rho^2} = \mathcal{O}(q^0)\,, \\
&\frac{1}{K^2 - M_\rho^2} = \mathcal{O}(q^{-1}) \quad \text{(see text above)}\,,
\end{aligned} \tag{3.2}$$

where k represents a small momentum and K a momentum with at least one large component, say the zeroth, corresponding to the large mass of a rho meson.

3.2 REFORMULATED INFRARED REGULARIZATION

This section illustrates the calculation of the analytic subtraction terms following [18]. They are necessary to renormalize the one-loop integrals such that they satisfy the power counting. As an example, the following one-loop scalar integral is considered,

$$H = i \int \frac{d^n k}{(2\pi)^n} \frac{1}{\left[(k-p)^2 - m^2 + i0^+\right]\left[k^2 - M^2 + i0^+\right]}, \tag{3.3}$$

where m denotes the large mass of the resonance, M the small pion mass and n the number of space-time dimensions. For example, this integral appears in the calculation of the two-point function of the rho meson with external momentum p. Here and henceforth, the method of dimensional regularization, whose key feature is preserving the Ward identities, is employed [69, 70]. Using the standard Feynman parametrization formula [71]

$$\frac{1}{ab} = \int_0^1 \frac{dz}{\left[az + b(1-z)\right]^2}, \tag{3.4}$$

with $a = (k-p)^2 - m^2 + i0^+$ and $b = k^2 - M^2 + i0^+$, interchanging the order of integrations and carrying out the integration over $d^n k$, the integral in equation (3.3) reads

$$H = -\frac{1}{(4\pi)^{n/2}} \Gamma(2 - n/2) \int_0^1 dz \left[A(z)\right]^{n/2-2}, \tag{3.5}$$

where

$$A(z) = -p^2(1-z)z + m^2 z + M^2(1-z) - i0^+ \tag{3.6}$$

and $\Gamma(z)$ is the well-known Gamma function. According to the infrared (IR) regularization scheme of Becher and Leutwyler [17], the integral $H = I + R$ is divided into the IR singular part I and the regular part R defined as

$$I = -\frac{1}{(4\pi)^{n/2}} \Gamma(2 - n/2) \int_0^\infty dz \left[A(z)\right]^{n/2-2}, \tag{3.7}$$

$$R = \frac{1}{(4\pi)^{n/2}} \Gamma(2 - n/2) \int_1^\infty dz \left[A(z)\right]^{n/2-2}. \tag{3.8}$$

It can be shown that the IR singular part I obeys power counting and that the IR regular part R is analytic in the square of the pion mass and

external momenta. Therefore, one can simply replace the integral H by its IR-regularized part

$$H^{\mathrm{IR}} = H - R = I\,, \tag{3.9}$$

considering that the part R can be compensated by redefined parameters of the most general Lagrangian. Note that the splitting might introduce additional divergences in I and R which cancel in the sum $I + R$. In general, infinities are neglected according to the so-called $\widetilde{\mathrm{MS}}$ renormalization scheme, i.e. terms proportional to the infinite quantity

$$\lambda = \frac{1}{16\pi^2}\left\{\frac{1}{n-4} - \frac{1}{2}\Big[\ln(4\pi) + \Gamma'(1) + 1\Big]\right\} \tag{3.10}$$

are set to zero, arguing that they also can be absorbed in counter-terms of the most general Lagrangian. The part R in equation (3.9) is also denoted subtraction term since the regularized integral is obtained by subtracting R from the original integral. Furthermore, the regular part R satisfies the Ward identities separately from I and, hence, the IR regularization preserves the symmetries of the theory.

In the original approach of Becher and Leutwyler [17], the crucial step is to calculate the singular part I directly in order to obtain the regularized integral, see also [68]. This turns out to be difficult in generalized situations. However, the subtraction terms can also be obtained order by order by expanding the integrand in equation (3.5) directly in small Lorentz-invariant quantities, say M^2 and $p^2 - m^2$, and interchanging the series and the integration. It has been shown that this procedure is equivalent to the original approach order by order, see [18] for details. In the following, this approach is termed reformulated IR regularization.

In practical calculations, the reformulated procedure provides an easier method of finding the renormalized version of the results. This concerns the integration as well as the identification of R, e.g. in two-loop calculations. After a standard Passarino-Veltman reduction [72, 73] in n space-time dimensions, the scalar integrals containing only pion masses and small momenta, such as the external photon momentum, are kept, whereas integrals containing only large masses and external momenta are discarded. This implies that diagrams with loops containing only heavy degrees of freedom can be discarded directly. Next, integrals which contain both scales are calculated in n dimensions as explained above up to a sufficient order in the small invariant quantities. Finally, the subtraction terms are obtained by the expansion around $n = 4$, neglecting divergences according to $\widetilde{\mathrm{MS}}$ scheme. Note that even after

expressing the integrals in Feynman parametrization and expanding the integrand, the analytic integration and subsequent expansion around $n = 4$ might turn out to be a formidable problem. Additionally, due to the Passarino-Veltman reduction, small quantities might appear in the denominator as so-called Gram determinants, which necessitates the calculation of subtraction terms with a higher order than the desired accuracy of the results. These subtleties are detailed in chapter 7 by means of an explicit example.

4 CLASSICAL CONSTRAINT ANALYSIS

4.1 PRELIMINARY REMARKS

The inclusion of massive particles with non-zero integer spin in an effective quantum field theory necessitates non-trivial considerations even on a classical level. Naturally, one prefers to use objects with a well-defined behavior under Lorentz transformations in order to construct Lorentz-invariant Lagrangian densities $\mathcal{L}$. For example, a four-vector V_μ, which is used to describe a spin-one particle, transforms under a Lorentz transformation Λ as

$$V_\mu \to V'_\mu = \Lambda_\mu{}^\nu V_\nu \,. \tag{4.1}$$

Consequently, the building block $V_\mu V^\mu$ is convenient for the construction of $\mathcal{L}$ since it is invariant under Λ, i.e.

$$V_\mu V^\mu \to V'_\mu V'^\mu \,. \tag{4.2}$$

However, a four-vector field V^μ has four degrees of freedom or an antisymmetric tensor field $W^{\mu\nu}$ has six degrees of freedom, but a spin-one particle[1] has only $2 \times 1 + 1 = 3$. Hence, one inevitably introduces more degrees of freedom than are physically realized. In canonical quantization, this leads to the appearance of so-called primary constraints in deriving the Hamiltonian density, i.e. equations of the form[2]

$$\phi_1(V, \Pi) \approx 0 \,, \tag{4.3}$$

from which some of the velocities $\dot{V}$ are not solvable. Here, V denotes the fields—neglecting the Lorentz structure—and $\Pi = \partial\mathcal{L}/\partial\dot{V}$ denotes the corresponding canonically conjugated momenta. In equation (4.3), the condition holds only after the evaluation of Poisson brackets. This is termed a weak equation in Dirac's sense [74]. There is a crucial difference between particles with and without mass. The former is the case discussed here and thus the constraints in equation (4.3) belong to a

1 The irreducible $2S+1$ dimensional representations of SU(2) are interpreted as particles with spin S.

2 Note that the Lorentz structure and internal indices are suppressed and therefore ϕ_1 can represent several non-equivalent expressions.

system of so-called second-class constraints. For the latter, so-called first-class constraints appear, which requires the introduction of additional constraints, i.e. gauge fixing terms. A well-known example for the massless case is Maxwell's theory for classical electrodynamics. In [75], a thorough review of these issues is available.

Next, the non-solvable velocities are simply regarded as unknown phase space functions $z(V, \Pi)$ and the Hamiltonian density is obtained by Legendre transformation,

$$\mathcal{H}_1 = \phi_1 z + \mathcal{H}\,, \tag{4.4}$$

where $\mathcal{H}$ depends on the particular form of $\mathcal{L}$. The unknown functions z, which can also be interpreted as generalized Lagrangian multipliers, can eventually be determined by the *physical* requirement that the constraints are conserved in time, i.e. the Poisson bracket of the Hamiltonian with the constraint must vanish,

$$\{H_1, \phi_1\} = \{\phi_1, \phi_1\}\, z + \{H, \phi_1\} \approx 0\,, \tag{4.5}$$

where $H_{(1)} = \int d^3x \mathcal{H}_{(1)}$. In general, the parameters a of the Lagrangian specify the properties of the „matrix" $\{\phi_1, \phi_1\}$. Thus, the parameters determine if the unknown functions z, interpreted as a „vector", can be solved from the „linear system of equations" in (4.5). In this manner, one should keep in mind how many constraints are physically meaningful, i.e. the number of constraints plus the number of physical degrees of freedom must equal the number of degrees of freedom[3] in the Hamiltonian $\mathcal{H}$, in short

$$\big(\#\text{DoF in } \mathcal{H}\big) - \big(\#\text{Constraints}\big) = \big(\#\text{DoF of particles}\big)\,. \tag{4.6}$$

This reasoning can lead to different options for conditions among the parameters a and further second-class constraints $\phi_2, \phi_3, \ldots$ can appear. Of course, they themselves must fulfill the physical requirement of conservation in time, which might in turn lead to more conditions for the parameters a. This procedure is illustrated as a cycle of the flowchart in figure 4.1. There, the term „depends on a" exactly refers to the case if the unknown functions z can only be solved for a certain choice of a. Additionally, an example is provided in section 4.2, which also prepares the concepts for the antisymmetric tensor model describing massive vector particles in chapter 6. In summary, the crucial result of a constraint analysis is to impose conditions on the parameters a and thus to restrict the variety of effective field theories to self-consistent ones.

3 That equals the number of fields plus the number of canonically conjugated momenta in the Hamiltonian formalism.

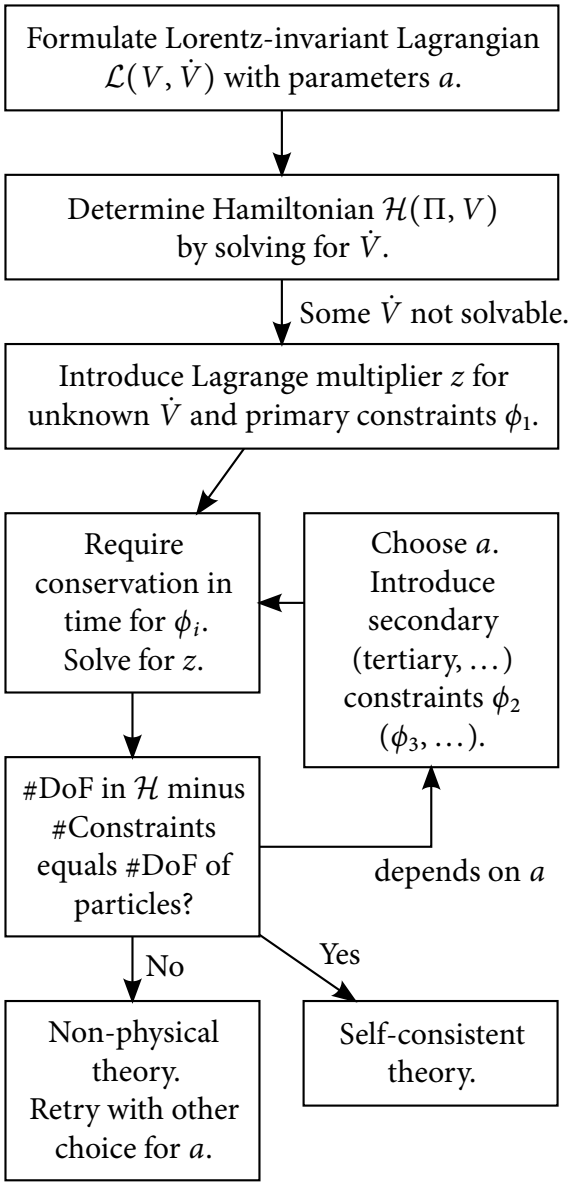

Figure 4.1: Constraint analysis as a flowchart. The number of degrees of freedom is abbreviated with #DoF. The physical requirement that the constraints are conserved in time is crucial for the resulting conditions on the parameters a. The case that no primary constraints appear is trivial. Note that one can obtain a non-physical theory even though $\mathcal{L}$ is the most general Lagrangian. Refer to section 4.1 for further explanation, especially for the option „depends on a“.

4.2 CONSTRAINT ANALYSIS OF THE FREE ANTISYMMETRIC TENSOR MODEL

As an example for the previous remarks, the Lagrangian density

$$\mathcal{L} = a\,\partial^\mu W_{\mu\nu}\partial_\rho W^{\rho\nu} + b\,\partial^\rho W_{\mu\nu}\partial_\rho W^{\mu\nu} + c\,W_{\mu\nu}W^{\mu\nu} \tag{4.7}$$

of an antisymmetric tensor field $W_{\mu\nu} = -W_{\nu\mu}$ is considered, analogous to [76, app. A]. In the Hamiltonian formalism the particle is described by six pairs of canonically conjugated variables $(W_{\mu\nu}, \Pi_{\mu\nu})$, hence twelve degrees of freedom, which must be reduced to the six physical degrees of freedom of a spin-one particle by six independent constraints. This requirement leads to conditions for the parameters a, b, c.

Henceforth, a non-covariant formulation is employed for practical reasons. This means explicitly that the Lagrangian is expressed in the six fields

$$W_{01},\ W_{02},\ W_{03},\ W_{12},\ W_{13},\ W_{23} \tag{4.8}$$

by exploiting the antisymmetry $W_{\mu\nu} = -W_{\nu\mu}$. This choice can be made without loss of generality and leads to

$$\begin{aligned}
\mathcal{L} = \quad & a\Big[\dot W_{00}\dot W_{00} - \dot W_{0j}\dot W_{0j} - 2\big(\partial_i W_{i0}\dot W_{00} - \partial_i W_{ij}\dot W_{0j}\big) \\
& \quad + \partial_i W_{0i}\partial_j W_{0j} - \partial_i W_{ik}\partial_j W_{jk}\Big] \\
& + b\Big[\dot W_{00}\dot W_{00} - \partial_k W_{00}\partial_k W_{00} - \dot W_{i0}\dot W_{i0} + \partial_k W_{i0}\partial_k W_{i0} \\
& \quad - \dot W_{0j}\dot W_{0j} + \partial_k W_{0j}\partial_k W_{0j} + \dot W_{ij}\dot W_{ij} - \partial_k W_{ij}\partial_k W_{ij}\Big] \\
& + c\Big[W_{00}W_{00} - W_{i0}W_{i0} - W_{0j}W_{0j} + W_{ij}W_{ij}\Big] \\
= \quad & a\Big[-\dot W_{0j}\dot W_{0j} + 2\big(\partial_i W_{ij}\dot W_{0j} - \partial_j W_{ij}\dot W_{0i}\big) + \partial_i W_{0i}\partial_j W_{0j} \\
& \quad - \partial_i W_{ik}\partial_j W_{jk} + \partial_i W_{ki}\partial_j W_{jk} + \partial_i W_{ik}\partial_j W_{kj} - \partial_i W_{ki}\partial_j W_{kj}\Big] \\
& + 2b\Big[-\dot W_{0j}\dot W_{0j} + \partial_k W_{0j}\partial_k W_{0j} + \dot W_{ij}\dot W_{ij} - \partial_k W_{ij}\partial_k W_{ij}\Big] \\
& + 2c\Big[-W_{0j}W_{0j} + W_{ij}W_{ij}\Big],
\end{aligned} \tag{4.9}$$

where Latin indices i, j, k range from 1 to 3. In the last step, the convention was introduced that a factor W_{ij} (including $\dot W_{ij}$) restricts any

implicit sum involving i or j to $i < j$. This convention will be kept from now on. As a result, the six canonically conjugated momenta read

$$\Pi_{0j} = \frac{\partial \mathcal{L}}{\partial \dot{W}_{0j}} = -2(a+2b)\dot{W}_{0j} + 2a\big(\partial_i W_{ij} - \partial_i W_{ji}\big)\,, \tag{4.10a}$$

$$\Pi_{ij} = \frac{\partial \mathcal{L}}{\partial \dot{W}_{ij}} = 4b\dot{W}_{ij}\,, \quad i<j\,. \tag{4.10b}$$

Next, four cases of parameter choices need to be distinguished, of which two are easily seen to be physically meaningless. These read:

$b = 0,\ a = -2b = 0$: This corresponds to a Lagrangian without a kinetic term. All momenta vanish.

$b \neq 0,\ a \neq -2b$: Here all velocities are solvable from equations (4.10a) and (4.10b) and no constraints reduce the twelve degrees of freedom. Hence, not only a spin-one particle is described, which is not desired here.

In the following sections both the remaining, physically meaningful cases are discussed.

The Case $b = 0,\ a \neq -2b = 0$

From equation (4.10b) one obtains on the one hand, due to $i < j$, three primary constraints

$$\phi^1_{ij} = \Pi_{ij} \approx 0\,, \tag{4.11}$$

and from equation (4.10a) on the other hand three solvable velocities

$$\dot{W}_{0j} = -\frac{1}{2a}\Pi_{0j} + \partial_i W_{ij} - \partial_i W_{ji}\,. \tag{4.12}$$

The Hamiltonian density is found by a Legendre transformation to be

$$\begin{aligned}\mathcal{H}_1 &= \Pi_{0j}\dot{W}_{0j} + \Pi_{ij}\dot{W}_{ij} - \mathcal{L}\\ &= \phi^1_{ij} z_{ij} - \frac{1}{4a}\Pi_{0j}\Pi_{0j} - a\partial_i W_{0i}\partial_j W_{0j}\\ &\quad + 2c\big(W_{0j}W_{0j} - W_{ij}W_{ij}\big)\,,\end{aligned} \tag{4.13}$$

where the solvable velocities have been replaced and unknown functions $z_{ij} \equiv \dot{W}_{ij}$ have been introduced.

Next, these unknown functions should be determined iteratively by the physical requirement that the Poisson bracket of the constraints and the Hamiltonian function $H_1 = \int d^3x \mathcal{H}_1$ vanishes, i.e. that the constraints are conserved in time. This leads to

$$\begin{aligned}\{\phi^1_{lm}(t,\vec{y}), H_1(t)\} = 4c\, W_{lm}(t,\vec{y}) \\ + \partial^y_l \Pi_{0m}(t,\vec{y}) - \partial^y_m \Pi_{0l}(t,\vec{y}) \approx 0\,,\end{aligned} \tag{4.14}$$

where the canonical equal-time commutation relations

$$\{W_{ij}(t,\vec{y}), \Pi_{lm}(t,\vec{x})\} = \delta_{il}\delta_{jm}\delta^{(3)}(\vec{y}-\vec{x})\,, \tag{4.15a}$$

$$\{W_{0j}(t,\vec{y}), \Pi_{0m}(t,\vec{x})\} = \delta_{jm}\delta^{(3)}(\vec{y}-\vec{x})\,, \tag{4.15b}$$

have been used. As usual, all other Poisson brackets of the fields and momenta vanish. Furthermore, Poisson brackets containing the unknown functions $\{\ldots, z_{ij}\}$ can be ignored since these are always factors of a „weakly" vanishing constraint.

From equation (4.14) three secondary constraints result, namely

$$\phi^2_{lm} = 4c\, W_{lm} + \partial_l \Pi_{0m} - \partial_m \Pi_{0l} \approx 0\,, \tag{4.16}$$

where the arguments of the functions are discarded here and henceforth for clarity. Imposing conservation in time again yields

$$\{\phi^2_{lm}, H_1\} = 4c\Big[z_{lm} - \big(\partial_l W_{0m} - \partial_m W_{0l}\big)\Big] \approx 0\,, \tag{4.17}$$

so that the unknown functions can be determined to $z_{lm} = \partial_l W_{0m} - \partial_m W_{0l}$ if $c \neq 0$. In the end, a self-consistent theory with 6 constraints and $12 - 6 = 6$ physical degrees of freedom is found as desired.

The Case $b \neq 0$, $a = -2b$

This case is analogously calculated to the one before, however, it is slightly more complicated. Here, equation (4.10a) yields the three constraints

$$\phi^1_{0j} = \Pi_{0j} + 4b\big(\partial_i W_{ij} - \partial_i W_{ji}\big) \approx 0\,, \tag{4.18}$$

as well as equation (4.10b), which yields the three solvable velocities

$$\dot{W}_{ij} = \frac{1}{4b}\Pi_{ij}\,. \tag{4.19}$$

The Hamiltonian density reads via Legendre transformation

$$\begin{aligned}\mathcal{H}_1 &= \Pi_{0j}\dot{W}_{0j} + \Pi_{ij}\dot{W}_{ij} - \mathcal{L} \\ &= \phi^1_{0j} z_{0j} + \frac{1}{8a}\Pi_{ij}\Pi_{ij} + 2c\Big(W_{0j}W_{0j} - W_{ij}W_{ij}\Big) \\ &\quad + 2b\Big(\partial_i W_{0i}\partial_j W_{0j} - \partial_k W_{0j}\partial_k W_{0j} + \partial_k W_{ij}\partial_k W_{ij} \\ &\qquad - \partial_i W_{ik}\partial_j W_{jk} + \partial_i W_{ki}\partial_j W_{jk} + \partial_i W_{ik}\partial_j W_{kj} \\ &\qquad - \partial_i W_{ki}\partial_j W_{kj}\Big)\,,\end{aligned} \tag{4.20}$$

where again three to be determined functions were introduced and the constraints in equation (4.18) were identified.

The following Poisson brackets are calculated as usual, except for the fact that an integration by parts is carried out with respect to the integral of the Hamiltonian function $H_1 = \int d^3x \mathcal{H}_1$ if necessary. From the conservation in time one obtains

$$\begin{aligned}\{\phi^1_{0l}, H_1\} &= 4b\partial_l\partial_i W_{0i} - 4b\partial_k\partial_k W_{0l} + 4c W_{0l} + \partial_n \Pi_{nl} - \partial_n \Pi_{ln} \\ &\equiv \phi^2_{0l} \approx 0\,.\end{aligned} \tag{4.21}$$

At this point the convention in use shall be stressed again, e.g. it holds for $l = 1$ that $\sum_{n<1} \partial_n \Pi_{n1} = 0$ in equation (4.21). Furthermore, one cannot solve for the unknown functions and thus equation (4.21) represents three more secondary constraints, as indicated in the second line of equation (4.21).

In order to calculate the conservation in time of ϕ^2_{0l}, the intermediate result

$$\begin{aligned}\{\Pi_{nl}, H_1\} = 4c W_{nl} - 4b\Big(&\partial_n\partial_i W_{il} - \partial_n\partial_i W_{li} \\ &- \partial_l\partial_i W_{in} + \partial_l\partial_i W_{ni} - \partial_k\partial_k W_{nl}\Big)\end{aligned} \tag{4.22}$$

is useful, which finally leads to

$$\begin{aligned}\{\phi^2_{0l}, H_1\} = {}& 4b\partial_l\partial_i z_{0i} - 4b\partial_k\partial_k z_{0l} + 4c z_{0l} \\ &- 4c\Big(\partial_n W_{ln} - \partial_n W_{nl}\Big) + 4b\partial_n\partial_n\Big(\partial_i W_{li} - \partial_i W_{il}\Big)\,.\end{aligned} \tag{4.23}$$

This differential equation (4.23) is solved by $z_{0l} = \partial_n W_{ln} - \partial_n W_{nl}$, since $\partial_i z_{0i} = 0$ holds in this choice. Moreover, the condition $c \neq 0$ is necessary to ensure invertibility of the differential operator in equation (4.23).

As in the previous case, one is led eventually to a self-consistent theory with the correct number of degrees of freedom. In both the self-consistent cases, the remaining non-vanishing parameter associated

with a or b can be eliminated by an appropriate normalization of the Lagrangian to obey the canonical commutation relations. Consequently, it can be shown that the parameter $c \neq 0$ is connected to the mass of the free particle. Thus, it is crucial that a *massive* free particle has been considered.

Part II

APPLICATIONS AND CALCULATIONS

5 SU(3)-INVARIANT GENERAL LAGRANGIAN

In this chapter, a short excursion to the SU(3) sector is undertaken. Mostly, the calculations have been carried out to implement the necessary algorithms on a computer while still having a cross-check with the very similar calculations in [62]. Here, an effective Lagrangian density for eight vector particles with same mass M including only interactions with dimensionless coupling constants g and h is considered, namely

$$\mathcal{L}_A = \mathcal{L}_2 + \mathcal{L}_3 + \mathcal{L}_4 \,, \tag{5.1}$$

where

$$\mathcal{L}_2 = -\frac{1}{4} V^a_{\mu\nu} V^{a\mu\nu} + \frac{M^2}{2} V^a_\mu V^{a\mu} \,, \tag{5.2a}$$

$$\mathcal{L}_3 = -g^{abc} V^a_\mu V^b_\nu \partial^\mu V^{c\nu} \,, \tag{5.2b}$$

$$\mathcal{L}_4 = -h^{abcd} V^a_\mu V^b_\nu V^{c\mu} V^{d\nu} \,, \tag{5.2c}$$

with the usual notation $V^a_{\mu\nu} = \partial_\mu V^a_\nu - \partial_\nu V^a_\mu$. All Latin indices of the beginning of the alphabet range from 1 to 8. The aim of the following is the derivation of a consistent theory with a *global* SU(3) invariance assumed a priori. This theory could describe the vector mesons in figure 5.1 on the next page, however, the global SU(3) invariance is broken due to the larger mass of the strange quark in comparison with the masses of the up- and down-quarks. The physical fields with well-defined quantum numbers in figure 5.1 are related to the Cartesian fields[1] as usual [76],

$$\frac{1}{\sqrt{2}} \sum_{a=1}^{8} \lambda^a V^a = \begin{pmatrix} \rho^0/\sqrt{2} + \omega_8/\sqrt{6} & \rho^+ & K^{\star +} \\ \rho^- & -\rho^0/\sqrt{2} + \omega_8/\sqrt{6} & K^{\star 0} \\ K^{\star -} & \overline{K^{\star 0}} & -2\omega_8/\sqrt{6} \end{pmatrix} . \tag{5.3}$$

Under a global infinitesimal SU(3) transformation the Cartesian fields behave as

$$V^a_\mu \to V^a_\mu + \epsilon^b f^{bca} V^c_\mu \,. \tag{5.4}$$

1 See also section A.1 on page 95 for the notation used.

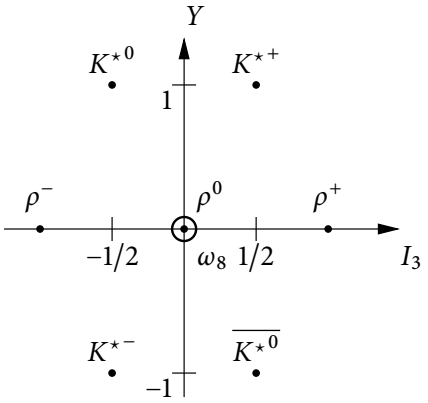

Figure 5.1: The vector meson octet as physical fields in a diagram of isospin three-component I_3 versus hypercharge $Y = B + S$. The variable S denotes the strangeness and the baryon number B vanishes for mesons.

Inserting equation (5.4) in equation (5.2b), thereby obtaining $\mathcal{L}_3'$, and demanding $\delta\mathcal{L}_3 = \mathcal{L}_3' - \mathcal{L}_3 = 0 + \mathcal{O}(\epsilon_a^2)$, one finds constraints for the coupling constants g^{abc}. These constraints can be used to parametrize $\mathcal{L}_3$ with only two independent coupling constants γ_1 and γ_2,

$$g^{abc} = \gamma_1 f^{abc} + \gamma_2 d^{abc} \,. \tag{5.5}$$

The explicit form of equation (5.5) is derived by contracting the SU(3)-invariant trace $\mathrm{Tr}(V_\alpha V_\beta \partial_\gamma V_\delta)$ of matrices $V_\mu \equiv V_\mu^a \lambda^a$ with Lorentz-invariant tensors of suitable rank.[2] An analogous consideration for $\mathcal{L}_4$ leads to three independent coupling constants η_1, η_2, and η_3 with

$$h^{abcd} = \eta_1 \delta^{ac}\delta^{bd} + \eta_2 \delta^{ab}\delta^{cd} + \eta_3 f^{abe} f^{cde} \,, \tag{5.6}$$

where other possible terms are equivalent due to the permutation symmetry of the Lorentz structure in equation (5.2c).

The constraint analysis is carried out identically to [62, sec. III], since the parameter range of the indices a, b, c, d is irrelevant there. In this manner, the canonically conjugated momenta read

$$\pi_0^a = \frac{\partial \mathcal{L}}{\partial \dot{V}_0^a} = -g^{bca} V_0^b V_0^c \,, \tag{5.7}$$

$$\pi_i^a = \frac{\partial \mathcal{L}}{\partial \dot{V}_i^a} = V_{0i}^a + g^{bca} V_0^b V_i^c \,, \tag{5.8}$$

2 Under the additional assumption that the resulting scalars should be even under parity.

and the three primary constraints are obtained as

$$\phi_1^a = \pi_0^a + g^{bca} V_0^b V_0^c \approx 0\,. \tag{5.9}$$

The Hamiltonian density $\mathcal{H}_1$ is constructed as in equation (4.4) on page 28 and conservation in time yields a linear system of equations

$$\{\phi_1^a, H_1\} = A^{ab} z^b + \chi^a \approx 0\,, \tag{5.10}$$

where χ^a are eight z-independent phase space functions and the crucial 8×8 matrix is given by

$$A^{ab} = \left(g^{bca} + g^{cba} - g^{acb} - g^{cab}\right) V_0^c\,. \tag{5.11}$$

Furthermore, to obtain the correct number of constraints, equation (5.10) must not be solvable for z. This reasoning leads to three secondary constraints

$$\phi_2^a = \chi^a \approx 0\,, \tag{5.12}$$

which are also required to be conserved in time, i.e.

$$\{\phi_2^a, H_1\} = \mathcal{M}^{ab} z^b + Y^a \approx 0\,. \tag{5.13}$$

Here, the crucial 8×8 matrix in equation (5.13) is given by

$$\begin{aligned} \mathcal{M}^{ab} = {} & M^2 \delta^{ab} - \left(g^{bca} + g^{cba}\right) \partial_i V_i^c \\ & - \left(g^{ace} g^{bde} - 4 h^{acbd}\right) V_i^c V_i^d \\ & - \left(h^{abcd} + h^{acbd} + h^{adcb}\right) V_0^c V_0^d \end{aligned} \tag{5.14}$$

and Y^a are some irrelevant functions. At this point it shall be emphasized that [62] gives a shortened form of equation (5.14). There, the relation only holds if the coupling constants obey the permutation conditions

$$\begin{aligned} h^{abcd} &= h^{bcda} = h^{cdab} = h^{dabc} \\ &= h^{cbad} = h^{adcb} = h^{dcba} = h^{badc}\,, \end{aligned} \tag{5.15}$$

which, in particular, are *not* satisfied by the parameter choice in equation (5.6) and by the Yang-Mills parametrization

$$\begin{aligned} g^{abc} &= g f^{abc}\,, \\ h^{abcd} &= \frac{1}{4} g^{abe} g^{cde}\,. \end{aligned} \tag{5.16}$$

No.	Fields	Factor in det $\mathcal{M}$	Inequality
1	$\partial_i V_i^3 = x$	$3M^4 - 4y_2^2x^2$	$y_2^2 \leq 0$
2	$V_0^1 = x,$	$M^2 + 4(\eta_1 + \eta_2)x^2$	$\eta_1 + \eta_2 \geq 0$
	$V_i^1 \equiv y$	$-12(\eta_1 + \eta_2)y^2$	$\eta_1 + \eta_2 \leq 0$

Table 5.1: Determinant of $\mathcal{M}$ in detail. For a given choice of fields all other fields are set to zero. Here, only the relevant factors of the determinant are displayed. Each step *depends* on the previous ones.

For example, consider the case $a = b = 1$ and $c = d = 2$ in equation (5.15), i.e. $h^{1122} = h^{1221}$, whereas in equation (5.16) $h^{1122} = 0$ but $h^{1221} = -g^2/4$ holds. This appears also in section 6.2 for the four-field interaction. It boils down to the fact that one is allowed to use the permutation symmetry as in equation (5.15) only *after* implementing the a priori assumed symmetry, e.g. global SU(3) or U(1).

In order to obtain a consistent theory, the parameters need to be chosen such that the determinant of A vanishes and the determinant of $\mathcal{M}$ is not equal to zero. Owing to the symmetry properties of f^{abc} and d^{abc}, it is easy to see that $A^{ab} \equiv 0$ and hence $\det A = 0$ is obviously satisfied. The analysis of $\det \mathcal{M}^{ab} \neq 0$ is carried out using that $\det \mathcal{M}$ must not vanish for all fields. This is detailed in table 5.1 and one obtains

$$\eta_1 = -\eta_2 \quad \text{and} \quad y_2 = 0\,, \tag{5.17}$$

besides several insignificant inequalities.

In order to carry out the renormalizability analysis, a general vector particle model has been implemented in FeynArts, see also section B.1. In this manner, the above derived relations for the coupling constants are employed in completely arbitrary three- and four-particle Feynman rules resulting from equations (5.2b) and (5.2c). Since $h^{1111} = 0$ holds, the infinite parts of the one-loop contribution to the four-vertex function of $V^1V^1V^1V^1$ must necessarily vanish. The relevant one-loop Feynman diagrams are topologically the same as in figure 6.2 of the next chapter. The calculation can be substantially simplified by neglecting terms which contain p^μ's as part of their Lorentz structure, since at tree level only $g^{\mu\nu}$

structures appear. Finally, this reasoning leads to the necessary, but not sufficient, condition

$$\begin{aligned} 0 &= 448\eta_1^2 - 96\eta_1\left(\gamma_1^2 - 4\eta_3\right) + 9\left(\gamma_1^2 - 4\eta_3\right)^2 \\ &= 9\left(\gamma_1^2 - 4\eta_3 - \frac{16}{3}\eta_1\right)^2 + 192\eta_1^2\,, \end{aligned} \tag{5.18}$$

which is equivalent to

$$\gamma_1^2 = 4\eta_3 \quad \text{and} \quad \eta_1 = 0\,. \tag{5.19}$$

Comparing equations (5.16) and (5.19), one is led from a *globally* SU(3)-invariant theory to a *locally* SU(3)-invariant one concerning the interaction terms—also known as a Yang-Mills theory with an additional mass term—only by requiring self-consistency of the constraints and perturbative renormalizability.

6

MASSIVE VECTOR PARTICLES IN THE ANTISYMMETRIC TENSOR MODEL

This chapter presents a detailed analysis of the antisymmetric tensor model for three massive vector particles including the interaction terms with coupling constants of mass unit eV^1 and eV^0. First, all available Lorentz structures relevant to three- and four-field interactions are derived. Consequently, the U(1) invariance is employed to reduce the number of free coupling constants. Next, a constraint analysis is used to impose self-consistency on the coupling constants. Finally, conditions for the renormalizability of the theory are calculated.

6.1 AVAILABLE LORENTZ STRUCTURES OF THE INTERACTION TERMS

From the Lagrangian density of the free tensor model in equation (4.7) on page 30 with mass unit eV^4 one derives[1] that the antisymmetric tensor field $W^{\mu\nu}$ has mass unit eV. Using the fact that all Lorentz indices in the interaction terms must be completely contracted, interaction terms with coupling constants possessing mass unit eV^{1-n}, where $n = 0, 1, 2, \ldots$, can be constructed. In the following, all available Lorentz structures for the cases $n = 0$, i.e. three fields, and $n = 1$, i.e. four fields, are motivated. Note that the derivative operator ∂_μ—with mass unit eV—needs not to be taken into account since possible terms

(1) must contain an even number of derivatives,
(2) must not represent a total divergence, and
(3) must not be equal to the kinetic term.

The Case $n = 0$: Three Fields

A general interaction term has the form of a rank-six tensor

$$W^{a\,\alpha_1\beta_1} W^{b\,\alpha_2\beta_2} W^{c\,\alpha_3\beta_3}\,, \tag{6.1}$$

1 The parameters a and b in equation (4.7) are dimensionless in order to be consistent with the fundamental commutation relations in canonical quantization.

where $a, b, c \in \{1, 2, 3\}$ denote the necessary internal indices for three particles. This expression can be contracted with all Lorentz-invariant rank-six tensors. These read—up to index permutations—

$$g_{\alpha_1\beta_1} g_{\alpha_2\beta_2} g_{\alpha_3\beta_3} \tag{6.2a}$$

and

$$\epsilon_{\alpha_1\beta_1\alpha_2\beta_2} g_{\alpha_3\beta_3} \,, \tag{6.2b}$$

where $(g_{\alpha\beta}) = \mathrm{diag}(1, -1, -1, -1)$ denotes the metric tensor and $\epsilon_{\alpha\beta\gamma\delta}$ denotes the totally antisymmetric Levi-Civita symbol with the convention $\epsilon^{0123} = -\epsilon_{0123} = 1$. Thereby, all $6! = 720$ index permutations of (6.2a) and (6.2b) are contracted with expression (6.1), additionally introducing a new coupling constant g^{abc} for each tuple (a, b, c).

This work has been carried out using a computer program, see section B.2, and one obtains for the case (6.2a) the term

$$\mathcal{L}_3 = -g^{abc} W^a{}_{\mu\nu} W^{b\,\mu\lambda} W^{c\,\nu}{}_{\lambda} \,. \tag{6.3}$$

The resulting terms for the case (6.2b) read

$$\begin{aligned} &\epsilon_{\beta\gamma\delta\varepsilon} W^{a\,\alpha\beta} W^b{}_{\alpha}{}^{\gamma} W^{c\,\delta\varepsilon} \,, \qquad \epsilon_{\beta\gamma\delta\varepsilon} W^{a\,\alpha\beta} W^{b\,\gamma\delta} W^c{}_{\alpha}{}^{\varepsilon} \,, \\ &\epsilon_{\alpha\beta\delta\varepsilon} W^{a\,\alpha\beta} W^{b\,\gamma\delta} W^c{}_{\gamma}{}^{\varepsilon} \,. \end{aligned} \tag{6.4}$$

However, these terms—which all are equivalent due to the suppressed coupling constants $\tilde{g}^{abc}$—are discarded in the further discussion since they are odd under parity transformation owing to the single Levi-Civita symbol. The latter statement can be seen as follows: Under the symmetry transformation parity P the fields behave as $W^{\mu\nu} \xrightarrow{P} W_{\mu\nu}$, whereas the Levi-Civita symbol behaves as $\epsilon^{\alpha\beta\gamma\delta} \xrightarrow{P} -\epsilon_{\alpha\beta\gamma\delta}$. This results in a change of sign, which shows the proposition.

The Case $n = 1$: Four Fields

A general interaction term has the form of a rank-eight tensor

$$W^{a\,\alpha_1\beta_1} W^{b\,\alpha_2\beta_2} W^{c\,\alpha_3\beta_3} W^{d\,\alpha_4\beta_4} \,, \tag{6.5}$$

with the same conventions as in the case $n = 0$. The invariant Lorentz tensors (up to permutations) which do not lead to odd-parity interactions read

$$g_{\alpha_1\beta_1} g_{\alpha_2\beta_2} g_{\alpha_3\beta_3} g_{\alpha_4\beta_4} \tag{6.6a}$$

and

$$\epsilon_{\alpha_1\beta_1\alpha_2\beta_2}\epsilon_{\alpha_3\beta_3\alpha_4\beta_4}\,. \tag{6.6b}$$

This time, 8! = 40320 permutations of Lorentz indices need to be considered for each term, which results for the case (6.6a) in six different terms:

$$\begin{aligned} &W^{a\,\alpha\beta}W^{b}{}_{\alpha\beta}\,W^{c\,\gamma\delta}W^{d}{}_{\gamma\delta}\,, \qquad W^{a\,\alpha\beta}W^{b\,\gamma\delta}W^{c}{}_{\alpha\beta}\,W^{d}{}_{\gamma\delta}\,,\\ &W^{a\,\alpha\beta}W^{b\,\gamma\delta}W^{c}{}_{\gamma\delta}\,W^{d}{}_{\alpha\beta}\,, \end{aligned} \tag{6.7a}$$

$$\begin{aligned} &W^{a\,\alpha\beta}W^{b}{}_{\alpha\gamma}\,W^{c}{}_{\beta\delta}\,W^{d}{}_{\gamma\delta}\,, \qquad W^{a\,\alpha\beta}W^{b}{}_{\alpha\gamma}\,W^{c\,\gamma\delta}W^{d}{}_{\beta\delta}\,,\\ &W^{a\,\alpha\beta}W^{b\,\gamma\delta}W^{c}{}_{\alpha\gamma}\,W^{d}{}_{\beta\delta}\,. \end{aligned} \tag{6.7b}$$

Note that the three terms in (6.7a) are structurally equivalent if taking the coupling constants into account, analogously to the terms in (6.4). The same reasoning holds for the terms in (6.7b). Hence, only two structurally independent interaction terms with arbitrary coupling constants are obtained:

$$\mathcal{L}_4^1 = -h_1^{abcd}\,W^{a\,\alpha\beta}W^{b\,\gamma\delta}W^{c}{}_{\alpha\beta}\,W^{d}{}_{\gamma\delta}\,, \tag{6.8a}$$

$$\mathcal{L}_4^2 = -h_2^{abcd}\,W^{a\,\alpha\beta}W^{b\,\gamma\delta}W^{c}{}_{\alpha\gamma}\,W^{d}{}_{\beta\delta}\,. \tag{6.8b}$$

In the case (6.6b), the same procedure yields eleven terms of which three are structurally independent. Including arbitrary coupling constants, these read

$$\mathcal{L}_4^3 = -h_3^{abcd}\epsilon^{\alpha\beta\gamma\delta}\epsilon^{\mu\nu\lambda\sigma}\,W^{a}{}_{\alpha\beta}\,W^{b}{}_{\gamma\delta}\,W^{c}{}_{\mu\nu}\,W^{d}{}_{\lambda\sigma}\,, \tag{6.8c}$$

$$\mathcal{L}_4^4 = -h_4^{abcd}\epsilon^{\alpha\beta\gamma\mu}\epsilon^{\delta\nu\lambda\sigma}\,W^{a}{}_{\alpha\beta}\,W^{b}{}_{\gamma\delta}\,W^{c}{}_{\mu\nu}\,W^{d}{}_{\lambda\sigma}\,, \tag{6.8d}$$

$$\mathcal{L}_4^5 = -h_5^{abcd}\epsilon^{\alpha\gamma\mu\lambda}\epsilon^{\beta\delta\nu\sigma}\,W^{a}{}_{\alpha\beta}\,W^{b}{}_{\gamma\delta}\,W^{c}{}_{\mu\nu}\,W^{d}{}_{\lambda\sigma}\,. \tag{6.8e}$$

At this point, it should be mentioned that the three Lagrangians in equations (6.8c) to (6.8e) do not have a linearly independent Lorentz structure from the first two in equations (6.8a) and (6.8b). This can be seen by virtue of the relation [77]

$$\epsilon^{\mu\nu\alpha\beta}\epsilon^{\lambda\rho\sigma\tau} = -\det\begin{pmatrix} g^{\lambda\mu} & g^{\lambda\nu} & g^{\lambda\alpha} & g^{\lambda\beta}\\ g^{\rho\mu} & g^{\rho\nu} & g^{\rho\alpha} & g^{\rho\beta}\\ g^{\sigma\mu} & g^{\sigma\nu} & g^{\sigma\alpha} & g^{\sigma\beta}\\ g^{\tau\mu} & g^{\tau\nu} & g^{\tau\alpha} & g^{\tau\beta} \end{pmatrix}, \tag{6.9}$$

which expresses an arbitrary product of two Levi-Civita symbols in terms of metric tensors. However, all Lagrangians are kept in order to provide a cross-check for the algorithm of the following section 6.2.

Summary

Altogether, the following Lagrangian density

$$\mathcal{L} = \mathcal{L}_2 + \mathcal{L}_{\text{int}} \tag{6.10}$$

with

$$\mathcal{L}_2 = -\frac{1}{2}\partial^\mu W^a{}_{\mu\nu}\,\partial_\rho W^{a\,\rho\nu} + \frac{M_a^2}{4} W^{a\,\mu\nu} W^a{}_{\mu\nu} \tag{6.11}$$

and

$$\mathcal{L}_{\text{int}} = \mathcal{L}_3 + \mathcal{L}_4^1 + \mathcal{L}_4^2 + \mathcal{L}_4^3 + \mathcal{L}_4^4 + \mathcal{L}_4^5$$

will be considered, referring to equations (6.3) and (6.8a) to (6.8e). Additionally, the choice $a = -1/2$, $b = 0$ and $c = M^2/4$ has been made for the free Lagrangian $\mathcal{L}_2$, including the generalization that the fields $W^{1\,\mu\nu}$ and $W^{2\,\mu\nu}$ have the mass parameter $M = M_1 = M_2$ and the field $W^{3\,\mu\nu}$ has the mass parameter M_3.[2] In the following sections, three physical requirements are employed:

1. invariance under U(1) transformations of the fields, i.e. conservation of charge,
2. self-consistency of the constraints with respect to their conservation in time, and
3. absorbability of the infinite parts in the vertex functions into the coupling constants.

Typically, these requirements reduce the number of the independent $3^3 + 5 \times 3^4 = 432$ coupling constants.[3]

6.2 REQUIREMENT OF THE U(1) INVARIANCE

The fields $W^{a\,\mu\nu}$ behave under an infinitesimal U(1) transformation as

$$W^{a\,\mu\nu} \to W'^{a\,\mu\nu} = W^{a\,\mu\nu} - \varepsilon\,\epsilon^{3ab} W^{b\,\mu\nu}\,. \tag{6.12}$$

The free part of the Lagrangian density is obviously invariant under this transformation, i.e. $\delta\mathcal{L}_2 = \mathcal{L}_2' - \mathcal{L}_2 = 0$, whereas the invariance

2 Strictly speaking, the mass term should be written with the help of a diagonal mass matrix $(M_{ab}^2) = \text{diag}(M^2, M^2, M_3^2)$, according to the sum convention.

3 As detailed in the following, this number does not account for the permutation symmetry due to the Lorentz structure.

of the interacting part imposes conditions on the coupling constants. These have been derived systematically with computer programs, see section B.2. In the following, the one three-field interaction and the five four-field interactions are discussed separately.

The Interaction Term $\mathcal{L}_3$

The interaction term

$$\mathcal{L}_3 = -g^{abc} W^a{}_{\mu\nu} W^{b\,\mu\lambda} W^{c\,\nu}{}_{\lambda} \tag{6.3}$$

can be expressed using only one parameter g_1 owing to the antisymmetry of the field $W^{\mu\nu}$. In fact, if one carries out the summation in equation (6.3) exploiting the aforementioned antisymmetry by replacing $W^{\mu\nu} \to V^{\mu\nu} - V^{\nu\mu}$, one finds that each prefactor of a non-vanishing three-field term has the form

$$g^{123} - g^{132} - g^{213} + g^{231} + g^{312} - g^{321}\,. \tag{6.13}$$

Furthermore, this part of the Lagrangian is invariant under equation (6.12) up to first order in ε if

$$\left(g^{abd}\epsilon^{3dc} + g^{adc}\epsilon^{3db} + g^{dbc}\epsilon^{3da}\right) W^a{}_{\mu\nu} W^{b\,\mu\lambda} W^{c\,\nu}{}_{\lambda} = 0 \tag{6.14}$$

holds. This condition is trivially satisfied owing to the antisymmetry of the fields.

Equation (6.13) justifies that the coupling constants g^{abc} can be expressed using only one parameter as follows:

$$g^{123} = g_1\,. \tag{6.15}$$

All other constants g^{abc} are set to zero without loss of generality.

The Interaction Terms $\mathcal{L}_4^1$ to $\mathcal{L}_4^5$

In the following, the sum of all four-field interactions needs to be considered:

$$\begin{aligned}\mathcal{L}_4 &= \mathcal{L}_4^1 + \mathcal{L}_4^2 + \mathcal{L}_4^3 + \mathcal{L}_4^4 + \mathcal{L}_4^5 \\ &= \sum_{i=1}^{5} h_i^{abcd}\, t_i^{\alpha\beta\gamma\delta\mu\nu\lambda\sigma}\, W^a{}_{\alpha\beta} W^b{}_{\gamma\delta} W^c{}_{\mu\nu} W^d{}_{\lambda\sigma}\,.\end{aligned} \tag{6.16}$$

Here, $t_i^{\alpha\beta\gamma\delta\mu\nu\lambda\sigma}$ corresponds to a Lorentz tensor directly given by the five four-field Lagrangians $\mathcal{L}_4^i$ for $i = 1, \ldots, 5$. Consequently, by applying the transformation in equation (6.12) to equation (6.16), one obtains the condition

$$\sum_{i=1}^{5}\left(h_i^{ebcd}\epsilon^{3ea} + h_i^{aecd}\epsilon^{3eb} + h_i^{abed}\epsilon^{3ec} + h_i^{abce}\epsilon^{3ed}\right) \times t_i^{\alpha\beta\gamma\delta\mu\nu\lambda\sigma} W^a{}_{\alpha\beta} W^b{}_{\gamma\delta} W^c{}_{\mu\nu} W^d{}_{\lambda\sigma} = 0 \tag{6.17}$$

up to order ε, which must hold for all fields $W^a_{\mu\nu}$. This results in 32 independent equations for the coupling constants $h_1, \ldots, h_5$ and, hence, reduces the number of independent parameters from $5 \times 3^4 = 405$ to 373.

As for the three-field interaction, one respects the antisymmetry by replacing the antisymmetric tensor field with an arbitrary tensor field, $W_{\mu\nu} \to V_{\mu\nu} - V_{\nu\mu}$, and carries out the summation over all indices in equation (6.16). Additionally, one eliminates 32 coupling constants owing to equation (6.17) in order to respect U(1) invariance. The resulting expression can be collected by the fields V, which yields prefactors consisting of linear combinations of the remaining couplings $h_1, \ldots, h_5$. In order to determine the truly independent parameters in this expression, which still respects U(1) invariance due to the prior elimination, one executes the following iterative replacement procedure:

1. Choose an arbitrary prefactor and replace it by a new parameter θ_1. This yields a relation of the form

$$\theta_1 = \xi_1(h_i)\,, \tag{6.18}$$

   where $\xi_1(h_i)$ denotes a linear combination in the coupling constants $h_1, \ldots, h_5$. Equation (6.18) can be solved uniquely for an arbitrarily chosen coupling constant, which is replaced in all other prefactors. In general, this introduces θ_1 in these other prefactors but eliminates the chosen coupling constant completely.

2. Choose the next prefactor which is not independent of the coupling constants $h_1, \ldots, h_5$—if any left—and replace it by a new parameter θ_2. In general, this yields a relation of the form

$$\theta_2 = \xi_2(h_i, \theta_1)\,. \tag{6.19}$$

   Again, solve for one arbitrarily chosen coupling constant and replace it in all other prefactors.

3. Repeat step 2 until all coupling constants are replaced by new parameters θ_j, $j = 1, \ldots, N$. Eventually, one obtains N linear equations of the form $\theta_j = \xi_j(h_i, \theta_i)$ which are used to replace N coupling constants by new parameters. All remaining coupling constants which cannot be replaced are set to zero without loss of generality.

As a trivial example, the above algorithm can be applied to the case of $\mathcal{L}_3$ discussed in the previous section. There, only one prefactor structure given in equation (6.13) exists and one solves for g^{123}. The newly introduced variable is $\theta_1 \equiv g_1$ according to equation (6.15). The subsequent replacement automatically eliminates all other coupling constants g^{abc} which are thus set to zero without loss of generality.

Note that these two steps „satisfying the U(1) invariance“ and „eliminating superfluous parameters“ do not commute in general, which has already been mentioned in chapter 5. In this manner, the presented algorithm was cross-checked against parametrizations used in the vector field formalism.

Finally, this reasoning leads to $N = 10$ truly independent parameters for the four-field interaction. The resulting choice of parameters reads:

$$
\begin{aligned}
h_1^{1111} &= h_1^{2222} = d_1\,, \\
h_1^{1122} &= 2(d_1 - d_2)\,, \\
h_1^{1133} &= h_1^{2233} = d_3\,, \\
h_1^{1212} &= 2d_2\,, \\
h_1^{1313} &= h_1^{2323} = d_4\,, \\
h_1^{3333} &= d_5\,, \\
h_2^{1111} &= h_2^{2222} = 2(d_6 - d_1)\,, \\
h_2^{1122} &= 4(2d_2 - d_1 + d_6 + d_7)\,, \\
h_2^{1133} &= h_2^{2233} = -2(d_3 - d_4 + d_8 + d_9)\,, \\
h_2^{1212} &= -4(2d_2 + d_7)\,, \\
h_2^{1313} &= h_2^{2323} = 2(d_9 - 2d_4)\,, \\
h_2^{3333} &= 2(d_{10} - d_5)\,.
\end{aligned}
\tag{6.20}
$$

All other constants are set to zero without loss of generality, which simplifies the following calculations significantly. Note that the parametrization for h_1 is equivalent to the one in [62] and that Lorentz structures of the last three interaction terms $\mathcal{L}_4^3, \ldots, \mathcal{L}_4^5$ can be completely incorporated by the first two owing to equation (6.9).

Interaction Term	Number of Parameters	Symbol
$\mathcal{L}_3$	1	g_1 in (6.15)
$\mathcal{L}_4^1 + \cdots + \mathcal{L}_4^5$	10	d_i in (6.20)

Table 6.1: Summary of the coupling constants after requiring U(1) invariance. Note that only the truly independent parameters are counted.

Summary

Finally, the number of coupling constants have been reduced from 432 to $1 + 10 = 11$ by requiring U(1) invariance and exploiting the permutation symmetry including the antisymmetry of the fields. An overview is given in table 6.1. In the vector-field formalism, one finds analogously 7 parameters for the three-field interaction and 5 parameters for the four-field interaction, which is in total 12 parameters [62].

6.3 CONSTRAINT ANALYSIS

The constraint analysis can be carried out analogously to section 4.2, however, the interaction terms are taken into account and the fields carry an additional internal index. Again, the same non-covariant formalism with its choice of fields is applied, but the parametrization in equation (6.20) is used only if beneficial.

The following calculations have been carried out with a FORM program, see section B.2, and have mostly been cross-checked by hand. Initially, the first four parts of the Lagrangian density of equation (6.10) are given in this formalism by

$$\begin{aligned}\mathcal{L}_2 = -\frac{1}{2}\Big[&\partial_i W^a_{0i}\partial_j W^a_{0j} - \dot{W}^a_{0k}\dot{W}^a_{0k} + 2\big(\partial_i W^a_{ik} - \partial_i W^a_{ki}\big)\dot{W}^a_{0k} \\ &- \partial_i W^a_{ik}\partial_j W^a_{jk} + \partial_i W^a_{ki}\partial_j W^a_{jk} + \partial_i W^a_{ik}\partial_j W^a_{kj} \\ &- \partial_i W^a_{ki}\partial_j W^a_{kj}\Big] + \frac{M_a^2}{2}\Big(-W^a_{0j}W^a_{0j} + W^a_{ij}W^a_{ij}\Big),\end{aligned} \tag{6.21a}$$

$$\begin{aligned}\mathcal{L}_3 = -g^{abc}\Big(&-W^a_{0i}W^b_{ik}W^c_{0k} + W^a_{0k}W^b_{ik}W^c_{0i} + W^a_{ij}W^b_{0i}W^c_{0j}\\ &- W^a_{ij}W^b_{0j}W^c_{0i} + W^a_{0j}W^b_{0k}W^c_{jk} - W^a_{0k}W^b_{0j}W^c_{jk}\\ &- W^a_{ij}W^b_{ik}W^c_{jk} + W^a_{ji}W^b_{ik}W^c_{jk} + W^a_{ij}W^b_{ki}W^c_{jk}\\ &- W^a_{ji}W^b_{ki}W^c_{jk} + W^a_{ij}W^b_{ik}W^c_{kj} - W^a_{ji}W^b_{ik}W^c_{kj}\\ &- W^a_{ij}W^b_{ki}W^c_{kj} + W^a_{ji}W^b_{ki}W^c_{kj}\Big),\end{aligned} \tag{6.21b}$$

$$\begin{aligned}\mathcal{L}^1_4 = -4h^{abcd}_1\Big(&W^a_{0j}W^b_{0l}W^c_{0j}W^d_{0l} - W^a_{0j}W^b_{0l}W^c_{0j}W^d_{0l}\\ &- W^a_{0j}W^b_{0l}W^c_{0j}W^d_{0l} + W^a_{0j}W^b_{0l}W^c_{0j}W^d_{0l}\Big),\end{aligned} \tag{6.21c}$$

$$\begin{aligned}\mathcal{L}^2_4 = -h^{abcd}_2\Big[&W^a_{0i}W^c_{0i}W^b_{0j}W^d_{0j}\\ &+ \big(W^a_{0i}W^c_{il} - W^a_{0i}W^c_{li}\big)\big(W^b_{lj}W^d_{0j} - W^b_{jl}W^d_{0j}\big)\\ &+ \big(W^a_{ik}W^c_{0i} - W^a_{ki}W^c_{0i}\big)\big(W^b_{0j}W^d_{kj} - W^b_{0j}W^d_{jk}\big)\\ &+ \big(W^a_{0k}W^c_{0l} - W^a_{ik}W^c_{il} + W^a_{ki}W^c_{il}\\ &\quad + W^a_{ik}W^c_{li} - W^a_{ki}W^c_{li}\big)\\ &\times \big(W^b_{0l}W^d_{0k} - W^b_{lj}W^d_{kj} + W^b_{jl}W^d_{kj}\\ &\quad + W^b_{lj}W^d_{jk} - W^b_{jl}W^d_{jk}\big)\Big],\end{aligned} \tag{6.21d}$$

The term for $\mathcal{L}_2$ is similar to equation (4.9). The lengthy expressions for $\mathcal{L}^3_4$, $\mathcal{L}^4_4$, and $\mathcal{L}^5_4$ have been omitted for clarity, since they consist of 5, 34, and 64 terms, respectively, and cannot be simplified significantly. Anyway, they vanish for the parameter choice in equation (6.20) due to equation (6.9).

Owing to the absence of derivatives in the interaction terms, the canonically conjugated momenta can easily be determined from equation (6.10) to

$$\Pi^e_{0m} = \frac{\partial\mathcal{L}}{\partial\dot{W}^e_{0m}} = \frac{\partial\mathcal{L}_2}{\partial\dot{W}^e_{0m}} = \dot{W}^e_{0m} - \big(\partial_i W^e_{im} - \partial_i W^e_{mi}\big) \tag{6.22a}$$

and

$$\Pi^e_{mn} = \frac{\partial\mathcal{L}}{\partial\dot{W}^e_{mn}} = \frac{\partial\mathcal{L}_2}{\partial\dot{W}^e_{mn}} = 0\,, \tag{6.22b}$$

where equation (6.22b) is not solvable for the velocities $\dot{W}^e_{mn}$ and therefore represents nine constraints

$$\phi^{1e}_{mn} = \Pi^e_{mn} \approx 0\,, \quad m < n\,. \tag{6.23}$$

The Hamiltonian density can be derived via Legendre transformation, namely,

$$\begin{aligned}\mathcal{H}_1 = \phi^{1a}_{ij} z^a_{ij} + \frac{1}{2}\Pi^a_{0j}\Pi^a_{0j} + \Pi^a_{0j}\big(\partial_i W^a_{ij} - \partial_i W^a_{ji}\big) + \frac{1}{2}\partial_i W^a_{0i}\partial_j W^a_{0j} \\ + \frac{M_a^2}{2}\big(W^a_{0j}W^a_{0j} - W^a_{ij}W^a_{ij}\big) - \mathcal{L}_{\text{int}}\big(W^a_{0j}, W^a_{ij}\big)\end{aligned} \tag{6.24}$$

with yet to be determined functions z^a_{ij}. Requiring conservation in time of the primary constraints yields[4]

$$\begin{aligned}\{\phi^{1e}_{mn}, H_1\} &= M_e^2 W^e_{mn} + \partial_m \Pi^e_{0n} - \partial_n \Pi^e_{0m} - \{\Pi^e_{mn}, L_{\text{int}}\} \\ &=: \phi^{2e}_{mn}\,,\end{aligned} \tag{6.25}$$

which represents nine secondary constraints, since the unknown functions z^a_{ij} cannot be solved in this step of the iteration. Again, requiring conservation in time of the secondary constraints yields

$$\begin{aligned}\{\phi^{2e}_{mn}, H_1\} &= \{M_e^2 W^e_{mn}, \Pi^a_{ij} z^a_{ij}\} \\ &\quad + \partial_m \{\Pi^e_{0n}, \frac{1}{2}\partial_i W^a_{0i}\partial_j W^a_{0j} + \frac{M_a^2}{2} W^a_{0j} W^a_{0j} - L_{\text{int}}\} \\ &\quad - \partial_n \{\Pi^e_{0m}, \frac{1}{2}\partial_i W^a_{0i}\partial_j W^a_{0j} + \frac{M_a^2}{2} W^a_{0j} W^a_{0j} - L_{\text{int}}\} \\ &\quad - \{\{\Pi^e_{mn}, L_{\text{int}}\}, \Pi^a z^a_{ij} + \frac{1}{2}\Pi^a_{0j}\Pi^a_{0j} + \Pi^a_{0j}\big(\partial_i W^a_{ij} - \partial_i W^a_{ji}\big)\} \\ &= \mathcal{M}^{ea}_{mnij} z^a_{ij} + Y^e_{mn}\end{aligned} \tag{6.26}$$

with

$$\mathcal{M}^{ea}_{mnij} = M_a^2 \delta^{ea}\delta^{im}\delta^{jn} + \{\Pi^a_{ij}, \{\Pi^e_{mn}, L_{\text{int}}\}\}\,, \tag{6.27}$$

where the explicit form of Y^e_{mn} is irrelevant. In the previous calculation it was used that L_{int}—including arbitrary Poisson brackets of that term—is a polynomial exclusively in the six fields W^a_{0j} and W^a_{ij}. It follows from

4 Note that we distinguish between the function and the corresponding density by a slightly different notation, e.g. $\mathcal{L}_{\text{int}}$ and $L_{\text{int}} = \int d^3x \mathcal{L}_{\text{int}}$.

No.	Fields	Factor in det $\mathcal{M}$	Inequality
1	$W^3_{01} = x$, $W^3_{23} = x$	$M^4 - x^2 g_1^2$	$g_1^2 \leq 0$
2a	$W^3_{01} = x$	$M_3^2 + 16x^2 d_{10}$,	$d_{10} \geq 0$
		$M^2 + 4x^2 d_9$	$d_9 \geq 0$
2b	$W^3_{12} = x$	$M_3^2 - 16x^2 d_{10}$,	$d_{10} \leq 0$
		$M^2 - 4x^2 d_9$	$d_9 \leq 0$
3a	$W^1_{01} = x$	$M^2 + 16x^2 d_6$,	$d_6 \geq 0$
		$M^2 - 8x^2 d_7$	$d_7 \leq 0$
3b	$W^1_{12} = x$	$M^2 - 16x^2 d_6$,	$d_6 \leq 0$
		$M^2 + 8x^2 d_7$	$d_7 \geq 0$
4	$W^2_{01} = x$, $W^3_{01} = y$	$M^2 M_3^2 - 64x^2 y^2 d_8^2$	$d_8^2 \leq 0$

Table 6.2: Analysis of the determinant of $\mathcal{M}$. For a given choice of fields all other fields are set to zero. Only the crucial factors of the determinant are mentioned. Each step *depends* on the previous ones.

equation (6.26) that the 9×9-matrix $\mathcal{M}$ from equation (6.27) needs a non-vanishing determinant in order to solve for the unknown functions z^a_{ij}. This reasoning leads finally to the correct number of constraints for three spin-one particles, i.e. the $2 \times 6 \times 3 = 36$ canonical variables are reduced by $2 \times 9 = 18$ constraints to the $2 \times 3 \times 3 = 18$ physical degrees of freedom. Furthermore, by exploiting the Jacobi identity one finds the property

$$\mathcal{M}^{ea}_{mnij} = \mathcal{M}^{ae}_{ijmn}\,, \tag{6.28}$$

i.e. $\mathcal{M}$ is symmetric, which simplifies further calculations.

The following analysis of the condition $\det \mathcal{M} \neq 0$ is only feasible with the help of computers, since every entry in the matrix contains about 11 terms despite using the parametrization in equation (6.20) satisfying U(1) invariance. Nevertheless, the test case $\mathcal{L}_{\text{int}} = \mathcal{L}_3$ has been calculated

by hand and cross-checked with the programs in use. The analysis is detailed in table 6.2 on the previous page and results in the equations

$$\begin{aligned} &d_6 = d_7 = d_8 = d_9 = d_{10} = 0\,, \\ &g_1 = 0\,, \end{aligned} \tag{6.29}$$

besides several insignificant inequalities. Applying these equations renders $\det \mathcal{M}$ independent of the fields W^a_{ij}, which are called „frozen-out" in [76]. This could be a hint that one cannot infer more conditions from this determinant analysis, although an estimate of the lower bound of the determinant[5] seems practically impossible due to the sheer size of the full expression. At this point, it shall be stressed that the three-field interaction governed by g_1 vanishes only by requiring self-consistency on a classical level owing to equation (6.29).

6.4 QUANTIZATION WITH CONSTRAINTS

The quantization including constraints is based on the path integral formalism, in which the generating functional plays the crucial role. On the classical level, the original variables are related by a canonical transformation to new ones, where the constraints are completely separated from the dynamical variables.[6] This allows for the construction of the correct generating functional using these new variables. However, the return to the original ones is accompanied by the introduction of non-physical fermionic scalar fields, which are called ghost fields. Before proceeding with the renormalizability analysis, one needs to verify that these ghost fields, e.g. denoted as c, $\bar{c}$, do not have a kinetic part, $\partial_\mu \bar{c} \partial^\mu c$, in the effective Lagrangian implementing the constraints. This ensures that one can simply derive naïve Feynman rules from interaction terms containing the tensor fields W only, since in dimensional regularization contributions from fields without kinetic parts can be ignored. In fact, this check is carried out analogously to [62, Ch. IV].

5 Note that $\det \mathcal{M} = M^{12} M_3^6$ for $W \equiv 0$ by virtue of equation (6.27). Therefore, $\det \mathcal{M} \neq 0 \,\forall\, W$ is equivalent to $\det \mathcal{M} > 0 \,\forall\, W$.

6 This separation is always possible owing to a fundamental theorem, see [75]. However, the proof does not yield an explicit form of the canonical transformation.

The generating functional, in which the variables Ω appearing in the constraints $\Omega = 0$ are separated from the dynamical variables ω appearing in the physical Hamiltonian $\mathcal{H}^{\mathrm{ph}}(\omega) \equiv \mathcal{H}(\omega, \Omega)\big|_{\Omega=0}$, reads

$$Z[J^\omega] = \int \mathcal{D}\omega\, \mathcal{D}\Omega\, \delta(\Omega) \times \exp\Big(i \int d^4x \left[\omega^2 \dot{\omega}^1 + \Omega^2 \dot{\Omega}^1 - \mathcal{H}(\omega, \Omega) + \omega J^\omega + \Omega J^\Omega\right]\Big), \tag{6.30}$$

where $\omega = (\omega^1, \omega^2)$, $\Omega = (\Omega^1, \Omega^2)$, and sources $J = (J^\omega, J^\Omega)$ have been introduced. Here, ω^1, Ω^1 and ω^2, Ω^2 denote the fields and momenta, respectively. Changing back to the original variables (W, Π) by a canonical transformation as well as to the original constraints (ϕ^1, ϕ^2), the δ-function behaves as

$$\delta(\Omega) = \delta(\phi)\sqrt{\det\big(\{\phi, \phi\}\big)}\,, \tag{6.31}$$

where

$$\{\phi, \phi\} = \begin{pmatrix} \{\phi^{1a}_{ij}, \phi^{1b}_{mn}\} & \{\phi^{1a}_{ij}, \phi^{2b}_{mn}\} \\ \{\phi^{2a}_{ij}, \phi^{1b}_{mn}\} & \{\phi^{2a}_{ij}, \phi^{2b}_{mn}\} \end{pmatrix} \tag{6.32}$$

is the 18×18-matrix consisting of the constraints given in equations (6.23) and (6.25). Since $\{\phi^{1a}_{ij}, \phi^{1b}_{mn}\} = 0$ holds according to equation (6.23), the relation

$$\sqrt{\det\big(\{\phi, \phi\}\big)} = \det\big(\{\phi^{2e}_{mn}, \phi^{1a}_{ij}\}\big) = \det \mathcal{M}\,, \tag{6.33}$$

is obtained, referring to equations (6.26) and (6.27). Since $\det \mathcal{M} \neq 0$ holds, the system of constraints is indeed of second class.

Furthermore, the action $S = \int d^4x \mathcal{L}$ is canonically invariant and the Jacobian determinant of a canonical transformation to the original values in equation (6.30) is unity. Now, expressing the determinant in equation (6.33) and the $\delta(\phi^2)$-function in $\delta(\phi) = \delta(\phi^1)\delta(\phi^2)$ as functional integrals over the aforementioned ghost fields,[7]

$$\begin{aligned} \delta(\phi^2) &\sim \int \mathcal{D}\lambda \exp\Big(i \int d^4x \sum_{i<j} \lambda^a_{ij} \phi^{2a}_{ij}\Big) \quad \text{and} \\ \sqrt{\det\big(\{\phi, \phi\}\big)} &\sim \int \mathcal{D}c\mathcal{D}\bar{c} \exp\Big(i \int d^4x \sum_{\substack{i<j \\ m<n}} \bar{c}^e_{mn} \mathcal{M}^{ea}_{mnij} c^a_{ij}\Big), \end{aligned} \tag{6.34}$$

7 Here, the summation convention of indices is noted explicitly once again.

the generating functional reads

$$\begin{aligned} Z[J] = \int \mathcal{D}W\,\mathcal{D}\Pi\,\mathcal{D}\lambda\,\mathcal{D}c\,\mathcal{D}\bar{c}\;\delta(\phi^1) \\ \times \exp\Big[i \int d^4x \left(\mathcal{K} + J^{a\,\mu\nu} W^a_{\mu\nu} \right) \Big], \end{aligned} \tag{6.35}$$

where

$$\begin{aligned} \mathcal{K} &= \Pi^a_{0j} \dot{W}^a_{0j} + \Pi^a_{ij} \dot{W}^a_{ij} - \mathcal{H}_1(W,\Pi) + \lambda^a_{ij} \phi^{2a}_{ij} + \bar{c}^e_{mn} \mathcal{M}^{ea}_{mnij} c^a_{ij} \\ &= \Pi^a_{0j} \dot{W}^a_{0j} + \Pi^a_{ij} \dot{W}^a_{ij} - \phi^{1a}_{ij} z^a_{ij} - \frac{1}{2} \Pi^a_{0j} \Pi^a_{0j} \\ &\quad - \Pi^a_{0j} \big(\partial_i W^a_{ij} - \partial_i W^a_{ji} \big) - \frac{1}{2} \partial_i W^a_{0i} \partial_j W^a_{0j} \\ &\quad + \frac{M_a^2}{2} \big(- W^a_{0j} W^a_{0j} + W^a_{ij} W^a_{ij} \big) + \mathcal{L}_{\text{int}} \\ &\quad + \lambda^a_{ij} \big(M_a^2 W^a_{ij} + \partial_i \Pi^a_{0j} - \partial_j \Pi^a_{0i} - \{ \Pi^a_{ij}, L_{\text{int}} \} \big) \\ &\quad + \bar{c}^e_{mn} \mathcal{M}^{ea}_{mnij} c^a_{ij} \end{aligned} \tag{6.36}$$

and sources $J^a_{\mu\nu}$ have been introduced.

The integration over the three momenta Π^a_{ij} can be carried out directly due to the factor $\delta(\phi^1) \equiv \prod_{m<n} \delta(\Pi^e_{mn})$ in the integrand and the fact that $\{\Pi^a_{ij}, L_{\text{int}}\}$ as well as $\bar{c}^e_{mn} \mathcal{M}^{ea}_{mnij} c^a_{ij}$ are indeed independent of Π^e_{mn}. Consequently, the integration over the remaining three momenta Π^a_{0j} is done by using the generalized formula for Gaussian integrals [78, Ch. 6.2]. This yields

$$Z[J] = \int \mathcal{D}W\,\mathcal{D}\lambda\,\mathcal{D}c\,\mathcal{D}\bar{c}\;\exp\Big[i \int d^4x \left(\tilde{\mathcal{K}} + J^{a\,\mu\nu} W^a_{\mu\nu} \right) \Big], \tag{6.37}$$

where

$$\begin{aligned} \tilde{\mathcal{K}} &= \frac{1}{2} \Big[\dot{W}^a_{0j} - \big(\partial_i W^a_{ij} - \partial_i W^a_{ji} \big) - \big(\partial_i \lambda^a_{ij} - \partial_i \lambda^a_{ji} \big) \Big] \\ &\quad \times \Big[\dot{W}^a_{0j} - \big(\partial_i W^a_{ij} - \partial_i W^a_{ji} \big) - \big(\partial_i \lambda^a_{ij} - \partial_i \lambda^a_{ji} \big) \Big] \\ &\quad - \frac{1}{2} \partial_i W^a_{0i} \partial_j W^a_{0j} + \frac{M_a^2}{2} \big(- W^a_{0j} W^a_{0j} + W^a_{ij} W^a_{ij} \big) + \mathcal{L}_{\text{int}} \\ &\quad + \lambda^a_{ij} \big(M_a^2 W^a_{ij} - \{ \Pi^a_{ij}, L_{\text{int}} \} \big) + \bar{c}^e_{mn} \mathcal{M}^{ea}_{mnij} c^a_{ij} \\ &= \frac{1}{2} \Big\{ \dot{W}^a_{0j} - \big[\partial_i (W^a_{ij} + \lambda^a_{ij}) - \partial_i (W^a_{ji} + \lambda^a_{ji}) \big] \Big\} \\ &\quad \times \Big\{ \dot{W}^a_{0j} - \big[\partial_i (W^a_{ij} + \lambda^a_{ij}) - \partial_i (W^a_{ji} + \lambda^a_{ji}) \big] \Big\} \\ &\quad + \frac{M_a^2}{2} \Big[- W^a_{0j} W^a_{0j} + \big(W^a_{ij} + \lambda^a_{ij} \big) \big(W^a_{ij} + \lambda^a_{ij} \big) - \lambda^a_{ij} \lambda^a_{ij} \Big] \\ &\quad - \frac{1}{2} \partial_i W^a_{0i} \partial_j W^a_{0j} + \mathcal{L}_{\text{int}} - \lambda^a_{ij} \{ \Pi^a_{ij}, L_{\text{int}} \} + \bar{c}^e_{mn} \mathcal{M}^{ea}_{mnij} c^a_{ij} \,. \end{aligned} \tag{6.38}$$

By shifting variables $W^a_{ij} \to W^a_{ij} - \lambda^a_{ij}$ in equation (6.37), an effective Lagrangian is finally obtained from equation (6.38) of the form

$$\mathcal{L}_{\text{eff}} = \mathcal{L} - \frac{M_a^2}{2}\lambda^a_{ij}\lambda^a_{ij} + \frac{M_a^2}{2}\bar{c}^a_{ij}c^a_{ij} + (\text{interactions of } \lambda, c, \bar{c}, W)\,, \quad (6.39)$$

with $\mathcal{L}$ given in equation (6.10). Since no kinetic terms of ghost fields appear in equation (6.39), one can continue with naïve Feynman rules resulting from $\mathcal{L}$ instead of $\mathcal{L}_{\text{eff}}$, which simplifies calculations.

6.5 NAÏVE FEYNMAN RULES

Propagator

The following explicit derivation of the propagator is guided by [78, Ch. 6], however, one must take into account not only the more complicated Lorentz structure but also the antisymmetry of the fields. As usual, one starts with the generating functional of the free Lagrangian density[8] from equation (6.11)

$$\begin{aligned} Z[J] &= \int \mathcal{D}W \exp\left\{ i \int d^4x \Big[\mathcal{L}_2\big(W^{\mu\nu}\big) + W_{\alpha\beta}J^{\alpha\beta} \Big] \right\} \\ &= \mathcal{N} \int \mathcal{D}V \exp\left\{ i \int d^4x \Big[\underbrace{\mathcal{L}_2\big(W(V^{\mu\nu})\big) + \big(V_{\alpha\beta} - V_{\beta\alpha}\big)J^{\alpha\beta}}_{(\star)} \Big] \right\}, \end{aligned} \quad (6.40)$$

where in the last step a tensor field $V^{\mu\nu}$, whose antisymmetric component equals $W^{\mu\nu} = \frac{1}{2}(V^{\mu\nu} - V^{\nu\mu})$, has been introduced. The path integration over the symmetric part of $V^{\mu\nu}$ has been compensated with a normalizing constant $\mathcal{N}$. Hence, one obtains for the exponent

$$(\star) = \frac{1}{2} V_{\alpha\beta}\Delta^{\alpha\beta\gamma\delta}V_{\gamma\delta} + \big(V_{\alpha\beta} - V_{\beta\alpha}\big)J^{\alpha\beta} \quad (6.41)$$

with the differential operator

$$\begin{aligned} \Delta^{\alpha\beta\gamma\delta} = g^{\beta\delta}\partial^\alpha\partial^\gamma + g^{\alpha\gamma}\partial^\beta\partial^\delta - g^{\alpha\delta}\partial^\beta\partial^\gamma - g^{\beta\gamma}\partial^\alpha\partial^\delta \\ + M^2\big(g^{\alpha\gamma}g^{\beta\delta} - g^{\alpha\delta}g^{\beta\gamma}\big)\,, \end{aligned} \quad (6.42)$$

8 The internal index structure is omitted in the following.

where here as in the following the divergence theorem has been employed. Via a change of variables $V_{\alpha\beta} \to V_{\alpha\beta} + \Psi_{\alpha\beta}$ in the path integral in equation (6.40), where $\Psi_{\alpha\beta}$ is some „constant" field, one obtains

$$\begin{aligned}(\star) \to \frac{1}{2} V_{\alpha\beta}\Delta^{\alpha\beta\gamma\delta}V_{\gamma\delta} + V_{\alpha\beta}\Delta^{\alpha\beta\gamma\delta}\Psi_{\gamma\delta} + \frac{1}{2}\Psi_{\alpha\beta}\Delta^{\alpha\beta\gamma\delta}\Psi_{\gamma\delta} \\ + V_{\alpha\beta}\left(J^{\alpha\beta} - J^{\beta\alpha}\right) + J_{\alpha\beta}\left(\Psi^{\alpha\beta} - \Psi^{\beta\alpha}\right),\end{aligned} \tag{6.43}$$

where the relation $\Psi_{\alpha\beta}\Delta^{\alpha\beta\gamma\delta}V_{\gamma\delta} = V_{\alpha\beta}\Delta^{\alpha\beta\gamma\delta}\Psi_{\gamma\delta}$ has been used. The field $\Psi_{\alpha\beta}$ is now chosen such that

$$\Delta^{\alpha\beta\gamma\delta}\Psi_{\gamma\delta} = -\left(J^{\alpha\beta} - J^{\beta\alpha}\right). \tag{6.44}$$

The solution of this differential equation can be determined by using a Green's function,

$$\Psi_{\gamma\delta}(x) = \int d^4y D_{\gamma\delta\mu\nu}(x-y)J^{\mu\nu}(y). \tag{6.45}$$

Inserting this in equation (6.44) and changing to momentum space representation, one finds

$$\tilde{\Delta}^{\alpha\beta\gamma\delta}(p)\tilde{D}_{\gamma\delta\mu\nu}(p) = -\left(\delta^\alpha_\mu\delta^\beta_\nu - \delta^\alpha_\nu\delta^\beta_\mu\right), \tag{6.46}$$

where the Fourier transform of the differential operator reads

$$\begin{aligned}\tilde{\Delta}^{\alpha\beta\gamma\delta} = -g^{\beta\delta}p^\alpha p^\gamma - g^{\alpha\gamma}p^\beta p^\delta + g^{\alpha\delta}p^\beta p^\gamma + g^{\beta\gamma}p^\alpha p^\delta \\ + M^2\left(g^{\alpha\gamma}g^{\beta\delta} - g^{\alpha\delta}g^{\beta\gamma}\right).\end{aligned} \tag{6.47}$$

An ansatz for the Lorentz structure of the to be determined Green's function reads

$$\begin{aligned}\tilde{D}_{\gamma\delta\mu\nu} = A_1 g_{\gamma\delta}g_{\mu\nu} + A_2 g_{\gamma\mu}g_{\delta\nu} + A_3 g_{\gamma\nu}g_{\delta\mu} \\ + B_1 g_{\gamma\delta}p_\mu p_\nu + B_2 g_{\gamma\mu}p_\delta p_\nu + B_3 g_{\gamma\nu}p_\delta p_\mu \\ + B_4 g_{\delta\mu}p_\gamma p_\nu + B_5 g_{\delta\nu}p_\gamma p_\mu + B_6 g_{\mu\nu}p_\gamma p_\delta \\ + C_1 p_\gamma p_\delta p_\mu p_\nu + D_1\epsilon_{\gamma\delta\mu\nu},\end{aligned} \tag{6.48}$$

where one could have already set $D_1 = 0$ due to the odd parity of $\epsilon_{\gamma\delta\mu\nu}$. This simplifies if one takes into account that

$$\Psi_{\gamma\delta}(x) = \frac{1}{(2\pi)^4}\iint d^4y d^4p\, e^{-ip\cdot(x-y)}\tilde{D}_{\gamma\delta\mu\nu}(p)J^{\mu\nu}(y) \tag{6.49}$$

is only contracted with antisymmetric tensors in equation (6.43). Therefore, one can ignore parts symmetric under $\gamma \leftrightarrow \delta$ by setting $A_1 = B_1 =$

$B_6 = C_1 = 0$ without loss of generality. Inserting the remaining ansatz in equation (6.46) yields conditions which can be expressed as

$$\begin{aligned} A_2 &= A_3 - \frac{1}{M^2}\,, & B_2 &= B_4 - \frac{1}{M^2(M^2-p^2)}\,, \\ B_3 &= B_5 + \frac{1}{M^2(M^2-p^2)}\,, & D_1 &= 0\,, \end{aligned} \tag{6.50}$$

where the coefficients A_3, B_4, B_5 are still arbitrary. Applying these conditions in the ansatz leads to

$$\begin{aligned} \tilde{D}_{\gamma\delta\mu\nu}(p) &= -\frac{1}{M^2(M^2-p^2)}\Big[\big(M^2-p^2\big)g_{\gamma\mu}g_{\delta\nu} + g_{\gamma\mu}p_\delta p_\nu - g_{\gamma\nu}p_\delta p_\mu\Big] \\ &\quad + A_3\big(g_{\gamma\nu}g_{\delta\mu} + g_{\gamma\mu}g_{\delta\nu}\big) + B_4\big(g_{\gamma\mu}p_\delta p_\nu + g_{\delta\mu}p_\gamma p_\nu\big) \\ &\quad + B_5\big(g_{\gamma\nu}p_\delta p_\mu + g_{\delta\nu}p_\gamma p_\mu\big) \\ &= -\frac{1}{M^2(M^2-p^2)}\Big[\big(M^2-p^2\big)g_{\gamma\mu}g_{\delta\nu} + g_{\gamma\mu}p_\delta p_\nu - g_{\gamma\nu}p_\delta p_\mu\Big], \end{aligned} \tag{6.51}$$

where again symmetric parts have been discarded without loss of generality.

Finally, one can absorb the path integral in the normalizing constant and one obtains

$$\begin{aligned} Z[J] = N\exp\Big\{-\frac{i}{2}\iint d^4z d^4z'\, J^{\gamma\delta}(z')\big[D_{\beta\alpha\gamma\delta}(z-z') \\ - D_{\alpha\beta\gamma\delta}(z-z')\big]J^{\alpha\beta}(z)\Big\}, \end{aligned} \tag{6.52}$$

from which the propagator as the two-point function follows as

$$\begin{aligned} \big\langle 0\big|T\big[W^a{}_{\mu\nu}(x)W^b{}_{\lambda\sigma}(y)\big]\big|0\big\rangle &= -\left.\frac{\delta^2 Z[J]}{\delta J^{a\,\mu\nu}(x)\delta J^{b\,\lambda\sigma}(y)}\right|_{J=0} \\ &= \frac{i\delta^{ab}}{2}\big[D_{\nu\mu\lambda\sigma}(x-y) - D_{\mu\nu\lambda\sigma}(x-y) \\ &\qquad + D_{\sigma\lambda\mu\nu}(x-y) - D_{\lambda\sigma\mu\nu}(x-y)\big] \\ &= \frac{i\delta^{ab}}{M_a^2}\int\frac{d^4p}{(2\pi)^4}e^{-ip\cdot(x-y)}\frac{1}{M_a^2-p^2-i0^+} \\ &\quad \times\Big[\big(M_a^2-p^2\big)g_{\mu\lambda}g_{\nu\sigma} + g_{\mu\lambda}p_\nu p_\sigma - g_{\mu\sigma}p_\nu p_\lambda - (\mu\leftrightarrow\nu)\Big]. \end{aligned} \tag{6.53}$$

This result is identical to [76, App. A] except for the internal index structure δ^{ab}, which has been added here for completeness. The term $-i0^+$ introduced in the last step indicates the usual Feynman boundary condition.

Three-Vertex

Although the constraint analysis has already shown that all couplings g^{abc} governing the three-field interaction vanish, the three-vertex is considered here again from a slightly different point of view. The naïve Feynman rule for the three-vertex can be derived from $\mathcal{L}_3$ as usual since it depends merely on index permutations and not on the tensor formalism itself. It reads:

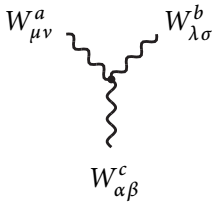

$$= -i \begin{pmatrix} g^{abc} \\ g^{bac} \\ g^{bca} \\ g^{acb} \\ g^{cab} \\ g^{cba} \end{pmatrix} \cdot \begin{pmatrix} g_{\mu\lambda}g_{\nu\alpha}g_{\sigma\beta} \\ g_{\mu\lambda}g_{\nu\beta}g_{\sigma\alpha} \\ g_{\mu\sigma}g_{\nu\beta}g_{\lambda\alpha} \\ g_{\mu\alpha}g_{\nu\lambda}g_{\sigma\beta} \\ g_{\mu\alpha}g_{\nu\sigma}g_{\lambda\beta} \\ g_{\mu\beta}g_{\nu\sigma}g_{\lambda\alpha} \end{pmatrix} . \tag{6.54}$$

Here and henceforth, the Feynman rules have been written as a „scalar product“ of a „vector“ containing only coupling constants and a „vector“ containing only kinematic terms. This is useful for the model implementation in FeynArts, see section B.2.

At this point, one should take into account that only parts which are antisymmetric in the index pairs $\mu\nu$, $\lambda\sigma$, and $\alpha\beta$ contribute to any physical quantity since (1) external legs are contracted with antisymmetric polarization tensors and (2) internal legs are contracted with the antisymmetric propagator in equation (6.53). The antisymmetric part of equation (6.54) can be written as

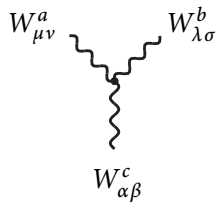

$$= \left(g^{abc} - g^{acb} - g^{bac} + g^{bca} + g^{cab} - g^{cba}\right) ggg^{[\mu\nu][\lambda\sigma][\alpha\beta]} , \tag{6.55}$$

where $ggg^{[\mu\nu][\lambda\sigma][\alpha\beta]}$ is a pairwisely antisymmetric Lorentz tensor, see also the remarks in section 6.6. Using the parametrization from equation (6.15), one finds that the right-hand side of equation (6.55) vanishes unless abc is a permutation of 123. In particular, the non-vanishing part has always the form

$$\pm g_1 ggg^{[\mu\nu][\lambda\sigma][\alpha\beta]} , \tag{6.56}$$

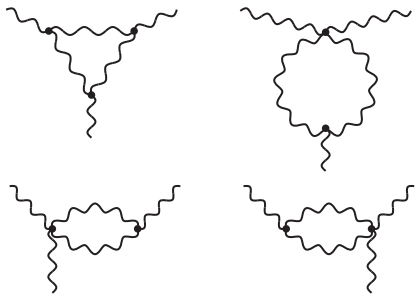

Figure 6.1: One-loop contributions to the three-point function. The wiggly line represents a spin-one particle. However, these contain always at least one three-vertex and can therefore be ignored due to the constraint analysis.

which, however, vanishes as soon as the results from the constraint analysis in equation (6.29) are applied. The three-vertex one-loop contributions are depicted in figure 6.1. In summary, all contributions which contain three-vertices can be neglected in a self-consistent theory without loss of generality.

Four-Vertex

The more complicated naïve Feynman rule for the four-vertex reads

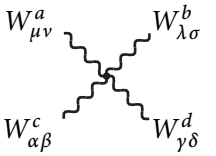

$$= \xi_1 + \xi_2 + \underbrace{\xi_3 + \xi_4 + \xi_5}_{=0}, \tag{6.57}$$

where the five summands $\xi_1, \ldots, \xi_5$ represent the parts resulting from the Lagrangian densities $\mathcal{L}_4^1, \ldots, \mathcal{L}_4^5$ with four fields. For the first two Lagrangians they are given explicitly in the following, the other three expressions have been omitted since they can be set to zero without loss of generality due to equation (6.9) as indicated:

$$\xi_1 = -i \begin{pmatrix} h_1^{acbd} + h_1^{adbc} + h_1^{bcad} + h_1^{bdac} \\ \quad + h_1^{cadb} + h_1^{cbda} + h_1^{dacb} + h_1^{dbca} \\ h_1^{abcd} + h_1^{adcb} + h_1^{badc} + h_1^{bcda} \\ \quad + h_1^{cbad} + h_1^{cdab} + h_1^{dabc} + h_1^{dcba} \\ h_1^{abdc} + h_1^{acdb} + h_1^{bacd} + h_1^{bdca} \\ \quad + h_1^{cabd} + h_1^{cdba} + h_1^{dbac} + h_1^{dcab} \end{pmatrix} \cdot \begin{pmatrix} g_{\mu\lambda} g_{\nu\sigma} g_{\alpha\gamma} g_{\beta\delta} \\ g_{\mu\alpha} g_{\nu\beta} g_{\lambda\gamma} g_{\sigma\delta} \\ g_{\mu\gamma} g_{\nu\delta} g_{\lambda\alpha} g_{\sigma\beta} \end{pmatrix}, \tag{6.58a}$$

$$\xi_2 = -i \begin{pmatrix} h_2^{adbc} + h_2^{bcad} \\ h_2^{acbd} + h_2^{bdac} \\ h_2^{bcda} + h_2^{dabc} \\ h_2^{bdca} + h_2^{cabd} \\ h_2^{adcb} + h_2^{cbad} \\ h_2^{abcd} + h_2^{cdab} \\ h_2^{cbda} + h_2^{dacb} \\ h_2^{bacd} + h_2^{cdba} \\ h_2^{acdb} + h_2^{dbac} \\ h_2^{abdc} + h_2^{dcab} \\ h_2^{cadb} + h_2^{dbca} \\ h_2^{badc} + h_2^{dcba} \end{pmatrix} \cdot \begin{pmatrix} g_{\mu\lambda} g_{\nu\alpha} g_{\sigma\gamma} g_{\beta\delta} \\ g_{\mu\lambda} g_{\nu\gamma} g_{\sigma\alpha} g_{\beta\delta} \\ g_{\mu\sigma} g_{\nu\beta} g_{\lambda\gamma} g_{\alpha\delta} \\ g_{\mu\sigma} g_{\nu\delta} g_{\lambda\alpha} g_{\beta\gamma} \\ g_{\mu\alpha} g_{\nu\lambda} g_{\sigma\delta} g_{\beta\gamma} \\ g_{\mu\alpha} g_{\nu\gamma} g_{\lambda\beta} g_{\sigma\delta} \\ g_{\mu\beta} g_{\nu\sigma} g_{\lambda\delta} g_{\alpha\gamma} \\ g_{\mu\beta} g_{\nu\delta} g_{\lambda\alpha} g_{\sigma\gamma} \\ g_{\mu\gamma} g_{\nu\lambda} g_{\sigma\beta} g_{\alpha\delta} \\ g_{\mu\gamma} g_{\nu\alpha} g_{\lambda\delta} g_{\sigma\beta} \\ g_{\mu\delta} g_{\nu\sigma} g_{\lambda\beta} g_{\alpha\gamma} \\ g_{\mu\delta} g_{\nu\beta} g_{\lambda\gamma} g_{\sigma\alpha} \end{pmatrix}. \tag{6.58b}$$

The four-vertex one-loop contributions are depicted in figure 6.2 on the facing page.

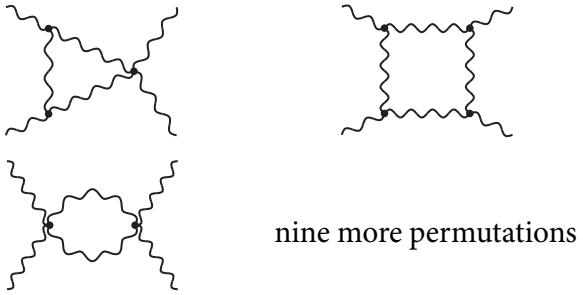

Figure 6.2: One-loop contributions to the four-point function. The wiggly line represents a spin-one particle. The omitted permutations can be obtained by crossing the external legs.

6.6 RENORMALIZABILITY ANALYSIS

Basically, one requires that Lorentz structures of divergent parts at one-loop level have the same structure of prefactors as the corresponding Lorentz structures at tree level. This ensures that infinite quantities can be absorbed in the parameters of the theory—a crucial condition for a physical theory—by using, for example, the minimal subtraction renormalization scheme.

Remarks about Antisymmetrization

The vertex functions at tree and one-loop level are pairwisely decomposed in antisymmetric and symmetric parts as follows:

$$\begin{aligned} t^{\cdots[\mu\nu]\cdots} &= \frac{1}{2}\left(t^{\cdots\mu\nu\cdots} - t^{\cdots\nu\mu\cdots}\right), \\ t^{\cdots(\mu\nu)\cdots} &= \frac{1}{2}\left(t^{\cdots\mu\nu\cdots} + t^{\cdots\nu\mu\cdots}\right). \end{aligned} \tag{6.59}$$

This is convenient since the polarization tensors are antisymmetric and, hence, symmetric parts do not contribute to physically meaningful quantities. In other words, this pairwise antisymmetrization ensures that merely necessary conditions are deduced in the following renormalizability analysis.

As an example, the contributions to a three-vertex function Γ with fixed internal indices $a, b, c \in \{1, 2, 3\}$ are regarded at tree and one-loop

level for vanishing momenta. These can be expressed in $6!/(3!2!2!2!) = 15$ products[9] of three metric tensors $ggg_i^{\mu\nu\lambda\sigma\alpha\beta}$ as follows:

$$\begin{aligned}\Gamma_{\text{tree}}^{\mu\nu\lambda\sigma\alpha\beta} &= \sum_{i=1}^{15} \kappa_i ggg_i^{\mu\nu\lambda\sigma\alpha\beta}\,,\\ \Gamma_{\text{1-loop}}^{\mu\nu\lambda\sigma\alpha\beta}\Big|_{p_i=0} &= \sum_{i=1}^{15} \tilde{\kappa}_i ggg_i^{\mu\nu\lambda\sigma\alpha\beta} + (\text{non-divergent parts})\,.\end{aligned} \tag{6.60}$$

For example, $ggg_1^{\mu\nu\lambda\sigma\alpha\beta}$ is given by[10]

$$ggg_1^{\mu\nu\lambda\sigma\alpha\beta} = g^{\mu\nu} g^{\lambda\sigma} g^{\alpha\beta}\,. \tag{6.61}$$

Each of these tensors can be decomposed into $2^3 = 8$ parts according to equation (6.59), however, only the pairwisely antisymmetric part needs to be considered. As seen in section 6.5, only one such structure $ggg^{[\mu\nu][\lambda\sigma][\alpha\beta]}$ remains. The expression reads

$$\Gamma_{\text{tree}}^{[\mu\nu][\lambda\sigma][\alpha\beta]} = \frac{1}{8}\left(\kappa_5 - \kappa_6 - \kappa_8 + \kappa_9 - \kappa_{10} + \kappa_{11} + \kappa_{13} - \kappa_{14}\right) ggg^{[\mu\nu][\lambda\sigma][\alpha\beta]} \tag{6.62}$$

and an analogous expression for the divergent part of the one-loop contribution. Since κ and $\tilde{\kappa}$ are functions of the coupling constants, one can derive conditions by requiring the same structure at tree and one-loop level. However, it has been shown in section 6.5 that the prefactor in equation (6.62) is always zero for all three-vertices and, hence, no conditions can be deduced.

Regarding the four-vertex function, the contributions are expressed in terms of $8!/(4!2!2!2!2!) = 105$ products of four metric tensors $gggg_i^{\mu\nu\lambda\sigma\alpha\beta\gamma\delta}$ as follows:[11]

$$\begin{aligned}\Gamma_{\text{tree}}^{\mu\nu\lambda\sigma\alpha\beta\gamma\delta} &= \sum_{i=1}^{105} \kappa_i gggg_i^{\mu\nu\lambda\sigma\alpha\beta\gamma\delta}\,,\\ \Gamma_{\text{1-loop}}^{\mu\nu\lambda\sigma\alpha\beta\gamma\delta}\Big|_{p_i=0} &= \sum_{i=1}^{105} \tilde{\kappa}_i gggg_i^{\mu\nu\lambda\sigma\alpha\beta\gamma\delta} + (\text{non-divergent parts})\,.\end{aligned} \tag{6.63}$$

9 As indicated, the figure 15 is given by 6! combinations of the Lorentz indices of Γ divided by 3! combinations of positions of the metric tensor and divided three times by 2! to account for the symmetry of the metric tensor in its Lorentz indices.

10 At this point, a certain order of the structures $ggg_i^{\mu\nu\lambda\sigma\alpha\beta}$ with κ_i or $\tilde{\kappa}_i$ as coefficients in equation (6.60) has been chosen.

11 The κ_i used here are not related to the ones in equation (6.60).

The pairwisely antisymmetric part is then written as

$$\begin{aligned}
\Gamma_{\text{tree}}^{[\mu\nu][\lambda\sigma][\alpha\beta][\gamma\delta]} = \quad & \frac{1}{4}\left(\kappa_{89} - \kappa_{90} - \kappa_{104} + \kappa_{105}\right) \gggg_1^{[\mu\nu][\lambda\sigma][\alpha\beta][\gamma\delta]} \\
& + \frac{1}{16}\left(\kappa_{56} - \kappa_{57} - \kappa_{59} + \kappa_{60} - \kappa_{71} + \kappa_{72}\right. \\
& \qquad + \kappa_{74} - \kappa_{75} - \kappa_{83} + \kappa_{84} + \kappa_{86} - \kappa_{87} \\
& \qquad \left. + \kappa_{98} - \kappa_{99} - \kappa_{101} + \kappa_{102}\right) \gggg_2^{[\mu\nu][\lambda\sigma][\alpha\beta][\gamma\delta]} \\
& + \frac{1}{4}\left(\kappa_{53} - \kappa_{54} - \kappa_{68} + \kappa_{69}\right) \gggg_3^{[\mu\nu][\lambda\sigma][\alpha\beta][\gamma\delta]} \\
& + \frac{1}{16}\left(\kappa_{25} - \kappa_{26} - \kappa_{28} + \kappa_{29} - \kappa_{40} + \kappa_{41}\right. \\
& \qquad + \kappa_{43} - \kappa_{44} - \kappa_{76} + \kappa_{77} + \kappa_{79} - \kappa_{80} \\
& \qquad \left. + \kappa_{91} - \kappa_{92} - \kappa_{94} + \kappa_{95}\right) \gggg_4^{[\mu\nu][\lambda\sigma][\alpha\beta][\gamma\delta]} \\
& + \frac{1}{16}\left(\kappa_{20} - \kappa_{21} - \kappa_{23} + \kappa_{24} - \kappa_{35} + \kappa_{36}\right. \\
& \qquad + \kappa_{38} - \kappa_{39} - \kappa_{47} + \kappa_{48} + \kappa_{50} - \kappa_{51} \\
& \qquad \left. + \kappa_{62} - \kappa_{63} - \kappa_{65} + \kappa_{66}\right) \gggg_5^{[\mu\nu][\lambda\sigma][\alpha\beta][\gamma\delta]} \\
& + \frac{1}{4}\left(\kappa_{17} - \kappa_{18} - \kappa_{32} + \kappa_{33}\right) \gggg_6^{[\mu\nu][\lambda\sigma][\alpha\beta][\gamma\delta]} ,
\end{aligned} \tag{6.64}$$

where $\gggg_i^{[\mu\nu][\lambda\sigma][\alpha\beta][\gamma\delta]}$ denote six independent pairwisely antisymmetric tensors. An analogous expression holds for the one-loop contribution. For example, $\gggg_1^{[\mu\nu][\lambda\sigma][\alpha\beta][\gamma\delta]}$ is given by

$$\begin{aligned}
\gggg_1^{[\mu\nu][\lambda\sigma][\alpha\beta][\gamma\delta]} = \; & g^{\alpha\sigma} g^{\beta\lambda} g^{\gamma\nu} g^{\delta\mu} - g^{\alpha\sigma} g^{\beta\lambda} g^{\gamma\mu} g^{\delta\nu} \\
& - g^{\alpha\lambda} g^{\beta\sigma} g^{\gamma\nu} g^{\delta\mu} + g^{\alpha\lambda} g^{\beta\sigma} g^{\gamma\mu} g^{\delta\nu} .
\end{aligned} \tag{6.65}$$

Each of the six prefactors in equation (6.64) at one-loop level needs to be absorbed in the corresponding coefficient at tree level simultaneously. This requires the same structures of coupling constants and therefore leads to the conditions for specific vertices, presented in the following sections.

Moreover, this procedure of antisymmetrization has been successfully cross-checked by pairwisely antisymmetrizing the whole expression first and then comparing coefficients of metric tensor products one by one.

The Vertex abcd = 3333.

The following prefactors of antisymmetric Lorentz structures are obtained at tree level and one-loop level:

Lorentz structure	Tree	Loop (divergent part)
	$-2d_5$	$-\frac{1}{\pi^2}\left(3d_3^2 - 4d_3d_4 + 2d_4^2 + 12d_5^2\right)$
	d_5	$\frac{1}{2\pi^2}\left(3d_3^2 - 4d_4d_3 + d_4^2 + 10d_5^2\right)$

The divergent part can only be absorbed if $d_4^2 + 2d_5^2 = 0$ holds, which is equivalent to

$$d_4 = d_5 = 0\,. \tag{6.66}$$

This result is used in the analysis of the following two vertices.

The Vertex abcd = 2233

The following prefactors of antisymmetric Lorentz structures are obtained at tree level and one-loop level:

Lorentz structure	Tree	Loop (divergent part)
	0	$-\frac{\left(M^4 + M_3^4\right)d_3^2}{16M^2M_3^2\pi^2}$

The divergent part must vanish, hence

$$d_3 = 0\,. \tag{6.67}$$

The Vertex abcd = 1111

The following prefactors of antisymmetric Lorentz structures are obtained at tree level and one-loop level:

Lorentz structure	Tree	Loop (divergent part)
	$-2d_1$	$-\frac{1}{4\pi^2}\left(72d_1^2 - 80d_2d_1 + 72d_2^2 + 6d_3^2\right)$
	d_1	$\frac{1}{4\pi^2}\left(32d_1^2 - 40d_2d_1 + 32d_2^2 + 3d_3^2\right)$

The divergent part can only be absorbed if $d_1^2 + d_2^2 = 0$ holds, which is equivalent to

$$d_1 = d_2 = 0\,. \tag{6.68}$$

Summary

All other non-mentioned vertices or Lorentz structures lead to either equivalent or trivial conditions. Collecting all the results above, one finds the conditions

$$d_1 = d_2 = d_3 = d_4 = d_5 = 0\,. \tag{6.69}$$

According to table 6.1 on page 50, the 13 parameters (including M and M_3) have been reduced due to equation (6.29) on page 54 and equation (6.69) to 2. All couplings g_i and d_i vanish and only the mass parameters remain. Therefore, no self-consistent interacting tensor model exists. Further implications of this result are discussed in chapter 8, and the findings of a cross-check starting from a global SU(2) symmetry are presented in the following section.

6.7 CONSISTENCY CHECK WITH GLOBAL SU(2) INVARIANCE

Using the fact that $d^{abc} \equiv 0$ and $f^{abc} = \epsilon^{abc}$ holds in SU(2), a global SU(2) invariance[12] is established by the following choice of coupling constants:

$$\begin{aligned} g^{abc} &= g_1 \epsilon^{abc}\,, & h_1^{abcd} &= f_1 \delta^{ac}\delta^{bd} + f_1' \delta^{ab}\delta^{cd}\,, \\ h_2^{abcd} &= f_2 \delta^{ac}\delta^{bd} + f_2' \delta^{ab}\delta^{cd}\,, & h_3^{abcd} &= f_3 \delta^{ac}\delta^{bd} + f_3' \delta^{ab}\delta^{cd}\,, \\ h_4^{abcd} &= f_4 \delta^{ac}\delta^{bd} + f_4' \delta^{ab}\delta^{cd}\,, & h_5^{abcd} &= f_5 \delta^{ac}\delta^{bd} + f_5' \delta^{ab}\delta^{cd}\,. \end{aligned} \tag{6.70}$$

Additionally, all three particles have the same mass, i.e. $M_3 = M$. Here, the three Lagrangians containing the product of Levi-Civita symbols are directly discarded owing to equation (6.9), i.e.

$$f_3 = f_3' = f_4 = f_4' = f_5 = f_5' = 0 \tag{6.71}$$

is set in equation (6.70) without loss of generality.[13]

12 Compare also chapter 5 and section A.1.

13 The calculation was also carried out *without* using equation (6.71) and it led to the same result.

No.	Fields	Factor in det $\mathcal{M}$	Inequality
1a	$W^1_{01} = x$	$8x^2(2f_1+f_2+2f_1'+f_2')+M^2$	$2f_1+f_2+2f_1'+f_2' \geq 0$
1b	$W^1_{12} = x$	$M^2-24x^2(2f_1+f_2+2f_1'+f_2')$	$2f_1+f_2+2f_1'+f_2' \leq 0$
2a	$W^1_{13} = x,$	$4x^2(4f_1+f_2)+M^2$	$4f_1+f_2 \geq 0$
	$W^3_{23} = x$	$M^2-4x^2(4f_1+f_2)$	$4f_1+f_2 \leq 0$
2b	$W^1_{01} = x,$	$M^4-36x^2g_1^2$	$g_1^2 \leq 0$
	$W^3_{23} = x$		

Table 6.3: Analysis of the determinant of $\mathcal{M}$ including global SU(2) symmetry. See table 6.2 on page 53 for further explanation.

A constraint analysis is carried out analogously to section 6.3 using the parameters given above.[14] One finds

$$g_1 = 0\,, \quad f_2 = -4f_1\,, \quad f_2' = 2(f_1 - f_1')\,. \tag{6.72}$$

Details for this analysis are given in table 6.3. Again, the three-vertex, which is determined by g_1, vanishes as do therefore all its one-loop contributions since in those a three-vertex is always present, see figure 6.1 on page 61.

Subsequently, the renormalizability analysis is restricted to the four-vertex. One can divide all vertices with non-vanishing divergences into two classes,

$$abcd \in \{1111, 2222, 3333\} \quad \text{and} \quad abcd \in \{1122, 1133, 2233, \dots\}\,, \tag{6.73}$$

where ... denotes more permutations. One finds that all Lorentz structures which *do not* appear at tree level vanish also at loop level after pairwise antisymmetrization. In order to ensure renormalizability, the linear combinations of coefficients at tree level need to be identical to the ones at loop level. This leads for the first class of vertices to one equation

$$2f_1^2 + \left(f_1 + f_1'\right)^2 = 0 \tag{6.74a}$$

14 However, note that in this section g_1 *does not* coincide with g_1 from the previous sections.

and for the second class to three equations:

$$f_1^2 + 4 f_1 f_1' = 0\,, \tag{6.74b}$$

$$2 f_1^2 - 2 f_1 f_1' + f_1'^2 = 0\,, \tag{6.74c}$$

$$f_1^2 - 6 f_1 f_1' + f_1'^2 = 0\,. \tag{6.74d}$$

Since equation (6.74a) can be interpreted as a parabolic surface in three dimensions which only intersects the $f_1 f_1'$ plane in the origin, all four equations are equivalent to

$$f_1 = f_1' = 0\,. \tag{6.75}$$

Employing these conditions in the constraint analysis again, one finds that $\det \mathcal{M} = (M^2)^9 \neq 0$, i.e. no further conditions can be deduced. In summary, twelve parameters in equation (6.70) (including M) have been reduced due to equations (6.72) and (6.75) to two. As in section 6.6, one finds that all three- and four-vertex functions vanish. This is consistent with the findings of the previous sections since the more restrictive global symmetry group SU(2) has been required here which should at least reproduce the results obtained by assuming the global symmetry group U(1) a priori.

7 MAGNETIC MOMENT OF THE RHO MESON

This chapter presents the calculation of the magnetic moment of the rho meson in the framework of chiral effective field theory up to order $\mathcal{O}(q^3)$. This is the first step towards form factors of vector mesons, which are helpful to describe a physical process depicted in figure 7.1. Furthermore, the results for the magnetic moment can, in principle, be used in Lattice QCD extrapolations. Simply speaking, Lattice QCD is another approach to non-perturbative QCD and regularizes the theory by discretizing the Minkowski space-time. Due to current limitations in computing power, results are calculated with pion masses of about $M \approx 300\,\text{MeV}$, i.e. far away from the physical value. Therefore, so-called chiral expansions are helpful to extrapolate the results obtained by Lattice QCD to physical values of the input parameters, such as the pion mass [79].

The chiral Lagrangians for pions and vector mesons discussed in the first part of this work are used. Some lengthier results are given in appendix C in order to keep the following presentation as clear as possible.

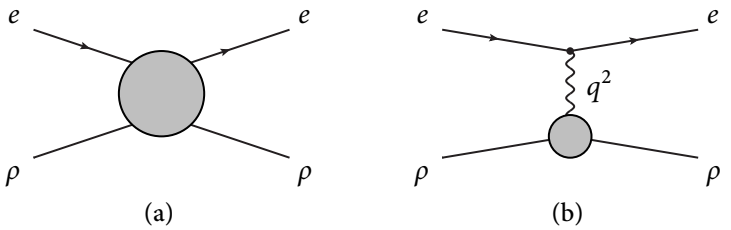

Figure 7.1: Exemplary subprocess to which the magnetic moment of the rho meson contributes. Process (a) represents a scattering process of an electron with a rho meson including all possible interactions, whereas process (b) represents the one-photon-exchange approximation, which is justified since the QED vertex is proportional to $\sqrt{\alpha} \approx 1/\sqrt{137} \ll 1$. The photon is represented by a wiggly line and carries the squared momentum q^2.

7.1 MODEL DEFINITION AND PRELIMINARY REMARKS

The inclusion of the lightest vector mesons in ChPT is a reasonable step in the construction of a chiral effective field theory. This was motivated in sections 2.2 and 2.3 and the introduced notation is employed here. Additionally, in figure 7.1b the incoming and outgoing large momenta of the rho meson are denoted as p_i and p_f, respectively, and the incoming photon momentum is q.

In this manner, the most general Lagrangian describing pions and vector mesons consistent with the assumed symmetries reads

$$\mathcal{L} = \mathcal{L}_\pi + \mathcal{L}_{\rho\pi} + \mathcal{L}_{\omega\rho\pi} + \dots\,, \tag{7.1}$$

where

$$\mathcal{L}_\pi = \frac{F^2}{4}\,\mathrm{Tr}\Big[D_\mu U\big(D^\mu U\big)^\dagger\Big] + \frac{F^2M^2}{4}\,\mathrm{Tr}\Big(U+U^\dagger\Big)\,, \tag{7.2a}$$

$$\begin{aligned}\mathcal{L}_{\rho\pi} = {}& -\frac{1}{2}\,\mathrm{Tr}\big(\rho_{\mu\nu}\rho^{\mu\nu}\big) + id_x\,\mathrm{Tr}\big(\rho_{\mu\nu}\Gamma^{\mu\nu}\big) + f_V\,\mathrm{Tr}\big(\rho_{\mu\nu}f_+^{\mu\nu}\big)\\ & + \frac{M_\rho^2 + c_xM^2\,\mathrm{Tr}(U+U^\dagger)/4}{g^2}\,\mathrm{Tr}\Big[\big(g\rho_\mu - i\Gamma_\mu\big)\big(g\rho^\mu - i\Gamma^\mu\big)\Big]\\ & + i\frac{g_{\rho\pi}}{g^2}\,\mathrm{Tr}\Big[\big(g\rho_\mu - i\Gamma_\mu\big)\big(g\rho_\nu - i\Gamma_\nu\big)f_+^{\mu\nu}\Big]\,,\end{aligned} \tag{7.2b}$$

$$\mathcal{L}_{\omega\rho\pi} = -\frac{1}{4}\omega_{\mu\nu}\omega^{\mu\nu} + \frac{M_\omega^2}{2}\omega_\mu\omega^\mu + \frac{F}{2}g_{\omega\rho\pi}\epsilon_{\mu\nu\alpha\beta}\omega^\nu\,\mathrm{Tr}\big(\rho^{\alpha\beta}u^\mu\big)\,. \tag{7.2c}$$

Here, only terms relevant to the calculation of the magnetic moment have been taken into account. Furthermore, the building block χ has been replaced by the square of the pion mass M^2, which is allowed within the desired accuracy of this calculation. Note that, for practical reasons, the definition of the LEC f_V is slightly different from the usual one, e.g. in [68]. The usual definition can be obtained by the replacement $f_V \to -f_V/(2\sqrt{2})$.

As already mentioned, the Kawarabayashi-Suzuki-Riazuddin-Fayyazuddin relation (KSRF) [63, 64] of the bare parameters is used to eliminate the pion decay constant F in the chiral limit from the results,

$$M_\rho^2 = 2g^2F^2\,. \tag{7.3}$$

Additionally, the term proportional to c_x in equation (7.2b) leads to a modification of the undressed rho meson propagator as follows

$$\frac{-i}{p^2 - (M_\rho^2 + c_xM^2)}\Big(g^{\mu\nu} - \frac{p^\mu p^\nu}{M_\rho^2 + c_xM^2}\Big)\,, \tag{7.4}$$

which transforms to the standard propagator for vector fields in the case $c_x = 0$, where M_ρ^2 is the squared mass of the rho meson in the chiral limit. Fortunately, FeynArts provides a technique to implement this modification easily. Since the physical mass of the rho meson is given by the pole of the dressed propagator, the on-mass-shell condition for an external rho momentum reads

$$p^2 = M_\rho^2 + c_x M^2 + \mathcal{O}(\hbar)\,, \tag{7.5}$$

where $\mathcal{O}(\hbar)$ denotes loop contributions.

Note that the so-called conventional dimensional regularization has been used here and henceforth and *not* dimensional reduction. This is favorable in computer-assisted calculations. In particular, the Levi-Civita symbol $\epsilon^{\mu\nu\lambda\sigma}$ in equation (7.2c) is treated as D-dimensional in contractions.[1] Consequently, these two methods yield different coefficients for finite terms, i.e. terms not proportional to a loop integral. Note that FeynCalc *does* treat the Levi-Civita symbol four-dimensionally by default, but FeynArts does *not*.

7.2 POWER COUNTING

As explained in section 3.1, the power counting takes all possible fluxes of external large momenta into account. Hence, they are shown for all one-loop topologies contributing to the self-energy and the magnetic moment in figures C.1 and C.2, respectively. For completeness, it is assumed that the external photon carries a small momentum, whereas the external rho mesons carry large momenta. The polarization vector of the photon ϵ^μ is counted as $\mathcal{O}(q^1)$, which implies that the covariant derivative D^μ can also be counted consistently as $\mathcal{O}(q^1)$. The last assignment is merely a convention since the polarization vector is an overall factor according to the LSZ formalism. However, this small quantity is included in the total accuracy of the calculation, namely $\mathcal{O}(q^3)$, but *not* in the orders given for the diagrams in figures 7.3 and 7.4.

An example shall illustrate the power counting scheme outlined in section 3.1. To this end, the one-loop diagram (13) in figure 7.4 is chosen. The rho meson is represented by a straight line, the pion by a dashed line, the external photon by a wiggly line and the omega meson by a curly

1 Conventional dimensional regularization is discussed in [70], based on [69]. For dimensional reduction see [80]. See also [81] for a comparison of the two schemes and more references.

line. The three possible cases and the resulting order of the vertices are discussed in the following separate paragraphs using the Feynman rules given in section C.1 on page 105. Here, fluxes of large momenta have already been indicated by thicker lines.

(1)

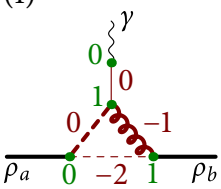

The $\gamma\rho$ vertex counts as $\mathcal{O}(q^0)$, since its leading order is $M_\rho^2 g^{\mu\nu}$. The $\rho\pi\pi$ vertex counts as $\mathcal{O}(q^0)$, since one of the pion momenta is large. Both $\omega\rho\pi$ vertices count as $\mathcal{O}(q^1)$, since either the ρ momentum or the π momentum is small, but not both. In total this yields $4 + 1 + 1 - 1 - 2 = 3$.

(2)

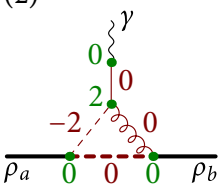

The $\gamma\rho$ vertex and the $\rho\pi\pi$ vertex are assigned the same order as for the first case. The upper $\omega\rho\pi$ vertex counts as $\mathcal{O}(q^2)$, since the ρ and the π momentum are both small. The lower $\omega\rho\pi$ vertex counts as $\mathcal{O}(q^0)$, since the ρ and the π momentum are both large. In total this yields $4 + 2 - 2 = 4$.

(3)

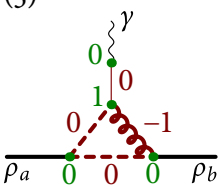

The $\gamma\rho$ vertex, the $\rho\pi\pi$ vertex and the upper $\omega\rho\pi$ vertex are assigned the same order as for the first case. All other vertices count as $\mathcal{O}(q^0)$, since there are always large momenta involved. In total this yields $4 + 1 - 1 = 4$.

In summary, the order $\mathcal{O}(q^3)$ is assigned to the diagram as the lowest order resulting from these three cases, excluding the order stemming from the polarization vector. This procedure has been carried out for each diagram in figure 7.4. Owing to the power counting of the corresponding propagators in table 3.1 on page 22, the lowest orders are usually obtained if pions carry small momenta and vector mesons large ones.

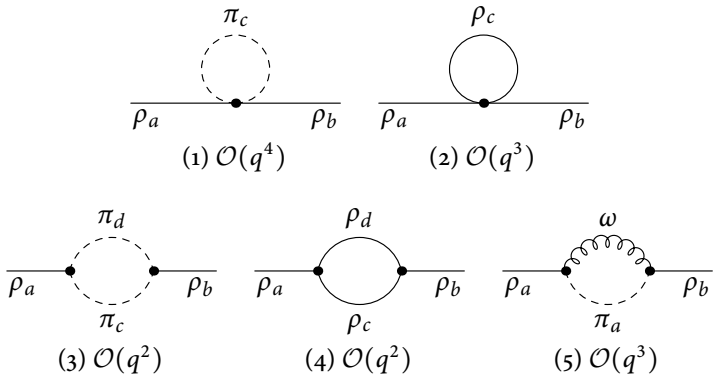

Figure 7.2: One-particle irreducible diagrams contributing to the two-point function of the rho meson.

7.3 TWO-POINT FUNCTION

The wave function renormalization constant Z_ρ is defined as the residue at the pole z_0 of the dressed propagator

$$D^{ab}_{\mu\nu}(p) = \delta^{ab}\frac{g_{\mu\nu} - p_\mu p_\nu/z_0}{p^2 - z_0}Z_\rho + (\text{non-pole parts})\,. \tag{7.6}$$

The sum of all one-particle-irreducible diagrams in figure 7.2 of the two-point function can be parametrized as

$$i\Pi^{ab}_{\mu\nu} = i\delta^{ab}\big[g_{\mu\nu}\Pi_1 + (g_{\mu\nu}p^2 - p_\mu p_\nu)\Pi_2(p^2)\big]\,, \tag{7.7}$$

where Π_1 is independent of p^2 and $\Pi_2(p^2)$ is regular at $p^2 = 0$. In terms of equation (7.7), the wave function renormalization constant of the rho meson reads[2]

$$Z_\rho = \frac{1}{1 - \Pi_2(z_0) - z_0\Pi_2'(z_0)} = 1 + \underbrace{\Pi_2(z_0) + z_0\Pi_2'(z_0)}_{=\delta Z_\rho} + \mathcal{O}(\hbar^2)\,, \tag{7.8}$$

where $\mathcal{O}(\hbar^2)$ denotes higher-order loop corrections.

2 The result is obtained by writing the dressed propagator symbolically as a self-similar series $iD = iD_0 + iD_0\, i\Pi\, iD_0 + iD_0\, i\Pi\, iD_0\, i\Pi\, iD_0 + \cdots = iD_0 + iD\, i\Pi\, iD_0$, where iD_0 is the undressed propagator in equation (7.4) and $i\Pi$ is the sum of all one-particle-irreducible diagrams in equation (7.7). The Lorentz structure can be taken into account by using a suitable ansatz for D as shown for the propagator in section 6.5. Since only the pole part is of interest, $i\Pi$ is expanded around $p^2 = z_0$.

Noting that equations (7.4) and (7.6) imply $z_0 = M_\rho^2 + c_x M^2 + \mathcal{O}(\hbar)$ and using the approximation $M_\rho \approx M_\omega$, the explicit calculation yields

$$\begin{aligned}
\delta Z_\rho = &-\frac{g^2}{576\pi^2 M_\rho^4 (M_\rho^2 + c_x M^2)} \Big\{ -258 M_\rho^4 A_0(M^2 c_x + M_\rho^2) \\
&- 24 A_0(M^2)(g d_x - 1)(3 g d_x - 1)(M^2 c_x + M_\rho^2)^2 \\
&+ (M^2 c_x + M_\rho^2)\big[12(g d_x - 1)(M^2 c_x + M_\rho^2) \\
&\quad \times B_0(M^2 c_x + M_\rho^2, M^2, M^2) \\
&\quad \times (M^2(3g(c_x - 2)d_x - c_x - 2) + M_\rho^2(3 g d_x - 1)) \\
&\quad + 99 M_\rho^4 B_0(M^2 c_x + M_\rho^2, M^2 c_x + M_\rho^2, M^2 c_x + M_\rho^2) \\
&\quad + 8 M^2 (c_x - 3) M_\rho^2 (g d_x - 1)(3 g d_x + 1) \\
&\quad + 4 M^4 (c_x - 6) c_x (g d_x - 1)(3 g d_x + 1) \\
&\quad + M_\rho^4 (4 g d_x (3 g d_x - 2) + 109)\big]\Big\} \\
&- \frac{g_{\omega\rho\pi}^2}{288\pi^2 (M_\rho^2 + c_x M^2)} \Big\{ -3 A_0(M_\rho^2)\big[2 M^2 c_x + M_\rho^2 + M^2\big] \\
&+ 3 A_0(M^2)\big[M^2(1 - 2c_x) - 3 M_\rho^2\big] \\
&- \big[M^2(17 c_x - 24) - 7 M_\rho^2\big]\big[M^2 c_x + M_\rho^2\big] \\
&+ 3 M^2\big[(3 c_x + 1) M_\rho^2 + M^2 (c_x - 1)(2 c_x + 1)\big] \\
&\quad \times B_0(M^2 c_x + M_\rho^2, M^2, M_\rho^2)\Big\} .
\end{aligned} \tag{7.9}$$

The above result is used in the calculation of the magnetic moment according to the LSZ formalism. This is detailed in the following section.

7.4 MAGNETIC MOMENT

In this section, the diagram depicted in figure 7.1a is calculated for $q^2 = 0$ in the one-photon-exchange approximation. To this end, the amplitude of the sub-diagram represented by the „blob“ in figure 7.1b is written as

$$\mathcal{M}^\lambda = \mathcal{M}_1^{a_1 \alpha} (-i) D_{\alpha\mu}^{a_1 a}(p_\mathrm{f}) \epsilon^{3ab} V^{\lambda\mu\nu}(p_\mathrm{f}, p_\mathrm{i}, q)(-i) D_{\nu\beta}^{b b_1}(p_\mathrm{i}) \mathcal{M}_2^{b_1 \beta} , \tag{7.10}$$

where $\mathcal{M}_1^{a_1 \alpha}$ and $\mathcal{M}_2^{b_1 \beta}$ are the polarization vectors of the outgoing and incoming rho meson, respectively, and the dressed propagator from equation (7.6) has been used. The SU(2) structure ϵ^{3ab} has already been

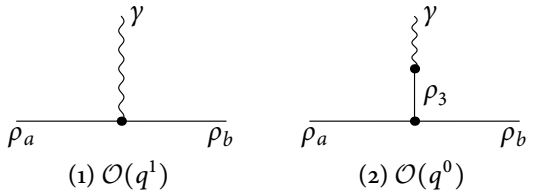

Figure 7.3: Tree diagrams contributing to the magnetic moment of the rho meson. Their order can be directly read off the corresponding Feynman rules.

separated from the vertex V. Next, the $\gamma\rho\rho$ vertex can be parametrized as

$$V^{\lambda\mu\nu}(p_\mathrm{f}, p_\mathrm{i}, q) = \sum_j t_j^{\lambda\mu\nu} V_j(p_\mathrm{f}^2, p_\mathrm{i}^2, q^2)\,, \tag{7.11}$$

where $t_j^{\lambda\mu\nu}$ are Lorentz structures. Expanding each V_j around the pole z_0 and substituting equation (7.6) in equation (7.10), the leading pole contribution is obtained as

$$\begin{aligned}\mathcal{M}^\lambda_\mathrm{pole} = &-\epsilon^{3ab}\mathcal{M}_1^{a\,\alpha} Z_\rho \frac{g_{\alpha\nu} - p_{\mathrm{f}\,\alpha} p_{\mathrm{f}\,\nu}/z_0}{p_\mathrm{f}^2 - z_0} \\ &\times \sum_j t_j^{\lambda\mu\nu} V_j(z_0, z_0, q^2) Z_\rho \frac{g_{\mu\beta} - p_{\mathrm{i}\,\mu} p_{\mathrm{i}\,\beta}/z_0}{p_\mathrm{i}^2 - z_0} \mathcal{M}_2^{b\,\beta}\,.\end{aligned} \tag{7.12}$$

In order to properly renormalize the $\gamma\rho\rho$ vertex function according to the LSZ reduction formula [44], equation (7.12) is rewritten as

$$\begin{aligned}\mathcal{M}^\lambda_\mathrm{pole} = &-\epsilon^{3ab}\sqrt{Z_\rho}\mathcal{M}_1^{a\,\alpha} \frac{g_{\alpha\nu} - p_{\mathrm{f}\,\alpha} p_{\mathrm{f}\,\nu}/z_0}{p_\mathrm{f}^2 - z_0} \\ &\times \sqrt{Z_\rho} \sum_j t_j^{\lambda\mu\nu} V_j(z_0, z_0, q^2) \sqrt{Z_\rho} \\ &\times \frac{g_{\mu\beta} - p_{\mathrm{i}\,\mu} p_{\mathrm{i}\,\beta}/z_0}{p_\mathrm{i}^2 - z_0} \sqrt{Z_\rho} \mathcal{M}_2^{b\,\beta}\,,\end{aligned} \tag{7.13}$$

so that the renormalized vertex function is given by

$$\begin{aligned}\sqrt{Z_\rho} \sum_j t_j^{\lambda\mu\nu} V_j(z_0, z_0, q^2) \sqrt{Z_\rho} &= Z_\rho V^{\lambda\mu\nu}(p_\mathrm{i}, p_\mathrm{f}, q) \\ &= -\Gamma^{\lambda\mu\nu}(p_\mathrm{i}, p_\mathrm{f}, q)\,.\end{aligned} \tag{7.14}$$

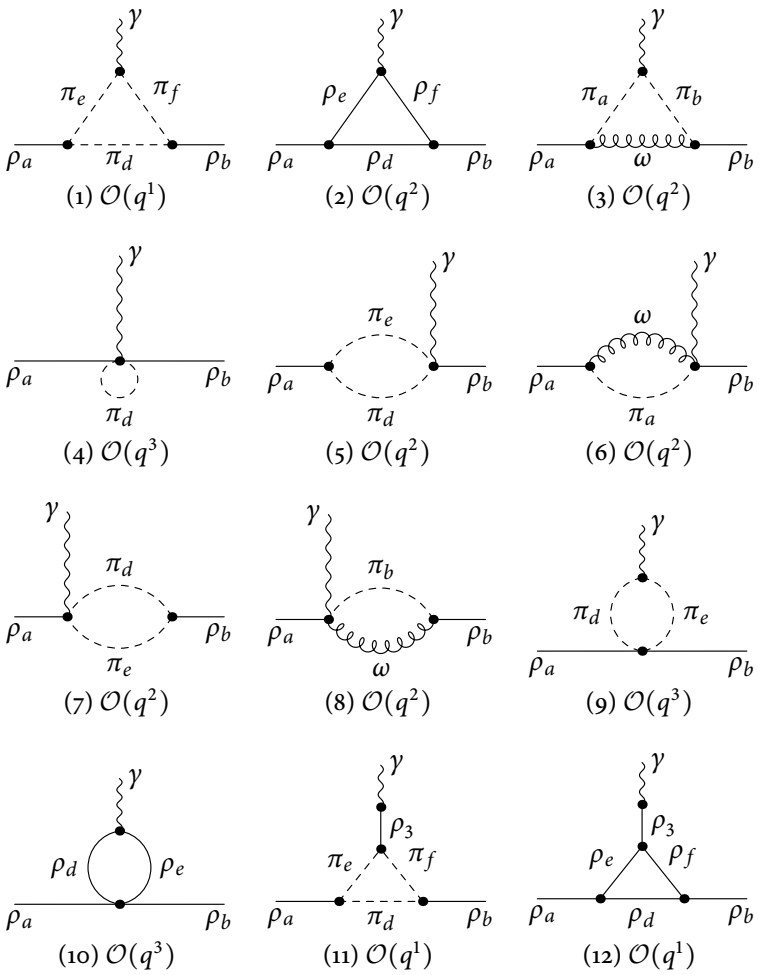

Figure 7.4: One-particle-irreducible loop diagrams contributing to the magnetic moment of the rho meson. Continued on page 79.

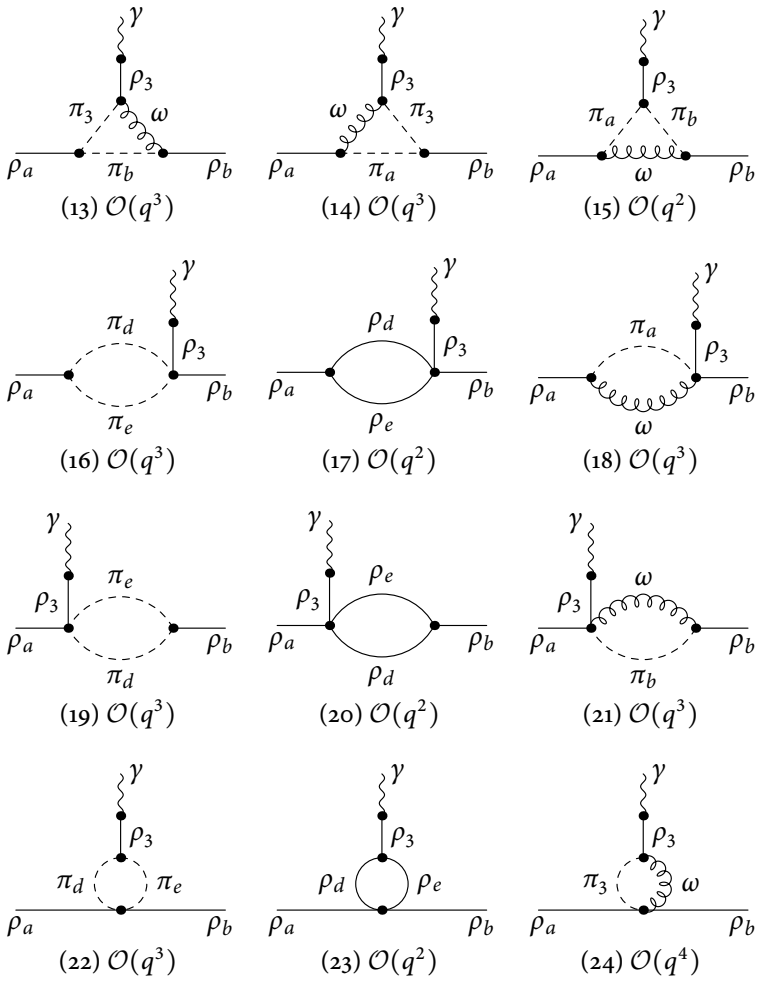

Figure 7.4: One-particle-irreducible loop diagrams contributing to the magnetic moment of the rho meson. (Cont.)

Noting that structures like $p_\mu D^{\mu\nu}(p)$ do not have a pole according to equation (7.6), structures containing p_i^μ or p_f^ν in $\Gamma^{\mu\nu\lambda}$ are dropped. Next, the „on-mass-shell" part of the vertex function Γ defined in equation (7.14) is parametrized as

$$\Gamma^{\mu\nu\lambda}(p_\mathrm{i}, p_\mathrm{f}, q) = f_1(q^2)(p_\mathrm{i}^\lambda + p_\mathrm{f}^\lambda)g^{\mu\nu} + f_2(q^2)(q^\nu g^{\lambda\mu} - q^\mu g^{\lambda\nu})\,, \quad (7.15)$$

where other Lorentz structures do not appear due to symmetries and gauge invariance. Here, the momenta p_i and q are defined as incoming and the momentum p_f is defined as outgoing. In particular, the on-shell condition

$$q_\lambda \Gamma^{\mu\nu\lambda} = 0\,, \quad (7.16)$$

which corresponds to the conservation of the U(1) current of quantum electrodynamics, justifies the parametrization in equation (7.15). This structure has been checked for the sum of the calculated diagrams. The electric charge e and the magnetic moment μ_ρ are then defined by $f_1(0)$ and $f_2(0)$ as

$$f_1(0) = e\,, \quad (7.17a)$$
$$f_2(0) = 2M_\rho \mu_\rho\,. \quad (7.17b)$$

According to equation (7.14), there are tree and loop contributions in these quantities, which are sorted symbolically in orders of $\hbar$ as follows:

$$\begin{aligned}\Gamma^{\mu\nu\lambda} &= -\big(1 + \hbar\delta Z_\rho\big)\big(V_\mathrm{tree}^{\lambda\mu\nu} + \hbar V_\mathrm{loop}^{\lambda\mu\nu}\big) + \mathcal{O}(\hbar^2) \\ &= -V_\mathrm{tree}^{\lambda\mu\nu} - \hbar\big(\delta Z_\rho V_\mathrm{tree}^{\lambda\mu\nu} + V_\mathrm{loop}^{\lambda\mu\nu}\big) + \mathcal{O}(\hbar^2)\,.\end{aligned} \quad (7.18)$$

The Feynman diagrams at tree level for $V_\mathrm{tree}^{\lambda\mu\nu}$ are given in figure 7.3 and at one-loop level for $V_\mathrm{loop}^{\lambda\mu\nu}$ in figure 7.4.

Finally, at tree level, the form factors are obtained as

$$f_1^\mathrm{tree}(0) = e\,, \quad (7.19a)$$
$$f_2^\mathrm{tree}(0) = e\big[2 + g_{\rho\pi} - g(d_x + 2f_V)\big]\,. \quad (7.19b)$$

Taking the tree-order results times the wave function renormalization constant according to equation (7.18) into consideration, one finds at one-loop level

$$f_1^\mathrm{loop}(0) = 0\,. \quad (7.20a)$$

This result is expected and serves as a reliable cross-check since hadronic corrections cannot contribute to the electric charge due to the Ward identity of quantum electrodynamics [46]. In the same way, using again the approximation $M_\omega \approx M_\rho$, the magnetic moment of the rho meson is obtained as

$$\begin{aligned} f_2^{\text{loop}}(0) = {} & \frac{e g^2}{576\pi^2 M_\rho^4 (M^2 c_x + M_\rho^2)} \Xi_1 \\ & + \frac{e g_{\omega\rho\pi}^2}{576\pi^2 M_\rho^2 (M_\rho^2 - M^2)} \Xi_2 \,, \end{aligned} \tag{7.20b}$$

where the lengthy expressions Ξ_1 and Ξ_2 are given in section C.3 on page 110.

Regarding power counting, the maximum order of terms to be taken into account in equation (7.18) is $\mathcal{O}(q^2)$, since the total accuracy is of order $\mathcal{O}(q^3)$ where the polarization vector counts as $\mathcal{O}(q^1)$ as an overall prefactor. This translates for the form factor f_1 to order $\mathcal{O}(q^2)$ and for the form factor f_2 to $\mathcal{O}(q^1)$ according to equation (7.15). Moreover, there is an important point concerning the power counting order of the wave function renormalization constant. Referring to equation (7.8), the minimal order of $\Pi_2(z_0)$ and $\Pi_2'(z_0)$ determines the order of Z_ρ since $z_0 = M_\rho^2 + \mathcal{O}(\hbar, q)$ is of order $\mathcal{O}(q^0)$. These two quantities can be seen as the coefficients of a Taylor expansion around $p^2 = z_0$ of the two-point function as follows:

$$\Pi_2(p^2) = \Pi_2(z_0) + \underbrace{(p^2 - z_0)}_{\mathcal{O}(q^1)} \Pi_2'(z_0) + \mathcal{O}\big((p^2 - z_0)^2\big) \,. \tag{7.21}$$

Since the tree level diagrams in figure 7.3 start with $\mathcal{O}(q^0)$, the wave function renormalization constant δZ_ρ contributes with $\mathcal{O}(q^2)$ in equation (7.18). By virtue of equation (7.21), this translates to $\mathcal{O}(q^3)$ as the maximum order of relevant diagrams in figure 7.2. Note that all these power counting considerations are only valid for particular expressions if the contributions of the diagrams are renormalized such that they respect their assigned chiral order. This is dealt with in the following section.

7.5 REFORMULATED INFRARED REGULARIZATION

The next step is to calculate the subtraction terms as explained in section 3.2 in order to give IR regularized expressions for the results in equation (7.20b) up to order $\mathcal{O}(q^1)$. Furthermore, one can check the correct calculation of subtraction terms up to order $\mathcal{O}(q^2)$ by virtue of equation (7.20a), since the IR regularization scheme satisfies the Ward identities. Nevertheless, there is a subtle point in calculating the subtraction terms for the wave function renormalization constant. It is not correct to calculate them on the basis of the per-diagram expressions in table C.1. During the derivation of equation (7.9), the relation for $\partial B_0/\partial p^2$ in equation (A.11) on page 97 has been used, which is only valid in $n = 4$ dimensions. However, this relation must not be used in the calculation of subtraction terms, where the expansion around $n = 4$ must take place as a last step. Consequently, one needs to calculate the subtraction terms off-mass-shell up to order $\mathcal{O}(q^3)$—noting that $p^2 - M_\rho^2$ is of order $\mathcal{O}(q^1)$—*before* taking the derivative with respect to p^2. Additionally, a similar complication appears in the case of diagrams for the magnetic moment. After the Passarino-Veltman reduction of tensor integrals, the small squared photon momentum q^2 can appear in the denominator as a so-called Gram determinant. Therefore, a numerator X containing loop integrals needs to be expanded around q^2 as $q^2 \to 0$, namely

$$\lim_{q^2\to 0} \frac{X}{q^2} = \lim_{q^2\to 0} \frac{1}{q^2}\Bigg(\underbrace{X|_{q^2=0}}_{=0} + \left.\frac{\partial X}{\partial q^2}\right|_{q^2=0} q^2 + \dots \Bigg) = \left.\frac{\partial X}{\partial q^2}\right|_{q^2=0} . \quad (7.22)$$

In other words, the derivatives of scalar one-loop integrals[3] are needed with respect to their momentum arguments. Again, one must not use formulas expressing the derivatives of C_0 integrals in terms of A_0 and B_0 integrals including finite parts stemming from $n \to 4$. Finally, one can resort to calculating the subtraction terms in n dimensions for arbitrary q^2 and then taking the limit $q^2 \to 0$. Note that this implies using the Passarino-Veltman reduction in n dimensions.[4] As a last step, the expression is expanded around $n = 4$.

3 See section A.2 on page 96 for the definition of the scalar loop integrals.

4 This is stressed here since FeynCalc takes the limit $n \to 4$ after Passarino-Veltman reduction by default, i.e. it automatically adds the finite terms from dimensional regularization.

In order to illustrate this, the test case is considered where only terms proportional to $g_{\omega\rho\pi}^2$ are taken into account and c_x is set to zero. Referring to the Feynman diagrams in figures 7.2 and 7.4, one concludes that only diagram (5) of the two-point function and diagram (15) of the magnetic moment contribute to f_1^{loop} up to order $\mathcal{O}(q^2)$.[5] Fortunately, the calculation of subtraction terms in this case necessitates only the expansion of one-point and two-point scalar loop integrals. Consequently, they read

$$\delta Z_\rho^{\text{sub, (5)}} = -\frac{g_{\omega\rho\pi}^2 M_\rho^2}{288\pi^2}\Big[3\ln(M_\rho^2) - 7\Big] + \mathcal{O}(q^3)\,, \tag{7.23a}$$

$$f_1(0)^{\text{sub, (15)}} = -\frac{e g_{\omega\rho\pi}^2}{288\pi^2}\Big[7M_\rho^2 + 3(M_\rho^2 + 3M^2)\ln(M_\rho^2) + 9M^2\Big] + \mathcal{O}(q^3)\,. \tag{7.23b}$$

Here and henceforth, the scale has been set to $\mu = 1\,\text{GeV}$ and divergences proportional to λ in equation (A.10) have not been shown. Next, the IR regularized expressions are obtained by subtracting the terms in equations (7.23a) and (7.23b) from the corresponding unrenormalized expressions in tables C.1 and C.2 on pages 112–113, respectively, and expanding the result up to M^2 with the help of the analytical expressions in equations (A.8) and (A.9) on pages 96–97. They read

$$\delta Z_\rho^{\text{IR, (5)}} = -\frac{(g_{\omega\rho\pi}^{\text{IR}})^2 M^2}{32\pi^2}\Big[\ln(M^2) + 3\Big] + \mathcal{O}(M^3)\,, \tag{7.24a}$$

$$f_1(0)^{\text{IR, (15)}} = \frac{e(g_{\omega\rho\pi}^{\text{IR}})^2 M^2}{32\pi^2}\Big[\ln(M^2) + 3\Big] + \mathcal{O}(M^3)\,. \tag{7.24b}$$

According to equations (7.18), (7.19a), and (7.20a) and to the fact that reformulated IR regularization preserves symmetries up to higher order, the condition

$$f_1(0)^{\text{IR, (15)}} + e\,\delta Z_\rho^{\text{IR, (5)}} = 0 + \mathcal{O}(M^3) \tag{7.25}$$

must hold, which is indeed true for equations (7.24a) and (7.24b). After the standard Passarino-Veltman reduction in n dimensions, it is convenient to analyze first which subtraction terms of the loop integrals are needed in particular. As motivated in equation (7.22), one can already set the external rho momenta on-shell, $p_{\text{i/f}}^2 = M_\rho^2 + c_x M^2$, whereas the

5 Compare also the particular contributions to $f_1(0)$ of each diagram in table C.2 on page 113 in the appendix.

photon momentum q^2 should be kept off shell. The analysis is achieved by replacing each specific scalar one-loop integral by a dummy series of sufficient[6] order, e.g.

$$\begin{aligned} &C_0(M_\rho^2 + c_x M^2, q^2, M_\rho^2 + c_x M^2, M^2, M^2, M^2) \\ &\qquad \to \mathcal{C}_0 + \aleph\mathcal{C}_1 + \aleph^2\mathcal{C}_2 + \aleph^3\mathcal{C}_3 + \dots , \end{aligned} \tag{7.26}$$

where $\aleph$ counts the small quantities and the $\mathcal{C}_i$ are unique with respect to the loop integral and its arguments. Next, small quantities in the prefactors of the integrals are identified with the replacements

$$\begin{aligned} M &\to \aleph M , \\ p_{\mathrm{i/f}}^2 &\to M_\rho^2 + \aleph(p_{\mathrm{i/f}}^2 - M_\rho^2) , \\ q^2 &\to \aleph^2 q^2 , \end{aligned} \tag{7.27}$$

where $p_{\mathrm{i/f}}$ denotes an external, not necessarily on-shell rho momentum and q^2 the squared photon momentum. Subsequently, the whole expression is expanded around $\aleph = 0$ up to order $\mathcal{O}(\aleph^2)$ and, afterwards, $\aleph$ is discarded by setting $\aleph = 1$. For diagram (11) in figure 7.4, this analysis leads to an expression which contains $\mathcal{C}_0, \mathcal{C}_1, \mathcal{C}_2$. Hence, the subtraction terms for the integral[7]

$$C_0(M_\rho^2 + c_x M^2, q^2, M_\rho^2 + c_x M^2, M^2, M^2, M^2) \tag{7.28}$$

up to order $\mathcal{O}(q^2)$ need to be calculated.

The procedure is carried out in a standard way [82] by using the Feynman parametrization

$$\frac{1}{p} = -i \int_0^\infty e^{ipx} dx , \tag{7.29a}$$

for the three propagator terms, integrating over $d^n k$ by using

$$\int d^n k \exp\Big(iAk^2 + 2iBk\Big) = i^{1-n/2} \pi^{n/2} A^{-n/2} \exp\Big(-i\frac{B^2}{A}\Big) , \tag{7.29b}$$

after interchanging both the integrations, substituting the Feynman parameters x_i by

$$x_1 = \lambda\xi_1 , \quad x_2 = \lambda(1-\xi_1)\xi_2 , \quad x_3 = \lambda(1-\xi_1)(1-\xi_2) , \tag{7.29c}$$

6 In practical calculations a maximum order of 10 was chosen.

7 See equation (A.12) on page 98 for its standard definition. Here, the $+i0^+$ prescription is noted explicitly again.

and, finally, integrating over λ by using

$$\int_0^\infty d\lambda \lambda^\alpha e^{-i\beta\lambda} = i^{-\alpha-1}\Gamma(\alpha+1)\beta^{-\alpha-1}. \tag{7.29d}$$

One obtains

$$\begin{aligned} &C_0(M_\rho^2 + c_x M^2, q^2, M_\rho^2 + c_x M^2, M^2, M^2, M^2) \\ &\quad = -(2\pi\mu)^{n-4}\pi^{n/2-2}\Gamma(3-n/2)\int_0^1 d\xi_1 d\xi_2\,(1-\xi_1) \\ &\qquad \times \Big[(M^2 - i0^+) - (M_\rho^2 + c_x M^2)\xi_1(1-\xi_1) \\ &\qquad\quad - q^2(1-\xi_1)^2(1-\xi_2)\xi_2\Big]^{n/2-3}. \end{aligned} \tag{7.30}$$

According to the reformulated IR regularization scheme, the integrand in equation (7.30) is expanded in small Lorentz-invariant quantities in order to obtain the subtraction terms. To this end, after employing the replacements in equation (7.27), the integrand is expanded up to $\aleph^2$ and, afterwards, $\aleph = 1$ is set. This yields

$$\begin{aligned} &C_0(M_\rho^2 + c_x M^2, q^2, M_\rho^2 + c_x M^2, M^2, M^2, M^2)^{\text{sub}} \\ &\quad = -(2\pi\mu)^{n-4}\pi^{n/2-2}\Gamma(3-n/2)\int_0^1 d\xi_1 d\xi_2\,(1-\xi_1) \\ &\qquad \times \Big\{\Big[-\xi_1(1-\xi_1)M_\rho^2 - i0^+\Big]^{n/2-3} \\ &\qquad\quad + \Big[n/2-3\Big]\Big[-\xi_1(1-\xi_1)M_\rho^2 - i0^+\Big]^{n/2-4} \\ &\qquad\qquad \times \Big[-q^2(1-\xi_1)^2(1-\xi_2)\xi_2 + M^2(1-c_x\xi_1(1-\xi_1))\Big]\Big\}. \end{aligned} \tag{7.31}$$

At this point, one respects the $-i0^+$ boundary condition correctly by using the auxiliary relation

$$\Big[-\xi_1(1-\xi_1)M_\rho^2 - i0^+\Big]^x = e^{-i\pi x}\xi_1^x(1-\xi_1)^x\Big(M_\rho^2\Big)^x, \tag{7.32}$$

where x is either $(n/2-3)$ or $(n/2-4)$. Note that the term $-\xi_1(1-\xi_1)M_\rho^2$ is always non-positive since the integration variable ξ_1 ranges between 0 and 1. Consequently, the integration over ξ_2 is trivial in equation (7.31) and the integration over ξ_1 can be carried out by employing the formula [83]

$$\int_0^1 d\xi_1 \xi_1^\alpha (1-\xi_1)^\beta = \frac{\Gamma(\alpha+1)\Gamma(\beta+1)}{\Gamma(\alpha+\beta+2)}. \tag{7.33}$$

The expansion around $n = 4$ is only necessary up to order $(n-4)^0$ for loop integrals since the n-dependent prefactors of the full expression cannot contain terms proportional to $1/(n-4)$. However, note that x in equation (7.32) is n-dependent, which leads to the correct imaginary parts of the subtraction terms due to the factor $e^{-i\pi x}$. Eventually, the first three coefficients in equation (7.26) are obtained as

$$\begin{aligned}
\mathcal{C}_0 &= \frac{1}{M_\rho^2}\Big[\ln\big(M_\rho^2\big) + 1 - i\pi\Big]\,, \\
\mathcal{C}_1 &= 0 \quad \text{(all odd coefficients vanish)}\,, \\
\mathcal{C}_2 &= \frac{q^2}{6M_\rho^4}\Big[\ln\big(M_\rho^2\big) + 2 - i\pi\Big] \\
&\quad - \frac{M^2}{M_\rho^4}\Big[(c_x - 2)\ln\big(M_\rho^2\big) - i\pi(c_x - 2) + 2\Big]\,.
\end{aligned} \tag{7.34}$$

By neglecting all diagrams in figure 7.4 with order $\mathcal{O}(q^3)$ or higher,[8] one finds that *after* the reformulated infrared reformulation procedure only diagram (15) contributes to $f_1^{\mathrm{IR}}(0)$ and $f_2^{\mathrm{IR}}(0)$ and the contribution of diagram (3) in figure 7.2 to $\delta Z_\rho^{\mathrm{IR}}$ vanishes. Hence, the already verified consistency condition in equation (7.25) stays the same if taking all diagrams into account. Finally, the result for the gyromagnetic ratio in reformulated infrared regularization reads

$$\begin{aligned}
f_2^{\mathrm{IR}}(0)/e &= \frac{1}{e}\big(f_2^{\text{tree, IR}} + f_2^{\text{loop, IR}}\big) \\
&= 2 + g_{\rho\pi}^{\mathrm{IR}} - g^{\mathrm{IR}}\big(d_x^{\mathrm{IR}} + 2f_V^{\mathrm{IR}}\big) + \frac{M}{64\pi}M_\rho\big(g_{\omega\rho\pi}^{\mathrm{IR}}\big)^2 + \mathcal{O}(M^2)\,.
\end{aligned} \tag{7.35}$$

8 That means that no calculation of subtraction terms has been carried out for these integrals since the corresponding C_0 integrals are cumbersome to integrate, despite using comprehensive integral tables [84, 85, 86]. Hence, no cross-check of the assignment of orders to those diagrams was done.

Method	μ_ρ	Reference
Current Dyson-Schwinger	2.01	[89]
Rel. QM: Light-front	1.92	[90]
QCD light cone sum rules	2.3 ± 0.5	[91]
QCD sum rules	2.0 ± 0.3	[92]
Previous Dyson-Schwinger	2.69	[93]
Rel. QM: Covariant	2.14	[94]
Rel. QM: Light-front	2.19, 2.17, 2.15, 2.48	[94]
Rel. QM: Light-front	2.26	[95]

Table 7.1: Comparison with other theoretical predictions. They are sorted by date of publication. The magnetic moment μ_ρ is given in units of $\mu = e/(2M_\rho)$. In general, all methods use some non-trivial assumptions concerning the effective interaction or validity of perturbative expansion.

7.6 DISCUSSION OF RESULTS

The main result obtained in this chapter is given in equation (7.35). The loop correction, which should be small in comparison to the tree-level result, can be estimated by numerical evaluation. Using the physical masses $M = 0.140\,\text{GeV}$, $M_\rho = 0.775\,\text{GeV}$ [36] and the heavily model-dependent numerical value for the LEC $g^{\text{IR}}_{\omega\rho\pi} \approx 16\,\text{GeV}^{-1}$ [87], one finds as a rough estimate

$$f_2^{\text{loop, IR}}(0)/e \approx 0.137\,. \tag{7.36}$$

Here, the width of the rho meson Γ_χ has been neglected as a higher-order correction. Assuming that the numerical value at tree level for the magnetic moment μ_ρ is 2 in units of $\mu = e/(2M_\rho)$ [88], the loop correction is indeed small.[9] However, at least the LEC $g^{\text{IR}}_{\rho\pi}$ at tree level in equation (7.35) is not known so far and thus no completely numerical result can be given.

In table 7.1 some other theoretical predictions are presented. They are in good agreement with the result obtained here if one takes into account that this calculation has an error of at least 15 % due to the numerical

9 Note that $f_2(0)/e$ is exactly the magnetic moment μ_ρ defined in equation (7.17b) in units of $\mu = e/(2M_\rho)$.

value of $g^{\mathrm{IR}}_{\omega\rho\pi}$ [87]. In Lattice QCD, the main problem is the calculation of this complex quantity at the physical pion mass due to the limited computational power resulting in large statistical errors [96, 97]. Hence, the results obtained there are not yet comparable. A higher-order calculation in the framework of chiral effective field theories could be used to give a more reliable numerical value for the magnetic moment as a chiral extrapolation of Lattice QCD results. Unfortunately, no experimental data for the magnetic moment exist at the moment and thus no final decision on the validity of the various theoretical assumptions compared in table 7.1 can be made.

8

SUMMARY AND CONCLUSION

This chapter gives a short summary of the results obtained in part II and draws conclusions from it. Consequently, some possible extensions of this work are proposed as a short outlook. Obstacles and difficulties, which may occur in future endeavors, are pointed out.

In chapter 5, a successful extension to the SU(3) sector of the constraint analysis in the vector field formalism has been presented. A massive Yang-Mills theory has been found for eight vector particles assuming a global SU(3) symmetry a priori. However, starting from a global U(1) symmetry, i.e. requiring only charge conservation, the analysis has not been feasible for eight fields due to the vast number of parameter choices during the constraint analysis. The same obstacle appears if requiring a global SU(2) symmetry as a subgroup of SU(3), i.e. for equal up- and down-quark masses, which leads to isospin symmetry. It is also a non-trivial task to find the number of truly independent parameters resulting from the permutation symmetries of the interaction terms. In conclusion, reducing the a priori assumptions for eight vector fields quickly leads to severe problems.

At this point, it shall be mentioned briefly that a constraint analysis for three *axial*-vector particles was carried out and led to conditions for the coupling constants. Unfortunately, the subsequent renormalizability analysis yielded lengthy equations which could not be simplified further. Nevertheless, little effort has been made to investigate this further.

In chapter 6, a challenging result has been found. Assuming U(1) invariance a priori, the most general Lagrangian for three vector particles described by antisymmetric tensor fields has been constructed. Here, interaction terms accompanied by couplings of negative energy dimension have been assumed to be suppressed by an intrinsic large scale. By applying a cumbersome constraint analysis, one directly finds that the three-vertex interaction must vanish. Taking absorbability of divergences into account, the four-vertex interaction must also vanish. This result would not have been obtained if one had not carried out the cumbersome constraint analysis. In conclusion, the only self-consistent theory in the antisymmetric tensor field formalism is the free theory.

This is in stark contrast to the findings in the vector field formalism. There, the same assumptions lead to a massive Yang-Mills theory.

An integral part of this work was cross-checking the results stemming from computer algorithms as far as possible by hand. Relying on that, one draws the conclusion that there is an astounding difference between the tensor field formalism and the vector field formalism in effective quantum field theories. Regarding the former, the assumption that terms with a higher number of fields and derivatives are suppressed does *not* lead to an expected self-consistent interacting theory as for the latter. However, the equivalence of both formalisms has been shown for various interaction terms in chiral effective field theories including vector mesons [60, 68]. There, different methods of implementing vector mesons are mutually consistent with respect to chiral symmetry, number of LECs, and power counting. In this sense, it is often argued that using either the vector or tensor field formalism does not matter and the formalism should be chosen as one prefers. Nevertheless, with a few exceptions [30], a proper constraint analysis for these interactions is not considered, although it is a crucial part in the reasoning presented here. Therefore, it would be a reasonable extension of this work to investigate interaction terms of vector mesons with pions or nucleons within the tensor field formalism including a constraint analysis. Of course, the increasing number of fields and thus the complexity of possible self-consistent parameter choices make life hard.

In chapter 7, the magnetic moment of the rho meson has been calculated in the framework of a chiral effective field theory including the rho and omega mesons. In comparison to work concerning the properties of nucleons, new difficulties appear. First, the power counting becomes more involved due to the different fluxes of large external momenta. Considering this, a chiral order was assigned to each diagram and the regularization scheme has been successfully confirmed for the relevant diagrams. Second, the rho meson can decay into two pions and thus loop integrals with imaginary parts appear. Additionally, the unstable rho meson should be implemented with a complex mass in order to absorb the complex counter-terms, however, it turned out that this is an effect of higher order in the calculated quantities. Up to order $\mathcal{O}(q^3)$, the calculation of the electromagnetic form factors at $q^2 = 0$ was successful in the reformulated infrared regularization scheme. The most important terms stemmed from the inclusion of the omega meson. Here, future work could focus on reinvestigating the correct construction of the most general Lagrangian, e.g. by using a constraint analysis, and on

cross-checking the renormalized quantities more thoroughly by considering the case $q^2 \neq 0$. Furthermore, the current Lattice QCD results need chiral expansions in the pion mass. Hence, a result valid for higher chiral orders could be advantageous.

Although the two last chapters cover different topics at first sight, both the results contribute to the endeavor how to create an effective field theory applicable in the low-energy regime up to 1 GeV. To this end, it is definitely necessary to include vector mesons as explicit degrees of freedom, which have been known as resonances in experiments for a long time. On the one hand, the sometimes favorable tensor field formalism for vector particles has shown *not* to be quasi-equivalent to the vector field formalism. This necessitates rethinking of the various descriptions of vector meson interactions with other hadrons. On the other hand, calculating physical properties of vector mesons turns out to be more complicated in comparison to nucleons. However, a successful calculation and comparison with future experiments and Lattice QCD extrapolations can increase the confidence in the validity of the effective field theory.

Part III

APPENDIX

A

NOTATIONS AND RELATIONS

In this chapter, the notation used throughout this thesis is briefly summarized. Furthermore, some important relations, which have been employed in the calculations, are given.

A.1 THE SPECIAL UNITARY GROUP

The following definitions and relations are also given in the comprehensive compendium of [77]. The special unitary group SU(N) is defined as

$$\mathrm{SU}(N) = \left\{ M \,\middle|\, M^\dagger M = \mathbb{1}, \det M = 1 \right\} , \tag{A.1}$$

where M is an $N \times N$ complex matrix. The unitary group U(N) is obtained by simply removing the constraint $\det M = 1$. Elements U of SU(N) can be parametrized as

$$U = \exp\left(-i\Theta_a T_a\right) , \tag{A.2}$$

where T_a represent the Hermitian and traceless $N^2 - 1$ generators. The totally antisymmetric structure constants f_{abc}, which encode the structure of the Lie group, are defined as

$$\left[T_a, T_b\right] = i f_{abc} T_c , \tag{A.3}$$

where $[A, B] = AB - BA$ denotes the commutator. Furthermore, the anticommutation relations can be written with the help of the totally symmetric tensor d_{abc} as

$$\left\{T_a, T_b\right\} = \kappa \delta_{ab} + d_{abc} T_c , \tag{A.4}$$

where κ is some N dependent constant.

For $N = 2$, the generators can be written in terms of the Pauli matrices, namely $T_i = \tau_i / 2$, where

$$\tau_1 = \begin{pmatrix} 0 & 1 \\ 1 & 0 \end{pmatrix} , \qquad \tau_2 = \begin{pmatrix} 0 & -i \\ i & 0 \end{pmatrix} , \qquad \tau_3 = \begin{pmatrix} 1 & 0 \\ 0 & -1 \end{pmatrix} . \tag{A.5}$$

The structure constants are equivalent to the Levi-Civita symbol, $f_{abc} = \epsilon_{abc}$, and the d_{abc} vanish. For convenience, τ_0 denotes the unit matrix.

For $N = 3$, the generators $T_a = \lambda_a/2$ are given by the Gell-Mann matrices

$$\lambda_1 = \begin{pmatrix} 0 & 1 & 0 \\ 1 & 0 & 0 \\ 0 & 0 & 0 \end{pmatrix}, \quad \lambda_2 = \begin{pmatrix} 0 & -i & 0 \\ i & 0 & 0 \\ 0 & 0 & 0 \end{pmatrix}, \quad \lambda_3 = \begin{pmatrix} 1 & 0 & 0 \\ 0 & -1 & 0 \\ 0 & 0 & 0 \end{pmatrix},$$

$$\lambda_4 = \begin{pmatrix} 0 & 0 & 1 \\ 0 & 0 & 0 \\ 1 & 0 & 0 \end{pmatrix}, \quad \lambda_5 = \begin{pmatrix} 0 & 0 & -i \\ 0 & 0 & 0 \\ i & 0 & 0 \end{pmatrix}, \quad \lambda_6 = \begin{pmatrix} 0 & 0 & 0 \\ 0 & 0 & 1 \\ 0 & 1 & 0 \end{pmatrix},$$

$$\lambda_7 = \begin{pmatrix} 0 & 0 & 0 \\ 0 & 0 & -i \\ 0 & i & 0 \end{pmatrix}, \quad \lambda_8 = \frac{1}{\sqrt{3}} \begin{pmatrix} 1 & 0 & 0 \\ 0 & 1 & 0 \\ 0 & 0 & -2 \end{pmatrix}. \tag{A.6}$$

The constants f_{abc} and d_{abc} can be calculated by the relations

$$f_{abc} = \frac{1}{4i} \operatorname{Tr}\big([\lambda_a, \lambda_b]\lambda_c\big) \quad \text{and} \quad d_{abc} = \frac{1}{4} \operatorname{Tr}\big(\{\lambda_a, \lambda_b\}\lambda_c\big), \tag{A.7}$$

respectively.

A.2 ONE-LOOP INTEGRALS

This section briefly summarizes the so-called scalar one-loop integrals in the notation of [98]. They typically appear as results of one-loop calculations after applying the standard Passarino-Veltman reduction [72]. The scheme reduces tensor loop integrals over $d^n k$, which carry quantities such as $k^\mu k^\nu$ in the numerator, to scalar ones. For a thorough review of Passarino-Veltman reduction schemes see [73]. The algorithms presented there are implemented in FeynCalc as well as in FormCalc, a part of FeynArts, see also appendix B. The calculation of loop integrals is detailed in [82].

In dimensional regularization [69], the one-point scalar integral is given by

$$\begin{aligned} A_0(m^2) &= \frac{(2\pi\mu)^{4-n}}{i\pi^2} \int d^n k \frac{1}{k^2 - m^2 + i0^+} \\ &= -32\pi^2 \lambda m^2 - m^2 \ln \frac{m^2}{\mu^2}. \end{aligned} \tag{A.8}$$

The mass scale μ gives the integral the mass unit eV^2 independent of the number of space-time dimensions n. It is usually set to $\mu = 1\,\mathrm{GeV}$ in this thesis, which simplifies results.

The two-point scalar integral can also be calculated explicitly for arbitrary arguments. It reads

$$\begin{aligned} &B_0(p^2, m_1^2, m_2^2) \\ &\quad = \frac{(2\pi\mu)^{4-n}}{i\pi^2} \int d^n k \frac{1}{\left[k^2 - m_1^2 + i0^+\right]\left[(k+p)^2 - m_2^2 + i0^+\right]} \\ &\quad = -32\pi^2\lambda + \ln\left(\frac{\mu^2}{m_2^2}\right) - 1 - \frac{\omega}{2}\, {}_2\mathrm{F}_1(1, 2; 3; \omega) \\ &\qquad - \frac{1}{2}\left[1 + \frac{m_2^2}{m_1^2(\omega - 1)}\right] {}_2\mathrm{F}_1\left(1, 2; 3; 1 + \frac{m_2^2}{m_1^2(\omega - 1)}\right), \\ &\omega = \frac{m_1^2 - m_2^2 + p^2 + \sqrt{(m_1^2 - m_2^2 + p^2)^2 - 4m_1^2 p^2}}{2m_1^2}, \end{aligned} \tag{A.9}$$

where ${}_2\mathrm{F}_1(a, b; c; z)$ is the standard hypergeometric function [83]. The divergent part of the one-point and two-point integrals is encoded in

$$\lambda = \frac{1}{16\pi^2}\left\{\frac{1}{n-4} - \frac{1}{2}\left[\ln(4\pi) + \Gamma'(1) + 1\right]\right\}. \tag{A.10}$$

According to the $\widetilde{\mathrm{MS}}$ renormalization scheme, quantities proportional to λ in equation (A.10) are compensated by appropriate counter-terms. Furthermore, the derivative of B_0 with respect to p^2 reads

$$\begin{aligned} \frac{\partial B_0(p^2, m_1^2, m_2^2)}{\partial p^2} = \frac{1}{D}\Big\{&\left(-p^2 + m_1^2 + m_2^2\right)p^2 - A_0(m_2^2)\left(p^2 + m_1^2 - m_2^2\right) \\ &- A_0(m_1^2)\left(p^2 - m_1^2 + m_2^2\right) \\ &+ B_0(p^2, m_1^2, m_2^2)\left[p^2(m_1^2 + m_2^2) - (m_1^2 - m_2^2)^2\right]\Big\}, \end{aligned} \tag{A.11}$$

where

$$D = p^2\left[m_1^4 - 2(p^2 + m_2^2)m_1^2 + (p^2 - m_2^2)^2\right].$$

This relation proves to be useful in the calculation of the wave function renormalization constant. Among more derivatives, this result can be found in [99, App. C.2.1]. However, note that some of these formulas exhibit parts not proportional to a one-loop integral. Therefore, they are only valid in $n = 4$ dimensions and cannot be used for the calculation of subtraction terms in the reformulated IR regularization scheme.

The non-divergent three-point scalar integral can only be calculated analytically for special arguments, so only its definition is given for completeness as

$$C_0(p_1^2, p_2^2, p_{12}^2, m_1^2, m_2^2, m_3^2) = \frac{(2\pi\mu)^{4-n}}{i\pi^2} \times \int d^n k \frac{1}{\left[k^2 - m_1^2\right]\left[(k+p_1)^2 - m_2^2\right]\left[(k+p_{12})^2 - m_3^2\right]}, \tag{A.12}$$

where $p_{12} = p_1 + p_2$ and the $+i0^+$ prescription in the denominator has been dropped for brevity. By virtue of the translation invariance in k, the following expressions are all equal:

$$\begin{aligned} &C_0(p_1^2, p_2^2, p_{12}^2, m_1^2, m_2^2, m_3^2)\,, \quad C_0(p_{12}^2, p_2^2, p_1^2, m_1^2, m_3^2, m_2^2)\,, \\ &C_0(p_1^2, p_{12}^2, p_2^2, m_2^2, m_1^2, m_3^2)\,, \quad C_0(p_2^2, p_{12}^2, p_1^2, m_2^2, m_3^2, m_1^2)\,, \\ &C_0(p_{12}^2, p_1^2, p_2^2, m_3^2, m_1^2, m_2^2)\,, \quad C_0(p_2^2, p_1^2, p_{12}^2, m_3^2, m_2^2, m_1^2)\,. \end{aligned} \tag{A.13}$$

Furthermore, the derivatives of C_0 with respect to an arbitrary argument is detailed in [100]. The corresponding algorithm is also given in [99, App. C.2.1] and has been implemented in Mathematica in order to express all C_0 at $q^2 = 0$ in terms of B_0 and A_0, compare also section 7.5 on page 82.

For completeness, the following relations for special arguments of C_0 integrals are given:

$$\begin{aligned} &C_0(p^2, 0, p^2, m_1^2, m_2^2, m_2^2) = \\ &\quad \left[m_2^4 - 2m_2^2(m_1^2 + p^2) + (m_1^2 - p^2)^2\right]^{-1} \\ &\quad \times \left[(m_2^2 - m_1^2 - p^2)(B_0(p^2, m_2^2, m_1^2) - 1)\right. \\ &\qquad \left. - (m_2^2 + m_1^2 - p^2)A_0(m_2^2)/m_2^2 + 2A_0(m_1^2)\right], \end{aligned} \tag{A.14a}$$

$$\begin{aligned} &C_0(p^2, p^2, 0, m_2^2, m_3^2, m_3^2) = \\ &\quad \left[B_0(p^2, m_2^2, m_3^2) - B_0(p^2, m_3^2, m_3^2)\right]/(m_2^2 - m_3^2)\,. \end{aligned} \tag{A.14b}$$

B

TECHNICAL DETAILS

This chapter gives a brief overview of the various tools and techniques which have been used to calculate the results throughout this work. Mostly, the comprehensive computer algebra system Wolfram Mathematica 7.0 and the programming language FORM [101, 102, 103] have been employed on a Linux-based 64bit machine. Note that a 32bit system is not sufficient due to some limitations of the FORM interpreter. Furthermore, both the Mathematica packages FeynCalc [104] and FeynArts/FormCalc [105] have been used in parallel for the calculation of diagram amplitudes.

B.1 EFFECTIVE FIELD THEORY MODEL IN FEYNARTS

Starting from the definition of the Lagrangian using the common building blocks of chiral effective field theories, the calculation is carried out in a semi-automatic way, i.e. all intermediate results are *not* transferred by hand at any point. This approach reduces possible sources of mistakes in general. However, its drawback is that interim consistency checks can become less transparent. The single calculation steps are detailed in the following and an overview is depicted in figure B.1.

The original FORM code for generating the Feynman rules in the mesonic sector—kindly provided by Sandro Gorini—was extended for the inclusion of the omega meson. Indeed, FORM is well-suited for the necessary expansion of the Lagrangian and the permutation operations involved in deriving Feynman rules of effective field theories. Next, a wrapper which automatically generates a complete FeynArts model has been developed in Mathematica as a first proof of concept. The wrapper obtains the Feynman rules via FormGet, a spin-off of FeynArts. Besides that, the Feynman rules are prepared for easy usage with respect to the FeynCalc package. The main difficulty concerning the wrapper was the correct separation of the Feynman rules in a so-called kinetic part and a part containing coupling constants according to the FeynArts manual, see also equations (6.58a) and (6.58b) on page 62. Basically, it boils down to the determination of coefficients of Lorentz structures and a rather cumbersome formatting of the output suitable for FeynArts.

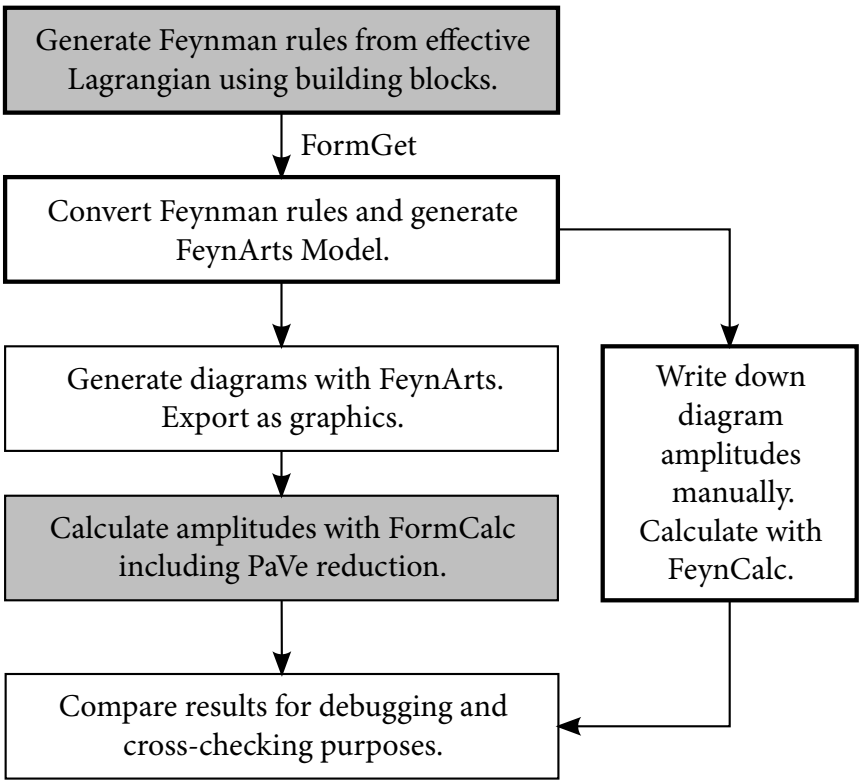

Figure B.1: Flowchart visualizing the necessary extension of FeynArts for effective field theories. The Feynman rules are also automatically converted for FeynCalc usage, which is a helpful tool for cross-checking. Boxes with thicker border indicate that the necessary code is mostly self-written. Boxes with gray background indicate that FORM is used instead of Mathematica.

Future developments should modify the FORM code output such that it is easily converted in a FeynArts model.

Regarding an effective field theory (EFT), typically much more complicated Feynman rules with various kinetic parts appear in comparison to the Standard Model, for which FeynArts has been originally designed. Furthermore, the photon-rho coupling requires appending a two-vertex to each generated topology. This is implemented by direct modification of already generated topology code, i.e. before inserting the particular fields. In summary, it turned out that FeynArts in conjunction with FormCalc is suitable for successful calculations in EFTs. Nevertheless, the calculation can take some hours since FormCalc is not optimized for typical amplitudes of EFTs. During the development process, some bugs in FormCalc have been identified by thorough comparison with FeynCalc results, especially in the SU(2) index handling and in the recently available Passarino-Veltman reduction code. They have already been fixed in the current official release. This was greatly supported by Thomas Hahn, the maintainer of FeynArts and FormCalc. Considering that FeynCalc is outdated and not well-maintained anymore, a future-proof approach should take FeynArts into account.

B.2 CONSTRAINT ANALYSIS IN FORM

As already mentioned in the previous section B.1, FORM is well-suited for algebraic transformations relevant to theoretical physics. For example, the contraction of a symmetric tensor with an antisymmetric one is automatically identified as zero. Furthermore, a very comprehensive replacement system and a useful preprocessor is provided.

The first part was the determination of available Lorentz structures discussed in section 6.1 on page 43. This is implemented in a brute-force approach by simply contracting all possible index permutations with the corresponding product of fields. Since FORM automatically sorts the indices in a standard order, only a few terms remain. They were finally reduced to the truly independent Lorentz structures by taking into account the contraction with the arbitrary coupling constants. These steps have also been cross-checked with independently developed Mathematica code. Admittedly, there are smarter ways of obtaining the possible Lorentz structures, but the brute-force method should be the most robust.

The second part concerned the requirement of the U(1) invariance in conjunction with the elimination of superfluous coupling parameters.

To this end, the summation over all Lorentz indices and internal indices is carried out in equations (6.14) and (6.17) on pages 47–48, respectively. Additionally, the antisymmetry of the tensor fields is incorporated as usual by the replacement $W^{\mu\nu} \to V^{\mu\nu} - V^{\nu\mu}$, where $V^{\mu\nu}$ is an arbitrary tensor field. The resulting expressions have been collected by the fields V. Fortunately, FormGet preserves this parenthesis structure of the expression. Using Mathematica, the conditions on the coupling constants due to U(1) invariance have been solved and converted to replacements again suitable for FORM. Finally, the whole Lagrangian is considered again in FORM and the solution ensuring U(1) invariance is inserted after explicit summation of all indices and antisymmetrization. This result is analyzed in Mathematica with respect to superfluous parameters according to the algorithm described in section 6.2 on page 46. In this part, the main problem was to figure out which tool is best-suited to carry out a specific step. For example, solving a linear equation algebraically is easily done in Mathematica, but hard in FORM. On the other hand, tensor structures and summations are much more efficiently handled by FORM in comparison to Mathematica.

The third part was the calculation of the matrix $\mathcal{M}$ in equation (6.27) on page 52, whose determinant was then analyzed in Mathematica. This problem boils down to the implementation of the Poisson algebra

$$\{f, gh\} = g\{f, h\} + \{f, g\}h\,, \tag{B.1}$$

where f, g, h are arbitrary functions of the canonical variables. Using equation (B.1), the expression is simplified to the fundamental Poisson brackets, which obey equation (4.15) on page 32. The algorithm uses replacements for the algebra and represents the poisson bracket by a so-called non-commuting function in FORM. The fact that no derivatives appear in the interaction part of the Lagrangian simplifies matters significantly since no integration by parts needs to be carried out. Finally, the output is prepared for Mathematica after applying the relations obtained from the U(1) invariance.

The last part consisted of the renormalizability analysis. It was carried out using a general tensor model file in FeynArts, analogously to the vector model file used in chapter 5. Fortunately, FeynArts supports tensor fields by design. Since the parametrization in equation (6.20) on page 49 is given for explicit internal indices, the infinite parts of the vertices needed to be calculated on „particles insertion level“. This calculation takes some hours and it has been parallelized using a small bash script and the MASH Perl script, which allows for treating Mathematica scripts

as usual shell scripts. This approach renders the process more stable. Note that FeynCalc is not suitable for such calculations, since the tensor rank of the loop integrals is quite high and the necessary simplification of the Lorentz structure is an elaborate problem.

C

RESULTS FOR THE MAGNETIC MOMENT IN DETAIL

C.1 FEYNMAN RULES

In the vertices, the rho meson is represented by a straight line, the pion by a dashed line, the (always external) photon by a wiggly line and the omega meson by a curly line. All the momenta in the following Feynman rules are incoming. These and the Lorentz indices $\mu, \nu, \lambda, \sigma, \alpha$ are ordered starting from the left upper corner in a counter-clockwise direction, e.g.

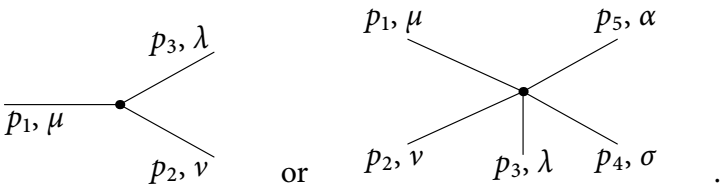

.

Additionally, note that the LEC f_V is defined differently in comparison to the usual definition, see e.g. [68] due to the implementation in FORM. Referring to equation (7.2b) on page 72, the usual definition can be obtained by the replacement $f_V \to -f_V/(2\sqrt{2})$. All rules presented here have been automatically calculated and inserted into this document, which reduces readability on the one hand, but increases correctness on the other hand. The Minkowski product $p_1 \cdot p_2$ of two four-vectors is written $p_1 p_2$ in the following Feynman rules.

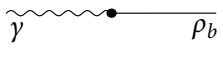

$$\frac{ie\delta^{3b}}{g}\Big(gp_1^\mu p_1^\nu(d_x+2f_V)+g^{\mu\nu}(M^2c_x - gp_1^2(d_x+2f_V)+M_\rho^2)\Big)$$

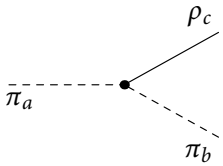

$$\frac{\epsilon^{abc}}{2F^2 g}\Big(p_2^\mu(M^2c_x+2g(p_1p_3)d_x+M_\rho^2) - p_1^\mu(M^2c_x+2g(p_2p_3)d_x+M_\rho^2)\Big)$$

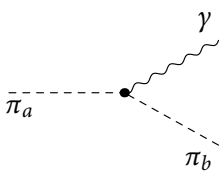

$$-\frac{e(p_1^\mu - p_2^\mu)\epsilon^{3ab}}{2F^2g^2}\Big(M_\rho^2+M^2c_x-2F^2g^2\Big)$$

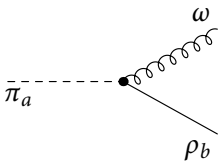

$$-g_{\omega\rho\pi}\delta^{ab}\epsilon^{p_1 p_2 \mu\nu}$$

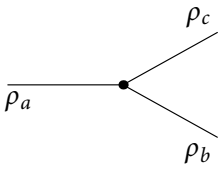

$$g\epsilon^{abc}\big((p_1^\lambda - p_2^\lambda)g^{\mu\nu} + (p_2^\mu - p_3^\mu)g^{\lambda\nu} + (p_3^\nu - p_1^\nu)g^{\lambda\mu}\big)$$

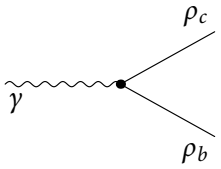

$$-e\epsilon^{3bc}\big(g_{\rho\pi} - g(d_x + 2f_V)\big)\big(p_1^\lambda g^{\mu\nu} - p_1^\nu g^{\lambda\mu}\big)$$

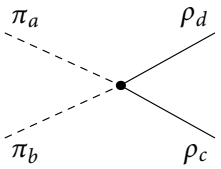

$$-\frac{i}{F^2}\big(M^2 c_x \delta^{ab}\delta^{cd} g^{\mu\nu} + g d_x (p_1^\mu p_2^\nu - p_2^\mu p_1^\nu)(\delta^{ad}\delta^{bc} - \delta^{ac}\delta^{bd})\big)$$

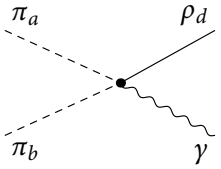

$$\begin{aligned}-\frac{ie}{2F^2 g}\big(&2\delta^{3d}\delta^{ab}(g^{\mu\nu}(2M^2 c_x + g(p_3p_4)(d_x + 2f_V) + g(p_1p_4 + p_2p_4)d_x + M_\rho^2) - g p_4^\mu (p_3^\nu (d_x + 2f_V) + d_x(p_1^\nu + p_2^\nu))) + \\ &\delta^{3a}\delta^{bd}(-g^{\mu\nu}(M^2 c_x + g(p_3p_4)(d_x + 2f_V) + 2g(p_1p_4)d_x - (p_1p_3)g_{\rho\pi} + (p_2p_3)g_{\rho\pi} + M_\rho^2) + g p_4^\mu (p_3^\nu (d_x + 2f_V) + 2d_x p_1^\nu) + g_{\rho\pi}(p_2^\mu - p_1^\mu)p_3^\nu) + \\ &\delta^{3b}\delta^{ad}(-g^{\mu\nu}(M^2 c_x + g(p_3p_4)(d_x + 2f_V) + 2g(p_2p_4)d_x + (p_1p_3)g_{\rho\pi} - (p_2p_3)g_{\rho\pi} + M_\rho^2) + g p_4^\mu (p_3^\nu (d_x + 2f_V) + 2d_x p_2^\nu) + g_{\rho\pi}(p_1^\mu - p_2^\mu)p_3^\nu)\big)\end{aligned}$$

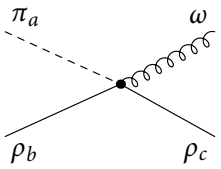

$$-igg_{\omega\rho\pi}\epsilon^{abc}\epsilon^{p_1\lambda\mu\nu}$$

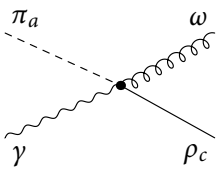

$$ieg_{\omega\rho\pi}\epsilon^{3ac}\epsilon^{-p_3\lambda\mu\nu}$$

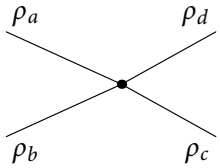

$$-ig^2\big(-\delta^{ab}\delta^{cd}(g^{\lambda\nu}g^{\mu\sigma}+g^{\lambda\mu}g^{\nu\sigma}-2g^{\lambda\sigma}g^{\mu\nu})-\delta^{ac}\delta^{bd}(g^{\lambda\nu}g^{\mu\sigma}-2g^{\lambda\mu}g^{\nu\sigma}+g^{\lambda\sigma}g^{\mu\nu})-\delta^{ad}\delta^{bc}(-2g^{\lambda\nu}g^{\mu\sigma}+g^{\lambda\mu}g^{\nu\sigma}+g^{\lambda\sigma}g^{\mu\nu})\big)$$

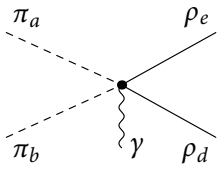

$$\frac{e}{8F^2}\big(-(p_3^\nu g^{\lambda\mu}-p_3^\lambda g^{\mu\nu})(3\epsilon^{3ad}\delta^{be}-3\epsilon^{3ae}\delta^{bd}+3\delta^{ae}\epsilon^{3bd}-3\delta^{ad}\epsilon^{3be}-2\delta^{ab}\epsilon^{3de}+\delta^{3b}\epsilon^{ade}+\delta^{3a}\epsilon^{bde})(g(d_x+2f_V)-g_{\rho\pi})-2gd_x(\delta^{ab}\epsilon^{3de}((p_1^\lambda+p_2^\lambda)g^{\mu\nu}-(p_1^\nu+p_2^\nu)g^{\lambda\mu})+\delta^{ae}\epsilon^{3bd}((2p_1^\nu+p_2^\nu)g^{\lambda\mu}-(2p_1^\lambda+p_2^\lambda)g^{\mu\nu})-\delta^{ad}\epsilon^{3be}((2p_1^\nu+p_2^\nu)g^{\lambda\mu}-(2p_1^\lambda+p_2^\lambda)g^{\mu\nu})+\epsilon^{3ad}\delta^{be}((p_1^\nu+2p_2^\nu)g^{\lambda\mu}-(p_1^\lambda+2p_2^\lambda)g^{\mu\nu})+\epsilon^{3ae}\delta^{bd}((p_1^\lambda+2p_2^\lambda)g^{\mu\nu}-(p_1^\nu+2p_2^\nu)g^{\lambda\mu})+\delta^{3a}\epsilon^{bde}(p_1^\nu g^{\lambda\mu}-p_1^\lambda g^{\mu\nu})+\delta^{3d}\epsilon^{abe}((p_2^\nu-p_1^\nu)g^{\lambda\mu}+(p_1^\lambda-p_2^\lambda)g^{\mu\nu})+\delta^{3b}\epsilon^{ade}(p_2^\nu g^{\lambda\mu}-p_2^\lambda g^{\mu\nu})+\delta^{3e}\epsilon^{abd}((p_1^\nu-p_2^\nu)g^{\lambda\mu}+(p_2^\lambda-p_1^\lambda)g^{\mu\nu}))\big)$$

C.2 FLUXES OF LARGE MOMENTA FOR EACH TOPOLOGY

In figures C.1 and C.2 the possible fluxes of large external momenta are given. They have been used to determine the chiral order of each diagram, see figures 7.2 and 7.4 on pages 75–78, respectively.

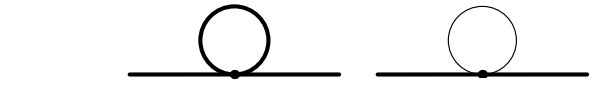

(a) Topology 1

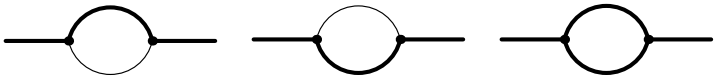

(b) Topology 2

Figure C.1: Possible fluxes of large momenta through each topology of one-loop diagrams for the two-point function. The external rho mesons are assumed to carry large momenta. The large momenta are indicated by a thicker propagator line. Note that these diagrams should be seen as naïve templates for a computer algorithm. Compare also figure 7.2 on page 75.

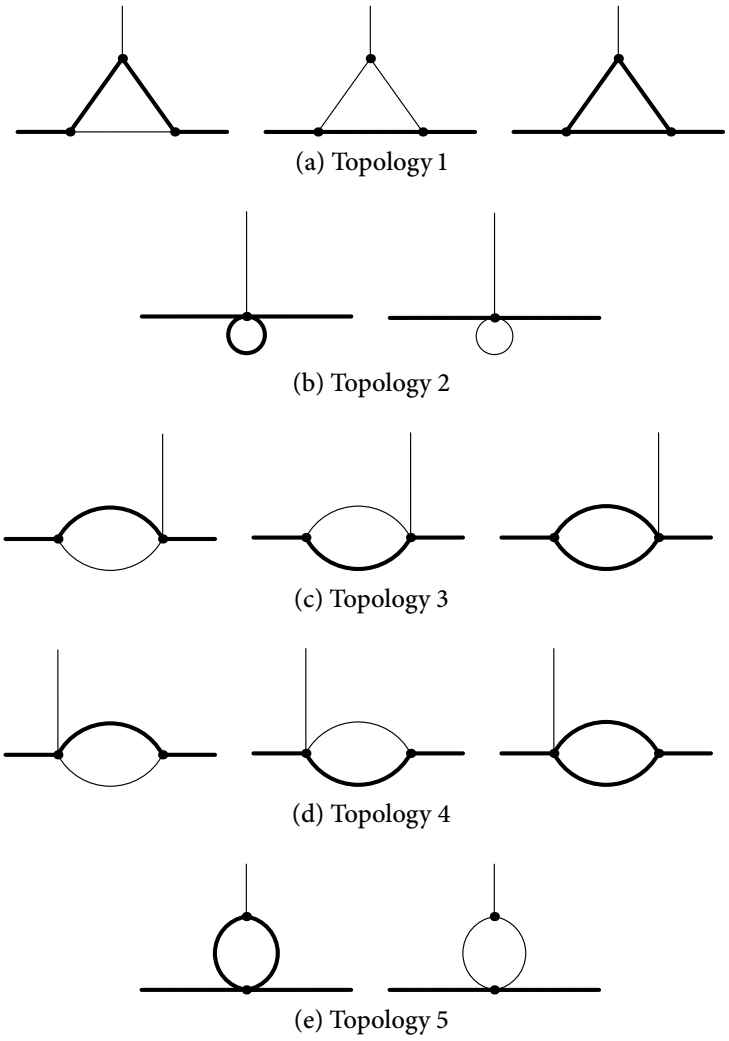

(a) Topology 1

(b) Topology 2

(c) Topology 3

(d) Topology 4

(e) Topology 5

Figure C.2: Possible fluxes of large momenta through each topology of one-loop diagrams relevant to the magnetic moment. Again, the external rho mesons are assumed to carry large momenta, whereas the photon momentum is assumed to be small. Compare also figure 7.4 on page 78.

C.3 Ξ_1 AND Ξ_2 FOR THE MAGNETIC MOMENT

Here, the two lengthy expressions for Ξ_1 and Ξ_2, which have been used in equation (7.20b) on page 81, are given in the following equations (C.1) and (C.2).

$$
\begin{aligned}
\Xi_1 = &-18M_\rho^4 A_0(M^2c_x + M_\rho^2)(3g(d_x + 2f_V) - 3g_{\rho\pi} - 5) \\
&- 24A_0(M^2)(M^2c_x + M_\rho^2)((gd_x - 1) \\
&\quad \times (M^2c_x(g(3d_x(g(d_x + 2f_V) - g_{\rho\pi} - 2) - 2f_V) \\
&\quad + 3(g_{\rho\pi} + 1)) + M_\rho^2(g(3d_x(g(d_x + 2f_V) - g_{\rho\pi} - 2) \\
&\quad - 2f_V) + 3g_{\rho\pi})) - 3M_\rho^2) \\
&+ (M^2c_x + M_\rho^2)(12(gd_x - 1)(M^2c_x + M_\rho^2) \\
&\qquad \times B_0(M^2c_x + M_\rho^2, M^2, M^2) \\
&\qquad \times (M^2(-g(3(c_x - 2)d_x g_{\rho\pi} + 3c_x d_x + 2c_x f_V + 4f_V) \\
&\qquad + 3g^2(c_x - 2)d_x(d_x + 2f_V) + 3(c_x - 2)g_{\rho\pi} + 6) \\
&\qquad + M_\rho^2(g(3d_x(g(d_x + 2f_V) - g_{\rho\pi} - 1) - 2f_V) + 3g_{\rho\pi})) \\
&\quad - 45M_\rho^4 B_0(M^2c_x + M_\rho^2, M^2c_x + M_\rho^2, M^2c_x + M_\rho^2) \\
&\qquad \times (g(d_x + 2f_V) - g_{\rho\pi} + 2) \\
&\quad - 8M^2c_x(3M^2 - M_\rho^2)(gd_x - 1)(g(3gd_x(d_x + 2f_V) \\
&\qquad - 3d_x g_{\rho\pi} + 2f_V) + 3(g_{\rho\pi} - 1)) \\
&\quad + 4M^4c_x^2(gd_x - 1)(g(3gd_x(d_x + 2f_V) - 3d_x g_{\rho\pi} + 2f_V) \\
&\qquad + 3(g_{\rho\pi} - 1)) \\
&\quad - 24M^2M_\rho^2(gd_x - 1)(g(3gd_x(d_x + 2f_V) - 3d_x g_{\rho\pi} + 2f_V) \\
&\qquad + 3(g_{\rho\pi} - 1)) \\
&\quad + M_\rho^4(g(d_x(4g(3d_x(g(d_x + 2f_V) - g_{\rho\pi} - 1) - 4f_V) \\
&\qquad + 3(8g_{\rho\pi} - 9)) - 38f_V) + 3(g_{\rho\pi} - 17)))
\end{aligned}
\tag{C.1}
$$

$$
\begin{aligned}
\Xi_2 = {} & (M^2 - M_\rho^2)(M^2 c_x + M_\rho^2)(M^2 M_\rho^2 (c_x(-5gd_x - 68gf_V + 34g_{\rho\pi} + 14) \\
& + 45gd_x + 96gf_V - 48g_{\rho\pi} - 9) \\
& + M^4 c_x (16c_x - 3)(gd_x - 1) + M_\rho^4 (27gd_x + 28gf_V - 14g_{\rho\pi} + 18)) \\
& + 6A_0(M_\rho^2)(M^4 M_\rho^2 (2c_x(-2g(2d_x + f_V) + g_{\rho\pi} + 4) + 2c_x^2(gd_x - 1) \\
& - 2gf_V + g_{\rho\pi} + 3) + M^2 M_\rho^4 (c_x(4g(d_x + f_V) - 2g_{\rho\pi} - 1) - 4gd_x - 2) \\
& + M^6 (c_x - 1)^2 c_x (gd_x - 1) + M_\rho^6 (2g(d_x + f_V) - g_{\rho\pi} + 4)) \\
& - 6A_0(M^2)(M^4 M_\rho^2 (-2c_x(3gd_x - 2gf_V + g_{\rho\pi} - 3) + 3c_x^2(gd_x - 1) \\
& - 2gf_V + g_{\rho\pi} + 3) + M^2 M_\rho^4 (2gc_x d_x - 4gc_x f_V + 2(c_x - 2)g_{\rho\pi} + c_x \\
& - gd_x + 8gf_V - 5) + M^6 c_x ((c_x - 3)c_x + 1)(gd_x - 1) \\
& + M_\rho^6 (-g(d_x + 6f_V) + 3g_{\rho\pi} + 7)) \\
& + 6(B_0(M^2 c_x + M_\rho^2, M^2, M_\rho^2)(-M^6 (c_x - 1) M_\rho^2 (2c_x(-5gd_x - 2gf_V \\
& + g_{\rho\pi} + 5) + 3c_x^2(gd_x - 1) - 2gf_V + g_{\rho\pi} + 3) \\
& - M^4 M_\rho^4 (c_x^2(4g(d_x + f_V) - 2(g_{\rho\pi} + 2)) \\
& + c_x(-20gd_x - 8gf_V + 4g_{\rho\pi} + 17) + 2(2gd_x - 2gf_V + g_{\rho\pi} + 4)) \\
& + M^2 M_\rho^6 (3c_x(-g(d_x + 2f_V) + g_{\rho\pi} + 1) + 7gd_x - 2gf_V + g_{\rho\pi} + 5) \\
& + M^8 (-(c_x - 1)^3) c_x (gd_x - 1) - 3M_\rho^8) \\
& + (gd_x - 1)(M^2(c_x - 4) + M_\rho^2)(M^2 c_x + M_\rho^2)^3 \\
& \times B_0(M^2 c_x + M_\rho^2, M^2, M^2))
\end{aligned}
\tag{C.2}
$$

C.4 NON-RENORMALIZED EXPRESSIONS PER DIAGRAM

The full non-renormalized expressions per diagram for the quantities δZ_ρ, $f_1(0)$, and $f_2(0)$ are given in tables C.1 to C.3, respectively. They have been included in this document in a fully automatic way. Concerning the magnetic moment, some diagrams have been grouped in order to ensure the current conservation, i.e. only their sum fulfills the Lorentz structure given in equation (7.15) on page 80. See also the corresponding Feynman diagrams in figures 7.2 and 7.4 on pages 75–78.

Diagram	δZ_ρ
(1)	0
(2)	0
(3)	$-\frac{g^2(gd_x-1)(M^2c_x+M_\rho^2)}{144\pi^2M_\rho^4}\big(A_0(M^2)(6-18gd_x)+(3gd_x+1)(M^2(c_x-6)+M_\rho^2)+3B_0(M^2c_x+M_\rho^2,M^2,M^2)(M^2(3g(c_x-2)d_x-c_x-2)+M_\rho^2(3gd_x-1))\big)$
(4)	$-\frac{g^2}{576\pi^2(M^2c_x+M_\rho^2)}\big(-258A_0(M^2c_x+M_\rho^2)+(M^2c_x+M_\rho^2)(99B_0(M^2c_x+M_\rho^2,M^2c_x+M_\rho^2,M^2c_x+M_\rho^2)+113)\big)$
(5)	$\frac{g_{\omega\rho\pi}^2}{288\pi^2(M^2c_x+M_\rho^2)}\big(3A_0(M_\rho^2)(2M^2c_x+M_\rho^2+M^2)+A_0(M^2)(M^2(6c_x-3)+9M_\rho^2)+(M^2(17c_x-24)-7M_\rho^2)(M^2c_x+M_\rho^2)+3M^2(M^2(-2c_x^2+c_x+1)-(3c_x+1)M_\rho^2)B_0(M^2c_x+M_\rho^2,M^2,M_\rho^2)\big)$

Table C.1: Contributions of each Feynman diagram in figure 7.2 to δZ_ρ defined in equation (7.8).

Diagram	$f_1(0)$
(1)	$-\frac{eg^2M^2c_x(gd_x-1)^2(M^2c_x+M_\rho^2)}{144\pi^2M_\rho^6}\big(-M_\rho^2-6A_0(M^2)-M^2(c_x-6)+3(M^2(c_x+2)+M_\rho^2)B_0(M^2c_x+M_\rho^2,M^2,M^2)\big)$
(2)	0
(3)	$\frac{eM^2c_xg_{\omega\rho\pi}^2}{288\pi^2M_\rho^2(M^2c_x+M_\rho^2)}\big(3A_0(M^2)(M^2(c_x-2)+3M_\rho^2)+3A_0(M_\rho^2)(M^2(c_x+2)-M_\rho^2)+(M^2c_x+M_\rho^2)(M^2(10c_x-3)+7M_\rho^2)-3M^2\big((3c_x+5)M_\rho^2+M^2(c_x^2+c_x-2)\big)B_0(M^2c_x+M_\rho^2,M^2,M_\rho^2)\big)$
(4)	0
(5)+(7)	$\frac{eg^3d_x(gd_x-1)(M^2c_x+M_\rho^2)}{144\pi^2M_\rho^4}\big(-6A_0(M^2)+2(M^2(c_x-6)+M_\rho^2)+3\big(M^2(c_x-4)+M_\rho^2\big)B_0(M^2c_x+M_\rho^2,M^2,M^2)\big)$
(6)+(8)	0
(9)	0
(10)	0
(11)	$\frac{eg^2(gd_x-1)^2}{144\pi^2M_\rho^6}\big((M^2c_x+M_\rho^2)^2\big)\big(-M_\rho^2-6A_0(M^2)-M^2(c_x-6)+3(M^2(c_x+2)+M_\rho^2)B_0(M^2c_x+M_\rho^2,M^2,M^2)\big)$
(12)	$\frac{eg^2}{1152\pi^2(M^2c_x+M_\rho^2)}\big(-534A_0(M^2c_x+M_\rho^2)+(M^2c_x+M_\rho^2)(495B_0(M^2c_x+M_\rho^2,M^2c_x+M_\rho^2,M^2c_x+M_\rho^2)+196)\big)$

Table C.2: Contributions of each Feynman diagram in figure 7.4 to the form factor $f_1(0)$ in equation (7.20a). Continued on page 114.

Diagram	$f_1(0)$
(13)+(14)	0
(15)	$\frac{eg_{\omega\rho\pi}^2}{288\pi^2 M_\rho^2}\big(3A_0(M_\rho^2)(M_\rho^2 - M^2(c_x+2)) - 3A_0(M^2)(M^2(c_x-2)+3M_\rho^2) - (M^2c_x + M_\rho^2)(M^2(10c_x-3)+7M_\rho^2) + 3M^2((3c_x+5)M_\rho^2 + M^2(c_x^2+c_x-2))B_0(M^2c_x+M_\rho^2, M^2, M_\rho^2)\big)$
(16)+(19)	$\frac{eg^3d_x(gd_x-1)(M^2c_x+M_\rho^2)}{144\pi^2M_\rho^4}\big(-6A_0(M^2) + 2(M^2(c_x-6)+M_\rho^2) + 3(M^2(c_x-4)+M_\rho^2)B_0(M^2c_x + M_\rho^2, M^2, M^2)\big)$
(17)+(20)	$\frac{eg^2}{384\pi^2(M^2c_x+M_\rho^2)}\big(6A_0(M^2c_x+M_\rho^2) - (M^2c_x + M_\rho^2)(99B_0(M^2c_x+M_\rho^2, M^2c_x+M_\rho^2, M^2c_x+M_\rho^2) - 10)\big)$
(18)+(21)	$\frac{eg_{\omega\rho\pi}^2}{288\pi^2(M^2c_x+M_\rho^2)}\big(14M_\rho^4 - 7M^4(c_x-3)c_x + 7M^2(c_x+3)M_\rho^2 - 3M^2A_0(M^2)(c_x+1) + 3A_0(M_\rho^2)(M^2(-c_x) - 2M_\rho^2 + M^2) + 3M^2(M^2(c_x-1)^2 - 4M_\rho^2)B_0(M^2c_x+M_\rho^2, M^2, M_\rho^2)\big)$
(22)	0
(23)	0
(24)	0

Table C.2: Contributions of each Feynman diagram in figure 7.4 to the form factor $f_1(0)$ in equation (7.20a). (Cont.)

Diagram	$f_2(0)$
(1)	$-\frac{eg^2M^2c_x(gd_x-1)^2(M^2c_x+M_\rho^2)}{144\pi^2M_\rho^6}\big(M_\rho^2+6A_0(M^2)+M^2(c_x-6)+6(M^2(c_x-1)+M_\rho^2)B_0(M^2c_x+M_\rho^2,M^2,M^2)\big)$
(2)	$-\frac{eg^2}{144\pi^2(M^2c_x+M_\rho^2)}\big(-g_{\rho\pi}+g(d_x+2f_V)\big)\big(-51A_0(M^2c_x+M_\rho^2)+(M^2c_x+M_\rho^2)(36B_0(M^2c_x+M_\rho^2,M^2c_x+M_\rho^2,M^2c_x+M_\rho^2)+5)\big)$
(3)	$\frac{eM^2c_xg_{\omega\rho\pi}^2}{576\pi^2M_\rho^2(M^2c_x+M_\rho^2)}\big(6A_0(M_\rho^2)(M^2(c_x-1)+2M_\rho^2)+6A_0(M^2)(M^2(1-2c_x)-3M_\rho^2)+(M^2c_x+M_\rho^2)(M^2(11c_x+3)+14M_\rho^2)-6(M^2(3c_x-4)M_\rho^2+M^4(c_x-1)^2+3M_\rho^4)B_0(M^2c_x+M_\rho^2,M^2,M_\rho^2)\big)$
(4)	0
(5)+(7)	$\frac{eg^2(gd_x-1)(M^2c_x+M_\rho^2)(gd_x+2g_{\rho\pi})}{144\pi^2M_\rho^4}\big(-6A_0(M^2)+2(M^2(c_x-6)+M_\rho^2)+3(M^2(c_x-4)+M_\rho^2)B_0(M^2c_x+M_\rho^2,M^2,M^2)\big)$
(6)+(8)	0
(9)	$-\frac{eg^3M^2A_0(M^2)c_xd_x}{8\pi^2M_\rho^4}$
(10)	$\frac{3eg^2}{16\pi^2}\big(g_{\rho\pi}-g(d_x+2f_V)\big)$
(11)	$\frac{eg^2(gd_x-1)^2}{144\pi^2M_\rho^6}\big((M^2c_x+M_\rho^2)^2\big)\big(M_\rho^2+6A_0(M^2)+M^2(c_x-6)+6(M^2(c_x-1)+M_\rho^2)B_0(M^2c_x+M_\rho^2,M^2,M^2)\big)$
(12)	$\frac{eg^2}{1152\pi^2(M^2c_x+M_\rho^2)}\big(-546A_0(M^2c_x+M_\rho^2)+(M^2c_x+M_\rho^2)(513B_0(M^2c_x+M_\rho^2,M^2c_x+M_\rho^2,M^2c_x+M_\rho^2)-136)\big)$

Table C.3: Contributions of each Feynman diagram in figure 7.4 to the form factor $f_2(0)$ in equation (7.20b). Continued on page 116.

Diagram	$f_2(0)$
(13)+(14)	$-\frac{eg^2_{\omega\rho\pi}(gd_x-1)}{576\pi^2M_\rho^2(M_\rho^2-M^2)}\big(6A_0(M_\rho^2)(M^2(c_x-4)M_\rho^2+M^4(c_x-1)^2+M_\rho^4)-6A_0(M^2)(M^2(2c_x-5)M_\rho^2+M^4((c_x-3)c_x+1)+2M_\rho^4)-6M^2(2M^2(c_x-3)(c_x-1)M_\rho^2+M^4(c_x-1)^3-8M_\rho^4)B_0(M^2c_x+M_\rho^2,M^2,M_\rho^2)+(M^2c_x+M_\rho^2)(6(M^2(c_x-4)+M_\rho^2)(M^2c_x+M_\rho^2)B_0(M^2c_x+M_\rho^2,M^2,M^2)+(M-M_\rho)(M_\rho+M)(M^2(16c_x-3)+13M_\rho^2))\big)$
(15)	$\frac{eg^2_{\omega\rho\pi}}{576\pi^2M_\rho^2}\big(6A_0(M^2)(M^2(2c_x-1)+3M_\rho^2)+6A_0(M_\rho^2)(M^2(-c_x)-2M_\rho^2+M^2)-(M^2c_x+M_\rho^2)(M^2(11c_x+3)+14M_\rho^2)+6(M^2(3c_x-4)M_\rho^2+M^4(c_x-1)^2+3M_\rho^4)B_0(M^2c_x+M_\rho^2,M^2,M_\rho^2)\big)$
(16)+(19)	$\frac{eg^3d_x(gd_x-1)(M^2c_x+M_\rho^2)}{144\pi^2M_\rho^4}\big(-6A_0(M^2)+2(M^2(c_x-6)+M_\rho^2)+3(M^2(c_x-4)+M_\rho^2)B_0(M^2c_x+M_\rho^2,M^2,M^2)\big)$
(17)+(20)	$\frac{eg^2}{384\pi^2(M^2c_x+M_\rho^2)}\big(6A_0(M^2c_x+M_\rho^2)-(M^2c_x+M_\rho^2)(99B_0(M^2c_x+M_\rho^2,M^2c_x+M_\rho^2,M^2c_x+M_\rho^2)-10)\big)$
(18)+(21)	$\frac{eg^2_{\omega\rho\pi}}{288\pi^2(M^2c_x+M_\rho^2)}\big(14M_\rho^4-7M^4(c_x-3)c_x+7M^2(c_x+3)M_\rho^2-3M^2A_0(M^2)(c_x+1)+3A_0(M_\rho^2)(M^2(-c_x)-2M_\rho^2+M^2)+3M^2(M^2(c_x-1)^2-4M_\rho^2)B_0(M^2c_x+M_\rho^2,M^2,M_\rho^2)\big)$
(22)	$\frac{eg^3A_0(M^2)d_x(M^2c_x+M_\rho^2)}{8\pi^2M_\rho^4}$
(23)	$\frac{3eg^2}{32\pi^2(M^2c_x+M_\rho^2)}\big(4(M^2c_x+M_\rho^2)-3A_0(M^2c_x+M_\rho^2)\big)$
(24)	$\frac{eg^2_{\omega\rho\pi}}{64\pi^2(M^2-M_\rho^2)}\big(5M^4-5M_\rho^4-2M^2A_0(M^2)+2M_\rho^2A_0(M_\rho^2)\big)$

Table C.3: Contributions of each Feynman diagram in figure 7.4 to the form factor $f_2(0)$ in equation (7.20b). (Cont.)

BIBLIOGRAPHY

[1] H. Leutwyler, „Chiral dynamics," (2000), arXiv:hep-ph/0008124 [hep-ph] .

[2] E. D. Bloom, D. Coward, H. DeStaebler, J. Drees, G. Miller, *et al.*, Phys. Rev. Lett. **23**, 930 (1969).

[3] M. Breidenbach, J. I. Friedman, H. W. Kendall, E. D. Bloom, D. Coward, *et al.*, Phys. Rev. Lett. **23**, 935 (1969).

[4] R. Brandelik *et al.* (TASSO), Phys. Lett. B **86**, 243 (1979).

[5] M. Gell-Mann, Phys. Lett. **8**, 214 (1964).

[6] G. Zweig, „An SU(3) model for strong interaction symmetry and its breaking," (1964).

[7] D. Gross and F. Wilczek, Phys. Rev. Lett. **30**, 1343 (1973).

[8] S. Weinberg, Phys. Rev. Lett. **31**, 494 (1973).

[9] H. Fritzsch, M. Gell-Mann, and H. Leutwyler, Phys. Lett. B **47**, 365 (1973).

[10] D. Gross and F. Wilczek, Phys. Rev. D **8**, 3633 (1973).

[11] H. Politzer, Phys. Rev. Lett. **30**, 1346 (1973).

[12] S. Weinberg, *The Quantum Theory of Fields I* (Cambridge University Press, 1995).

[13] S. Weinberg, „What is quantum field theory, and what did we think it is?" (1996), arXiv:hep-th/9702027 [hep-th] .

[14] J. Gasser and H. Leutwyler, Annals Phys. **158**, 142 (1984).

[15] S. Weinberg, Physica A **96**, 327 (1979).

[16] J. Gasser, M. Sainio, and A. Svarc, Nucl. Phys. **B307**, 779 (1988).

[17] T. Becher and H. Leutwyler, Eur. Phys. J. C **9**, 643 (1999).

[18] M. R. Schindler, J. Gegelia, and S. Scherer, Phys. Lett. B **586**, 258 (2004).

[19] A. Erwin, R. March, W. Walker, and E. West, Phys. Rev. Lett. **6**, 628 (1961).

[20] B. Maglic, L. Alvarez, A. Rosenfeld, and M. Stevenson, Phys. Rev. Lett. **7**, 178 (1961).

[21] P. Schlein, W. Slater, L. Smith, D. Stork, and H. Ticho, Phys. Rev. Lett. **10**, 368 (1963).

[22] P. Connolly, E. Hart, K. Lai, G. London, G. Moneti, *et al.*, Phys. Rev. Lett. **10**, 371 (1963).

[23] M. Alston, L. Alvarez, P. Eberhard, M. Good, W. Graziano, *et al.*, Phys. Rev. Lett. **6**, 300 (1961).

[24] Y. Nambu, Phys. Rev. **106**, 1366 (1957).

[25] J. J. Sakurai, *Currents and Mesons* (University of Chicago Press, 1969).

[26] B. Kubis and U.-G. Meißner, Nucl. Phys. **A679**, 698 (2001).

[27] M. R. Schindler, J. Gegelia, and S. Scherer, Eur. Phys. J. A **26**, 1 (2005).

[28] J. Gegelia and S. Scherer, Eur. Phys. J. A **44**, 425 (2010).

[29] D. Djukanovic, J. Gegelia, A. Keller, and S. Scherer, Phys. Lett. B **680**, 235 (2009).

[30] D. Djukanovic, M. Schindler, J. Gegelia, G. Japaridze, and S. Scherer, Phys. Rev. Lett. **93**, 122002 (2004).

[31] S. Scherer and M. R. Schindler, *A Primer for Chiral Perturbation Theory* (Springer Verlag, 2011).

[32] S. Scherer and M. R. Schindler, „A Chiral perturbation theory primer," (2005), arXiv:hep-ph/0505265 [hep-ph] .

[33] S. Scherer, Adv. Nucl. Phys. **27**, 277 (2003).

[34] W. J. Marciano and H. Pagels, Phys. Rept. **36**, 137 (1978).

[35] G. Altarelli, Phys. Rept. **81**, 1 (1982).

[36] K. Nakamura *et al.* (PDG), J. Phys. G **37**, 075021 (2010).

[37] E. Noether, Gött. Nachr. , 235 (1918).

[38] J. Bell and R. Jackiw, Nuovo Cim. A **60**, 47 (1969).

[39] S. L. Adler, Phys. Rev. **177**, 2426 (1969).

[40] S. L. Adler and W. A. Bardeen, Phys. Rev. **182**, 1517 (1969).

[41] J. Goldstone, Nuovo Cim. **19**, 154 (1961).

[42] J. Goldstone, A. Salam, and S. Weinberg, Phys. Rev. **127**, 965 (1962).

[43] S. Coleman, J. Math. Phys. **7**, 787 (1966).

[44] H. Lehmann, K. Symanzik, and W. Zimmermann, Nuovo Cim. **1**, 205 (1955).

[45] M. E. Peskin and D. V. Schroeder, *An Introduction to Quantum Field Theory* (Westview Press, 1995).

[46] J. C. Ward, Phys. Rev. **78**, 182 (1950).

[47] E. Fradkin, Zh. Eksp. Teor. Fiz. **29**, 258 (1955).

[48] Y. Takahashi, Nuovo Cim. **6**, 371 (1957).

[49] M. Gell-Mann, Phys. Rev. **125**, 1067 (1962).

[50] J. Gasser and H. Leutwyler, Nucl. Phys. **B250**, 465 (1985).

[51] H. Leutwyler, Annals Phys. **235**, 165 (1994).

[52] M. Gell-Mann, R. Oakes, and B. Renner, Phys. Rev. **175**, 2195 (1968).

[53] S. R. Coleman, J. Wess, and B. Zumino, Phys. Rev. **177**, 2239 (1969).

[54] J. Callan, Curtis G., S. R. Coleman, J. Wess, and B. Zumino, Phys. Rev. **177**, 2247 (1969).

[55] J. S. Schwinger, Phys. Lett. B **24**, 473 (1967).

[56] J. Wess and B. Zumino, Phys. Rev. **163**, 1727 (1967).

[57] S. Weinberg, Phys. Rev. **166**, 1568 (1968).

[58] U. G. Meißner, Phys. Rept. **161**, 213 (1988).

[59] M. Bando, T. Kugo, and K. Yamawaki, Phys. Rept. **164**, 217 (1988).

[60] M. C. Birse, Z. Phys. A **355**, 231 (1996).

[61] G. Ecker, J. Gasser, H. Leutwyler, A. Pich, and E. de Rafael, Phys. Lett. B **223**, 425 (1989).

[62] D. Djukanovic, J. Gegelia, and S. Scherer, Int. J. Mod. Phys. A **25**, 3603 (2010).

[63] K. Kawarabayashi and M. Suzuki, Phys. Rev. Lett. **16**, 255 (1966).

[64] Riazuddin and Fayyazuddin, Phys. Rev. **147**, 1071 (1966).

[65] M. Veltman, Physica **29**, 186 (1963).

[66] A. Denner and S. Dittmaier, Nucl. Phys. Proc. Suppl. **160**, 22 (2006).

[67] T. Bauer, J. Gegelia, G. Japaridze, and S. Scherer, „Complex-mass scheme and perturbative unitarity," (2011), in preparation.

[68] P. C. Bruns and U.-G. Meißner, Eur. Phys. J. C **40**, 97 (2005).

[69] G. 't Hooft and M. Veltman, Nucl. Phys. **B44**, 189 (1972).

[70] J. Collins, *Renormalization* (Cambridge University Press, 1984).

[71] R. Feynman, Phys. Rev. **76**, 769 (1949).

[72] G. Passarino and M. Veltman, Nucl. Phys. **B160**, 151 (1979).

[73] A. Denner and S. Dittmaier, Nucl. Phys. **B734**, 62 (2006).

[74] P. A. M. Dirac, *Lectures on Quantum Mechanics* (Dover, 2001).

[75] D. M. Gitman and I. V. Tyutin, *Quantization of Fields with Constraints* (Springer Verlag, 1990).

[76] G. Ecker, J. Gasser, A. Pich, and E. de Rafael, Nucl. Phys. **B321**, 311 (1989).

[77] V. Borodulin, R. Rogalev, and S. Slabospitsky, „CORE: COmpendium of RElations: Version 2.1," (1995), arXiv:hep-ph/9507456 [hep-ph] .

[78] L. H. Ryder, *Quantum Field Theory*, 2nd ed. (Cambridge University Press, 1996).

[79] G. Colangelo, S. Durr, A. Juttner, L. Lellouch, H. Leutwyler, *et al.*, Eur. Phys. J. C **71**, 1695 (2011).

[80] W. Siegel, Phys. Lett. B **84**, 193 (1979).

[81] W. B. Kilgore, „Regularization Schemes and Higher Order Corrections," (2011), arXiv:1102.5353 [hep-ph] .

[82] V. A. Smirnov, *Evaluating Feynman Integrals* (Springer Verlag, 2004).

[83] M. Abramowitz and I. A. Stegun, *Handbook of Mathematical Functions* (National Bureau of Standards, 1964).

[84] A. P. Prudnikov, Y. A. Brychkov, and O. I. Marichev, *Integrals and Series I* (Gordon and Breach, 1986).

[85] A. P. Prudnikov, Y. A. Brychkov, and O. I. Marichev, *Integrals and Series II* (Gordon and Breach, 1986).

[86] A. P. Prudnikov, Y. A. Brychkov, and O. I. Marichev, *Integrals and Series III* (Gordon and Breach, 1986).

[87] M. Lublinsky, Phys. Rev. D **55**, 249 (1997).

[88] D. Djukanovic, M. R. Schindler, J. Gegelia, and S. Scherer, Phys. Rev. Lett. **95**, 012001 (2005).

[89] M. Bhagwat and P. Maris, Phys. Rev. C **77**, 025203 (2008).

[90] H.-M. Choi and C.-R. Ji, Phys. Rev. D **70**, 053015 (2004).

[91] T. Aliev, I. Kanik, and M. Savci, Phys. Rev. D **68**, 056002 (2003).

[92] A. Samsonov, JHEP **312**, 61 (2003).

[93] F. Hawes and M. Pichowsky, Phys. Rev. C **59**, 1743 (1999).

[94] J. de Melo and T. Frederico, Phys. Rev. C **55**, 2043 (1997).

[95] F. Cardarelli, I. Grach, I. Narodetsky, G. Salme, and S. Simula, Phys. Lett. B **349**, 393 (1995).

[96] M. Gurtler *et al.* (QCDSF), PoS LATTICE2008 , 051 (2008).

[97] B. Lasscock, J. Hedditch, D. Leinweber, and A. Williams, PoS LATTICE2006 , 114 (2006).

[98] T. Hahn and M. Perez-Victoria, Comput. Phys. Commun. **118**, 153 (1999).

[99] D. Djukanovic, *Virtual Compton scattering in baryon chiral perturbation theory*, Ph.D. thesis, Institut für Kernphysik, Mainz (2008).

[100] G. Devaraj and R. G. Stuart, Nucl. Phys. **B519**, 483 (1998).

[101] J. A. M. Vermaseren, „New features of FORM," (2000), arXiv:math-ph/0010025 [math-ph] .

[102] J. Vermaseren, Nucl. Phys. Proc. Suppl. **205-206**, 104 (2010).

[103] J. Vermaseren, „FORM development," (2011), arXiv:1101.0511 [hep-ph] .

[104] R. Mertig, M. Böhm, and A. Denner, Comput. Phys. Commun. **64**, 345 (1991).

[105] T. Hahn, Comput. Phys. Commun. **140**, 418 (2001).